

University of Witwatersrand

Long-term Reconstruction of Rainfall and Fire for the Kavango-East and Zambezi Regions, Namibia and the Impact of people on Past Fire Regimes

A Dissertation submitted to the Faculty of Science, University of
Witwatersrand, Johannesburg, in fulfilment of the requirements for the degree of
Master of Science.

**Keywords: Savanna, Fire, Rainfall, Radiocarbon, Sedimentary Charcoal,
Environmental Proxy**



Tamryn Hamilton 670775

9 September 2020



Supervisors: Dr Sally Archibald (APES, WITS) and Dr Stephan Woodborne (iThemba Labs, NRF)

Contents

Chapter 1: General Overview and Context	2
1.1. Introduction	2
1.1.1. Climate Variability in Southern Africa	2
1.1.2. The Drivers of Savanna Structure	3
1.1.3. No Savannas without Fire	4
1.1.4. Woody Encroachment - A Response to Rainfall and Fire?	5
1.1.5. People in African Savannas.....	6
1.1.6. The role of Palaeoecological data in understanding Climate.....	9
1.1.7. Sedimentary Charcoal as a Fire Proxy	10
1.1.8. Tree Cores as Indicators of Past Climate	12
1.2. Project Outline.....	14
1.3. Project Aim.....	16
1.4. Objective 1.....	16
1.5. Objective 2.....	16
1.6. Study Site.....	16
Chapter 2: Creating Chronologies	21
2.1. Introduction	21
2.1.1. Radiocarbon Dating.....	21
2.1.2. Radiocarbon Dating Sediments.....	22
2.1.3. Radiocarbon Dating Tree Rings	24
2.2. Chapter Outline.....	25
2.3. Methods	25
2.3.1. Field Sampling	25
2.3.2. Lab Sampling	25
2.3.3. Charcoal Counting.....	26
2.3.4. Radiocarbon Dating the Mukolo Sediment.....	27

2.3.5.	Radiocarbon Dating the Linyanti Tree Core	28
2.3.6.	Age-depth Modelling	29
2.4.	Results	29
2.4.1.	Mukolo Sediment Core Age-Depth model.....	29
2.4.2.	Linyanti Rainfall Record Age-Depth model	33
2.5.	Discussion.....	36
2.5.1.	Chronology for the sedimentary sequence from Mukolo	37
2.5.2.	Changes in the Fire Regime over time based on the Microscopic and Macroscopic Charcoal Records.....	38
2.5.3.	Linyanti Baobab Tree Core Chronology	38
2.5.4.	Reliability of Mukolo and Linyanti Climate Records.....	39
2.6.	Appendices	41
2.6.1.	Appendix 1 –Summary of the Methods and Results of Hamilton (2016), the generation of the Linyanti $1 \delta^{13}C$ record.....	41
	Chapter 3: Rainfall and Fire in the Kavango-Zambezi region.....	43
3.1.	Introduction	43
3.1.1.	Climate Proxies for Understanding the Past	45
3.1.2.	Forcing at different time scales (event vs regime)	45
3.1.3.	Forcing at different spatial scales (local vs regional).....	46
3.1.4.	Age precision and Proxy Comparison.....	47
3.2.	Aims and Objectives of this Chapter	48
3.3.	Methods	48
3.3.1.	Scaling Mukolo and Linyanti Records.....	48
3.3.2.	Morlet Wavelet Analysis.....	49
3.4.	Results	50
3.4.1.	Mukolo Fire Record	50
3.4.2.	Linyanti Rainfall Record.....	51
3.4.3.	Wavelet Analyses of Environmental Records.....	52

3.5.	Discussion.....	57
3.5.1.	The Linyanti Rainfall Record.....	57
3.5.2.	The Mukolo Fire record	60
3.5.3.	The Fire-Rainfall Relationship.....	61
3.5.4.	Conclusions	63
3.5.5.	Integration with current research.....	63
3.6.	Appendices	65
3.6.1.	Appendix 1	65
3.6.2.	Appendix 2	66
Chapter 4:	Interpretations of historic climate fire numbering.....	67
4.1.	Dissertation Overview	67
4.1.1.	Pre-1400	68
4.1.2.	Old Wood Burning: 1400-1600.....	69
4.1.3.	Fire Transition Zone: 1600-1800	70
4.1.4.	Degraded Fire-Rainfall Relationship: 1800 to 1880	71
4.1.5.	Regional Burning: 1880-1950.....	72
4.2.	Conclusions	73
4.3.	Reflections on the study aims and objectives.....	74
4.4.	Recommendations for Land-users and Policy-makers	74
4.5.	Potential Sources of Error.....	75
4.6.	How this study could be improved.....	75
References	78

Acknowledgements

This dissertation is a demonstration of patience and endurance. It would not be possible without the dedication, guidance and collaboration shown by my supervisors' Dr Sally Archibald and Dr Stephan Woodborne, the most valuable input of Dr Lindsey Gillson and help from Dr Glynis Humphrey. Thank you for the invaluable time spent at the Plant Conservation Unit of University of Cape Town with the Palaeoecology Lab. Thank you to the South African Environmental Observation Network (SAEON) and the Expanded Freshwater and Terrestrial Environmental Observation Network (EFTEON). I owe a special thanks for support to Ashley Shamrock, my family and friends for always keeping your faith in me.

In acknowledgement of partial funding received from the Southern African Science Service Centre for Climate Change and Adaptive Land Management (SASSCAL).

Abstract

African savanna structure is driven by climate and fire, which have been well documented in modern observations and palaeo-studies, but is lacking on intermediate (decades to centuries) timescales where much of the ecosystem dynamics occur. Long-term rainfall and fire records were generated from environmental proxies from the semi-arid Kavango-Zambezi region of South-Central Africa. The records were radiocarbon dated in high resolution and modelled with Bayesian accumulation models to generate ~600year chronologies. The proxy time series were analysed in time-frequency space to elucidate the relationship between rainfall and fire at different timescales within local and regional fire histories. Wavelet analysis shows periods of time in the past when fire had a positive relationship with rainfall, and also a negative relationship, and a switch from local to regional-scale fire response to rainfall is observed in the Little Ice Age (1700-1750). A shift to regionally dominated fire regime thereafter is attributed to human population increase and associated land-use change. The results show that over time savanna landscapes can shift between load-limited and moisture-limited fire regimes and that savanna structure has been affected by human activities both directly, and via changes in fire regimes.

Chapter 1: General Overview and Context

1.1. Introduction

Southern Africa is a semi-arid largely summer-rainfall region dominated by fire-prone savanna habitats with many large mammalian herbivores. Savannas are ecosystems which have existed for several million years in Southern Africa (Beerling and Osborne, 2006) the persistence of which suggests high variability and a resilient nature (Walker and Noy-Meir, 1982). Our understanding of the thresholds defining savanna habitats is based on recent definitions following centuries of human manipulation (Gillson, 2015), and yet there is no agreement on the exact controls for savanna structure and function or the responses of savannas to changing climate and disturbances. Annual rainfall is predicted to decrease by as much as 30% in southern Africa (Niang *et al.*, 2014) with biome shifts in response to increased aridity (Niang *et al.*, 2014) facilitated by increased fire frequency and a change in timing and intensity of burns (Scholes *et al.*, 2015). Long-term data providing information on the local resilience to fire regimes and how the environment has responded in the past would benefit predictions of future instability and environmental response of these savanna ecosystems in the face of warming climate.

Here I will outline and describe the underlying climate, ecology and human influences relevant to the environmental proxies analysed and interpreted in this dissertation. This literature review will introduce the reader to generalized concepts for Southern African and focus in towards local concepts specific to the Kavango-Zambezi region of Namibia.

1.1.1. Climate Variability in Southern Africa

Southern African rainfall is driven by the Intertropical Convergence Zone (ITCZ) and its annual migration during austral summer which feeds moisture to smaller Temperate-Tropical Troughs (TTTs) (Harrison, 1984; Todd *et al.*, 2004). Southern Africa is dominated by arid and semi-arid regions associated with summer rainfall experienced from November to February, with the exception of the south-western Cape which receives winter rainfall. With regards to the summer rainfall zone, the dominant

rain bearing systems are Temperate-Tropical Troughs (TTTs) (Harrison, 1984; Todd *et al.*, 2004) - a synoptic system responsible for the poleward transport of moisture from the Intertropical Convergence Zone (ITCZ) during the Southern Hemisphere summer.

The seasonal transition of the ITCZ between the Northern and Southern hemispheres is a major convective system which contributes to the global energy balance (Hu *et al.*, 2007; Nicholson, 2018). Migrations of the ITCZ, as the North or Southerly variations from its common latitudes, can result in energy changes within the coupled atmospheric and oceanic circulation affecting precipitation (Leduc *et al.*, 2009; Schneider *et al.*, 2014). Within the last 1000years the placement of the ITCZ has varied enough to cause up to $>0.5^{\circ}\text{C}$ temperature anomaly causing relatively wetter or drier conditions in the Southern hemisphere depending on its placement (Schneider *et al.*, 2014). The migrations of the ITCZ influence the Indian Ocean Monsoon which is responsible for delivering moisture inland across the Eastern coast of Africa (Jury *et al.*, 1994).

Additional rainfall variability in southern Africa has been linked to abnormalities in atmospheric and sea surface temperatures of the Equatorial Pacific Ocean (Fauchereau *et al.*, 2003a; 2003b). This phenomenon is known as El Niño/La Niña or El Niño Southern Oscillation (ENSO). ENSO events occur on average every three to five years with identified trends occurring at different timescales up to 66-year cycles (Kane, 2009). El Niño events manifest as a “dry period”, where warm, dry atmospheric conditions prevail over southern Africa (Scholes *et al.*, 2015), and they are generally associated with droughts. Analyses of mean annual rainfall and Indian Ocean sea surface temperature anomalies associated with ENSO suggest that rainfall variation in southern Africa is strongly linked to the occurrence of ENSO events (Fauchereau *et al.*, 2003a; 2003b; Nicholson and Kim, 1997; Usman and Reason, 2004). Singleton and Reason (2007) then confirmed the effect of ENSO on rainfall and that La Niña increased the frequency of rain-bearing synoptic systems in southern Africa between 1973 and 2002, however they identified no such relationship for El Niño during the same period.

1.1.2. *The Drivers of Savanna Structure*

A savanna is generally defined by the presence of a continuous layer of C4 grasses with a variable distribution of trees (Archibald *et al.*, 2019). The determinants of savannas vary across continents but can be widely attributed to temperature, rainfall and soil (Archibald *et al.*, 2019). Many studies have argued the importance of these aspects to different degrees; focusing on frost (Hoffmann *et al.*, 2019; Holdo, 2006), rainfall seasonality (Priyadarshini *et al.*, 2016), soil water content (Wei *et al.*, 2019) and soil fertility (Lehmann *et al.*, 2011). However, it is widely agreed that they require regular disturbance (Bond, 2008) in the form of herbivory and/or fire (Archibald, 2010; Archibald *et al.*, 2019; Archibald and Hempson, 2016; Sankaran *et al.*, 2005; Staver *et al.*, 2011) to maintain an open system.

In arid and semi-arid savannas water is the limiting resource (Bond, 2008); due to the seasonal occurrence of rainfall, vegetation experiences a defined growing season initiated by the wet season. Following a rainfall event vegetation experiences a pulse of increased productivity resulting in an increase in biomass, although this phenomenon has been appreciated and used to determine fire management activities by people living in them for millennia, the first reference to this was a colonial visitor in 1853 (Fleming, 1856). This concept of savanna greening is well-documented in recent studies (Collins *et al.*, 2008; Saha *et al.*, 2015; Schwinning and Sala, 2004; Williams *et al.*, 2009; Zhang *et al.*, 2019). However, the response time between trees and grasses differ; Schwinning and Sala (2004) observed that trees respond to long-term changes in the form of average pulses, while grasses rely on short-term pulses and are often event driven. Long-term experiments show that changes in the fire regime (Roques *et al.*, 2001), herbivore pressure (Ward, 2005) and rainfall (Joubert *et al.*, 2008) result in alterations in savanna vegetation – specifically affecting the density of woody vegetation.

1.1.3. No Savannas without Fire

Fire is a key disturbance that reduces tree cover which is essential to maintain savanna vegetation at high rainfalls (Sankaran *et al.*, 2005): Whittaker (1962) was the first to identify that savannas existed in areas where rainfall is high enough to support forests and specifically referred to these systems as not reaching their “climate potential”. These findings brought to light the significance of fire in maintaining woody

vegetation within savannas and lead to the concept of a savanna as an alternative stable state to forests maintained by fire (Staver *et al.*, 2011).

Forest systems are thought to occur only when the canopy is sufficiently high to evade fire and facilitate canopy closure and prevent growth of a flammable grassy understory (Favier *et al.*, 2004; Hennenberg *et al.*, 2005; Staver *et al.*, 2011). Fire, on the other hand, acts to prevent tree canopies closing because saplings need to grow through the fire trap in which trees are prevented from recruiting by the reoccurrence of fire which causes top-kill in saplings and stunts sapling growth (Grady and Hoffmann, 2012). The return interval of fire therefore plays a key role in limiting woody recruitment by preventing canopy closure and sapling growth.

Savanna fires are determined by rainfall through the amount of biomass accumulated during previous wet seasons and the duration of the dry season (Archibald *et al.*, 2009; Bond, 2008; Joubert *et al.*, 2008; Van Wilgen *et al.*, 2004), or more specifically by two years previous rainfall (Archibald, 2010). Long-term fire studies from South Africa have identified that changing fire regimes can influence the intensity of burns, frequency of fires and area burned (Archibald *et al.*, 2009; Bond & Keeley, 2005; Cromsigt *et al.*, 2017) with measurable differences in the savanna vegetation structure (Higgins *et al.*, 2007a). Van Wilgen *et al.* (2004) identified that frequent burning in savannas results in fires which are smaller and less intense, while long-term suppression of fire alternatively results in larger fires with greater fire intensity and impact on woody vegetation (Van Langevelde *et al.*, 2003; Van Wilgen *et al.*, 2004). Thus, changes in the fire regime caused by rainfall variability can have knock-on effects for vegetation structure within African savannas because fire has a strong effect on tree-grass dynamics.

1.1.4. Woody Encroachment - A Response to Rainfall and Fire?

Vegetation variability in southern African savannas is linked to the competition between trees and grasses for resources and space, facilitated by disturbances like fire and herbivory (Shorrocks and Bates, 2015). The complex arrangement of trees and tree patches, termed patch dynamics, within savannas has recently been under investigation as the encroachment of woody species has become a focus in savanna ecosystem ecology (Joubert, 2014; Roques *et al.*, 2001; Stevens *et al.*, 2017; Ward, 2005).

Savanna trees respond to rainfall and competition from grasses differently depending on the demographic stage (Bond, 2008; February *et al.*, 2013; Higgins *et al.*, 2000); and trees require favourable conditions in order for seedlings to successfully establish. Joubert *et al.* (2008) conducted field experiments which determined that *Acacia mellifera*, considered a prolific woody shrub species in Namibia, requires three years of above average rainfall to establish suggesting increased rainfall frequency and intensity as the cause of bush encroachment; but other drivers include the increased availability of carbon dioxide (Buitenwerf *et al.*, 2012); landscape degradation following intense farming practices (Ward, 2005); and fire management practices (Moleele *et al.*, 2002). Probably all of these factors are involved at varying extents depending on the landscape history and current use.

1.1.5. *People in African Savannas*

The point at which humans started using fire to manipulate the environment is unclear, but Daniau *et al.* (2010) argue that the effect of people on fire regimes would have taken place at the time that early humans acquired the ability to create fire - somewhere between 200 000 and 1 million years ago (Archibald *et al.*, 2012). The history of people in sub-Saharan Africa is limited with preferential preservation at archaeological sites within less favourable arid regions (Chemello and Davis, 2014). The earliest confirmed use of fire by humans is from Wonderwerk Cave in South Africa, where ash suggest the use of fire by *Homo erectus* to cook food as early as 1 million years ago (Kaplan, 2012). The consequence is that the African environments have already been manipulated by humans for thousands of years (Gillson, 2015).

Major developments in human culture and economies in southern Africa, such as iron technology around 2 000 years ago, led to increased fuelwood consumption to sustain furnaces for smelting of metals (Robertson, 2001), but did not mark a noticeable increase of fire in the landscape (Scott, 2002). Around the same time the introduction of agriculture and pastoralism (Pyne, 1997) in southern Africa lead to changes in the lifestyle and economy from seasonally-nomadic to permanent settlements as people started to keep livestock (Kinahan, 2011a). Early famers and pastoralists arrived in the Kavango Zambezi region around 1550 (Seddon, 1968) and there were many other groups of people within the region who are thought to have learned agriculture

technology thereafter (Kinahan, 2011a). Fire was a commonly used tool for land clearing for agriculture and protection around settlements (Pausas and Keeley, 2009) as well as to improve livestock feed (Van de Vijver *et al.*, 1999). Civilizations such as Mapungubwe (1220-1290AD) (Huffman, 2000) and Great Zimbabwe (1290-1450AD) (Huffman and Vogel, 1991) are well known for their development and complexity in agriculture, trade and society (Beach, 1998; Chirikure and Pikirayi, 2008; Huffman, 2000). The success and collapse of these societies has been attributed to rainfall variation in history – particularly related to drought conditions around 1300 (Huffman and Vogel, 1991; Huffman and Woodborne, 2016; O’connor and Kiker, 2004).

Pre-colonial history in South Central Africa shows that there were many different groups of people living within the region, most of which relied on seasonal agriculture and livestock farming (Boden, 2009; Kinahan, 2011a). Goats and cattle, as kept by the Fwe and other subsistence communities which have long histories within the Kavango-Zambezi region (Pretorius, 1975), are capable of facilitating and maintaining grazing lawns (Hempson *et al.*, 2015; Tlou, 1972). These finite areas which are characterized by short, less flammable grasses enhance the patchiness of burns (Hempson *et al.*, 2015). Historic accounts of the Yeyi people and their exceptional hippo harpooning skills (Pretorius, 1975) lends to the likely existence of grazing lawns in the Kavango-Zambezi region because of the concentrated grazing they perform (Hempson *et al.*, 2015). The most notable features of local history is the Lozi people who moved southwards from Zambia through the Kavango-Zambezi region displacing or absorbing other groups on their way to Southern Botswana from 1830-1900 (Boden, 2009; Pretorius, 1975). This was followed by the widespread Northward migration of Sotho-Tswana people in the early 19th century fleeing the reign of Shaka in the Eastern coast of South Africa, known as the Difaqane, which resulted in violence and chaos as many local people were displaced (Pretorius, 1975).

Colonial settlers first interacted with indigenous people in Namibia in the late 1700s, before the establishment of colonial settlement (Kinahan, 2011a). But it was in 1888 that Namibian legislation banned all fires (Goldammer, 2001) until the 1940s when ecological thinking shifted and burning for management was initiated with studies from Kruger National Park of South Africa that suggested fire management policies of suppression and prescribed burning had little impact on the area burned but was rather more influenced by rainfall (Pyne, 1997; Van Wilgen *et al.*, 2004). However,

a study from the Kwando East region (inhabited by pastoralist people) of Namibia, found no discernible relationship between pastoralist fire management and rainfall (Verlinden and Laamanen, 2006). These findings suggest that pastoralist fire management strategies weaken, if not disrupt, the relationship between fire and rainfall.

More recently studies using continental-scale satellite imagery suggest that human activity has impacted all fire regimes across southern Africa (Archibald, 2010). The influence of people on African fire regimes suggest that people increase the frequency of ignitions in the system and reduce burnt area through fragmentation of the landscape (Archibald, 2010). Thus, the presence of people increases the potential for smaller, more frequent and less intense fires, but these conclusions are based on modern observations where settlements are more permanent and does not account for the semi-nomadic movement of people as was frequent in history (Boden, 2009). Hence, realistic management within the Kavango-Zambezi region requires site-specific long-term data which shows the degree of change in the form of historical range and variability of the fire management (Gillson, 2015).

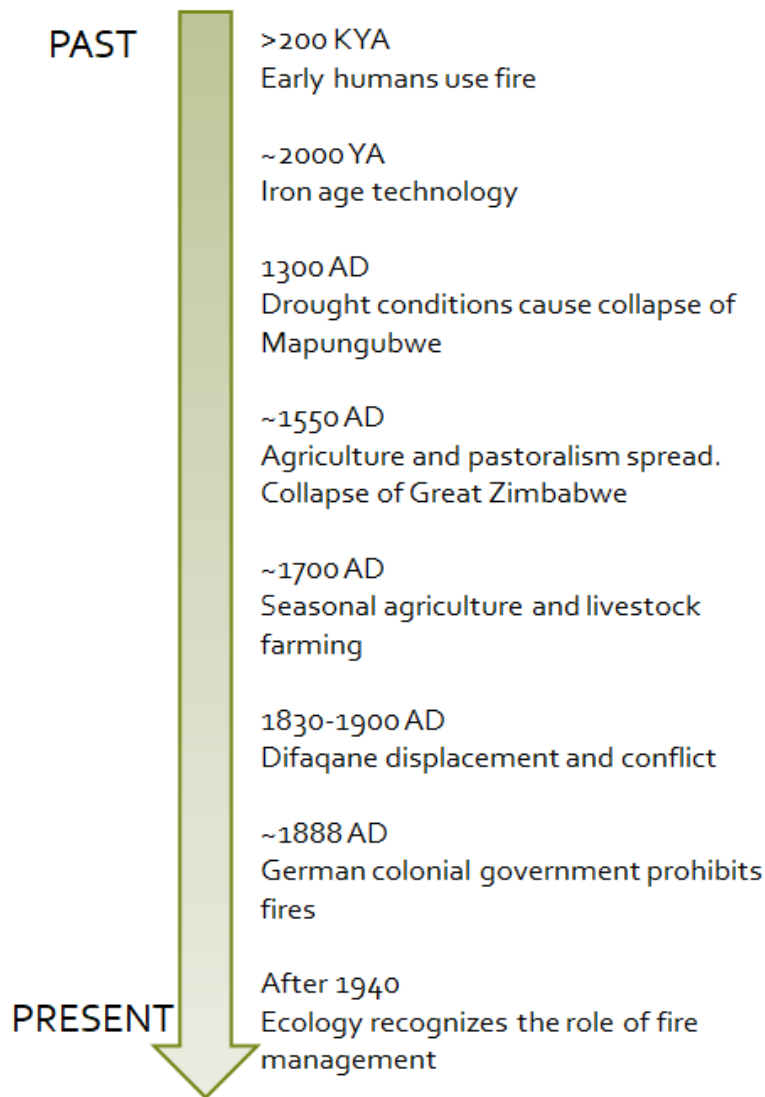


Figure 1. A timeline summarizing the important events in literature with regards to fire, rainfall and human activities specific to the Kavango-Zambezi region. Derived from information in (Goldammer, 2001; Huffman, 2008; Kinahan, 2011b; Patrut *et al.*, 2007; Pretorius, 1975; Robertson, 2001; Seddon, 1968; Van Wilgen *et al.*, 2004).

1.1.6. *The role of Palaeoecological data in understanding Climate*

Our understanding of semi-arid savannas is based on a maximum of 250-year documented account of a several-million-year-old landscape (Gillson, 2015). If past conditions approximate those expected for the future climate; could the savanna responses be similar? Accurately predicting future landscape change is dependent on modelling abilities (Pearson and Dawson, 2003); it requires understanding of the long-

term responses and is site specific (Giorgi and Mearns, 1991). Currently, investigations into historical landscape change in southern Africa are limited by the lack of long-term data (Scholes *et al.*, 2015) which could influence management practices and policy-making based on the understanding of the “natural” state of savanna landscapes (Gillson, 2015). Understanding ecosystem dynamics on longer timescales could change what we perceive “natural” vegetation states to be and give us a broader perspective on the concept of ecological thresholds (Gillson and Marchant, 2014) with implications for sustainable management practices. In the absence of long-term records, the development of environmental proxies has allowed for the investigation of past environmental responses to climate. For example palaeo-ecological studies from New Zealand and Madagascar used sedimentary charcoal and pollen to determine the state of ecosystems prior to the arrival of humans on the islands, which revealed that recent management goals tended towards a false “natural” state (Gillson, 2015).

Proxies for climate reconstruction provide limited information when used in isolation, but the use of multiple independent proxies provides a more reliable source of information (Mann and Rutherford, 2002). However proxies are not often directly comparable due to localized accumulation and taphonomy conditions (Gillson, 2015) and error ranges associated with dating techniques (Scott, 2007) which make direct comparisons heavily dependent on the timeline associated with each proxy. This means that comparing climatic events or variables observed on short timescales within climate proxies can yield poor relationships, whilst on the long-term timescale the relationship between climate factors can indicate a strong linkage.

1.1.7. Sedimentary Charcoal as a Fire Proxy

The use of sedimentary charcoal refers to plant material which has undergone incomplete combustion and accumulates in sediments over time (Whitlock and Larsen, 2002) - it is a measure for fire activity in the past. Sedimentary charcoal is quantified as a concentration within sediment relative to a known concentration additive (Whitlock and Larsen, 2002). The resultant concentrations are compared as relative abundances of fire activity within the proxy, higher concentrations of charcoal are attributed to increased fire activity (Clark, 1988; Duffin, 2008; Duffin *et al.*, 2008; Whitlock and

Larsen, 2002), but can be skewed by charcoal breakage during sieving (Schlachter and Horn, 2010; Whitlock and Larsen, 2002).

Sedimentary charcoal analyses were previously based on size-class characterisation (Clark, 1988), however, particle size has been strongly linked to distribution distances (Clark, 1988; Duffin *et al.*, 2008; Ekblom and Gillson, 2010; Higuera *et al.*, 2007; Whitlock and Larsen, 2002). Recent trends in charcoal analysis focus on two main size classes as indicators for different deposition areas: Microscopic charcoal (<150µm) which is assumed to be associated with regional distribution (Oris *et al.*, 2014; Scott, 2002; Tinner and Hu, 2003) and macroscopic charcoal (>150µm) which is assumed to be associated with more limited local distribution (Higuera *et al.*, 2007; Oris *et al.*, 2014; Peters and Higuera, 2007; Tinner *et al.*, 2006). Sediment trap studies have been employed in an effort to constrain deposition distances with strong correlations of both microscopic and macroscopic charcoal at 40km source areas when compared with MODIS fire data (Adolf *et al.*, 2018b, 2018a). However, the study area of Adolf *et al.*(2018b) was dominated by sites within and surrounded by mountains with potential to channel winds differently to open, flatter landscapes. It is important to note that the macroscopic charcoal sourced from open landcover classes, most similar to savanna landscapes, was limited to a source area of <15km (Adolf *et al.*, 2018b).

Charcoal production is dependent on the local context of fire within the landscape: the size of fires, location, and frequency of burn (Duffin *et al.*, 2008; Ekblom and Gillson, 2010; Higuera *et al.*, 2007; Peters and Higuera, 2007), which influences the potential for charcoal particles to be transported. The fuel source affects the morphology of charcoal particles produced, with elongated charcoal shapes associated with grasses and more compact shapes attributed to woody vegetation (Crawford and Belcher, 2014). These components of charcoal production and morphology are related to dispersal characteristics that are estimated by models which suggest a range of <5km distance for macroscopic charcoal and 5-32km distance for microscopic charcoal (Higuera *et al.*, 2007; Peters & Higuera, 2007). However, these models are limited to forest fires with generally greater fire intensity (Alexander, 1982; Tinner *et al.*, 2006) in comparison to savanna fires (Govender *et al.*, 2006) suggesting the microscopic charcoal particle dispersion associated with savannas would be <32km.

In an African context, there are very few studies which have actively explored charcoal transport and deposition, with no sediment trap studies to date or any physical measurements of the maximum distance travelled by charcoal particles. The Southern African Regional Science Initiative (SAFARI) 2000 project measured land-atmosphere interactions through emissions monitoring, however the particulate matter category (under which microscopic charcoal would be categorized) was limited to particles smaller than PM_{2.5} (Korontzi *et al.*, 2004), which refers particles less than 2.5 micrometres in length. Those particles are ten times smaller than the microscopic charcoal counted in sedimentary charcoal analyses. Hence the particulate matter (PM_{2.5}) described in the SAFARI publications has the potential to move much greater distances across the landscape and cannot be compared with sedimentary charcoal data.

The closest source for any quantifiable charcoal deposition measures in African savannas are those of Duffin *et al.* (2008) in which macroscopic charcoal >50µm is attributed to a maximum distance of 5km whilst microscopic charcoal (< 50µm) was sourced from 10-15km from the accumulation site. Considering that fire intensity also plays a role in the distance particles can be transported, the absence of high intensity fires by Duffin *et al.* (2008) suggest that charcoal particle transmission could be greater than their maximum observation of 15km. A comparison of sedimentary charcoal proxies and tree rings from the Kruger National Park in South Africa identified that periods characterized by increased charcoal concentrations in the past coincided with periods of higher rainfall (Duffin, 2008; Duffin *et al.*, 2008; Ekblom & Gillson, 2010; Lindsey Gillson & Ekblom, 2009). Other than the relatively short-term studies performed in the Kruger National Park, there is a lack of fire proxies in sub-Saharan Africa with most African sedimentary charcoal studies concentrated around large lakes which offer extremely long-chronologies but do not inform on shorter timescales (L. Gillson, 2015; Marlon *et al.*, 2013) such as those relevant to ecology.

1.1.8. Tree Cores as Indicators of Past Climate

Dendrochronological sequences are proxies used to indicate past climate, the basis for which is the growth rings which accumulate over time and can be interpreted as tree ring widths or, more recently as stable carbon isotopic fractionation values. Tree-ring width analyses require annual ring growth and correlation with climatic variables

(February, 2000) which is uncommon in African tree species (Woodborne *et al.*, 2015). Stable carbon isotopic analysis of tree rings relies on the inherent process of photosynthesis. When carbon is absorbed from the atmosphere and converted into energy used for growth of new tree rings the carbon isotopic composition is strongly correlated to rainfall (February, 2000; Fichtler *et al.*, 2004; Robertson *et al.*, 2006). Stable carbon isotopic analysis has been applied to various tree species in South Africa, with their climate interpretations applied generally for southern Africa (February, 2000; Gebrekirstos *et al.*, 2009; Hall *et al.*, 2009; Woodborne *et al.*, 2016, 2015).

The stable carbon isotopic signature measured from tree rings is controlled by two factors: the constant carbon fractionation of Rubisco and the physiological response of the individual plant species to water stress (Woodborne *et al.*, 2015). The uptake of carbon by Rubisco is selective, and discriminates against heavier ^{13}C isotopes (Farquhar *et al.*, 1982; Guy *et al.*, 1993). The physiological response refers to the stomatal conductance – when the stomata close to reduce water loss and in doing so restrict the exchange of gases within the leaf. Arid-specialised trees, such as baobabs, are able to close the stomata on the leaf surface during the day to prevent water loss (Fenner, 1980). However, this temporarily prevents gaseous exchange as there is no flow of carbon dioxide with the atmosphere (Farquhar & Sharkey, 1982). Under these conditions photosynthesis continues and whatever CO_2 is available inside the leaf is used incorporating increased amounts of heavy (^{13}C) as the light (^{12}C) isotopes of carbon are used up (Farquhar and Sharkey, 1982). Thus, under dry conditions baobab stomata close resulting in a greater abundance of heavier carbon isotopes incorporated into woody tissue, denoted as a greater $\delta^{13}\text{C}$ values.

Accessing these chronologically sequenced tissues through tree cores results in a quantifiable chronological records of water stress experienced by the plant over time. The degree of water-stress is plant-specific due to the Intrinsic Water-use Efficiency (iWUE) (Farquhar *et al.*, 1989) which generally describes plant performance of arid specialized plants. Microclimates and genetic lineage (Herrera *et al.*, 2015) can affect the iWUE, but can be quantified and corrected conserving the inter-annual climate trend (McCarroll *et al.*, 2009). In this way, woody plant tissue characterized by increased $\delta^{13}\text{C}$ values is used as an indicator of dry conditions synonymous with reduced rainfall.

1.2. Project Outline

Understanding interactions between climate, fire, vegetation and people in savanna contexts requires understanding both their direct and indirect impacts on each other (Figure 2). In the Caprivi context we know that climate affects vegetation and tree grass ratios, and it also affects fire regimes (from studies in other places we expect that more rainfall will result in more frequent, more intense fires). However, fire regimes also affect vegetation patterns so climate has both direct and indirect (via fire) influences on tree-grass ratios. Finally, human activities alter fire regimes, and potentially disrupt relationships between climate and fire.

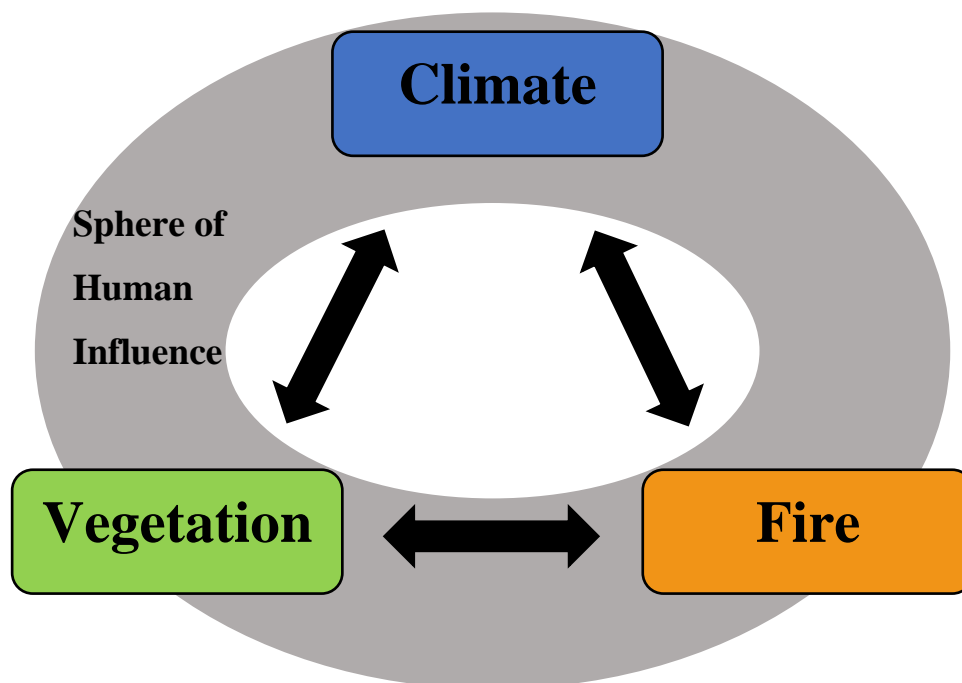


Figure 2. A diagram showing the interdependence of climate, fire and vegetation on one another as determinants of African savanna structure and the overarching influence of humans on savanna determinants. Derived from information in (Archibald *et al.*, 2009; Joubert *et al.*, 2008; Van Wilgen *et al.*, 2004).

This dissertation will focus on the relationship between fire and climate to identify and interpret the influence of people on the determinants of savanna structure (Figure 2.) in the past. It will be structured as four chapters: a general introduction and literature review; two data chapters and a synthesis chapter.

Chapter One (this chapter) introduces the reader to the underlying climate, ecology and human influences relevant to the environmental proxies analysed and interpreted in this dissertation. This literature review identifies generalized concepts for African savannas and focuses in towards local concepts specific to the Kavango-Zambezi region of Namibia.

Chapter Two is the first data chapter where the environmental proxies are dated and the chronologies which characterize each environmental proxy are developed. The chapter is structured with an introduction to proxy dating techniques; methods section describing the sampling, preparation and radiocarbon dating of the Mukolo sediment core and Linyanti 1 Baobab core; results section where radiocarbon dates and model outputs are presented; and a discussion section where the radiocarbon dates and chronologies are interpreted.

Chapter 3 is the second data chapter where the fire and rainfall records generated from the environmental proxies are compared. This chapter is structured with an introduction providing background into why we compare environmental proxies and some of the limitations around their comparison which lead to my use of time-frequency space. The methods section describes how the fire and rainfall records were converted into time series and compared using wavelet analysis. The results section is where wavelet plots are presented; and the discussion section where the environmental proxies are critically interpreted in terms of other African climate proxies and known climatic features.

Chapter 4 is a synthesis where the reader is reminded of the overall findings from this dissertation. Aspects from the radiocarbon dating and wavelet comparisons are interpreted in terms of the local human history of the Kavango-Zambezi region; or if unavailable, the broader South-Central African history. Ecological interpretations are made based on the relationship between fire and rainfall; and although vegetation is a key component for determining the state of African savannas, its role will be limited to literature as there are no pollen records available at this time.

1.3. Project Aim

To create a proxy climate record for rainfall and fire for South-Central Africa and to investigate the relationship between rainfall and fire over time and to assess the impact of human activities on the fire regime.

1.4. Objective 1

Define and constrain the temporal accumulations of the Linyanti Baobab tree core and Mukolo sediment core.

- Hypothesis 1: Radiocarbon dating at intervals from each climate proxy will yield a series of dates which can be interpolated to generate timeseries for the rainfall and fire records.

1.5. Objective 2

Investigate the relationship between rainfall and fire in the Kavango-Zambezi region through climate proxies.

- Hypothesis 1: There have been large-scale shifts in water availability which can be linked to rainfall variability in southern Africa in recent centuries.
- Hypothesis: Fire and rainfall proxies support current evidence that there is more fire during wetter periods in African savannas.
- Hypothesis 4: Human activity and land-use practices obscure the relationship between climate and fire.

1.6. Study Site

The North Eastern region of Namibia is centrally located in southern Africa (~18°S and 24°E). The region is bordered by Zambia (North), Zimbabwe (East), Botswana (South) and Angola (North West) (Figure 3.) It forms the centre of the Kavango-Zambezi Trans-Frontier Conservation Area (KAZA TFCA), a collaborative conservation effort between governments and international stakeholders. The KAZA

TFCA regions are world renowned as a corridor for wildlife which includes large mammals such as elephant, white rhinoceros and hippopotamus (Cumming, 2008).

The North-eastern region of Namibia is divided into two regions: the Kavango-East which includes the eastern section of Bwabwata National Park and Kavango River (Figure 3.); and the Zambezi region which is from Katima Mulilo (Figure 3.) eastward and includes the Zambezi River (Figure 3.). Within the Kavango-East and Zambezi regions there exist 15 communal conservancies, 1 tourism concession area and 3 state protected areas, each with community enacted management strategies (Mendelsohn *et al.*, 2002).

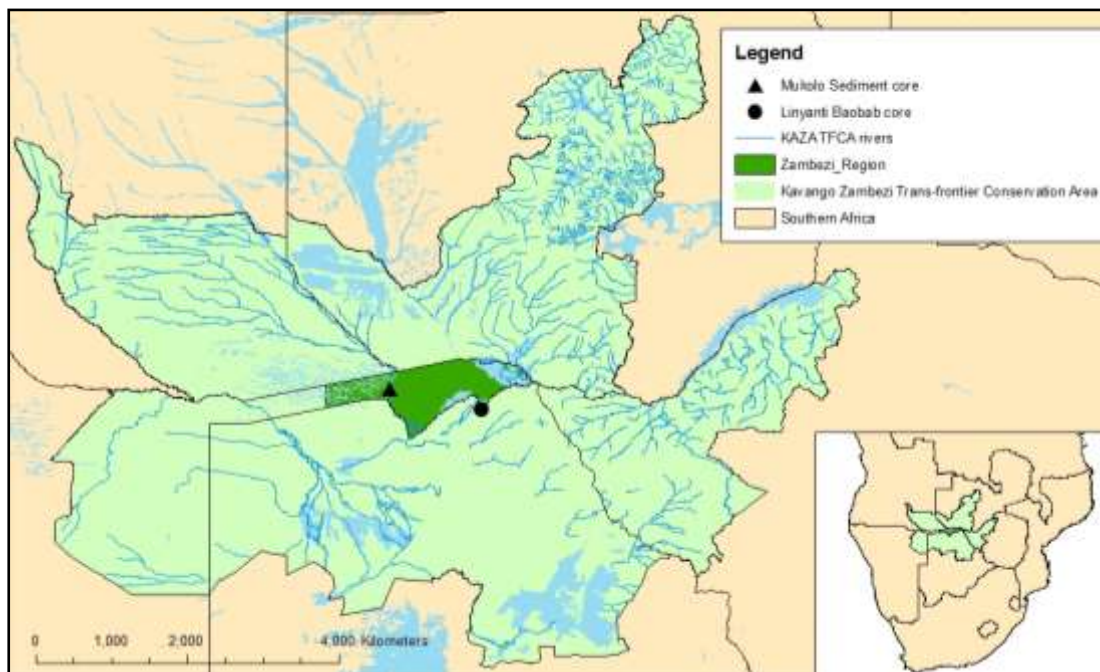


Figure 3. A map showing the central location of the Kavango-Zambezi region (dark green) within southern Africa. The location of proxy collection sites is shown, the Linyanti Baobab core (circle) and the Mukolo sediment core (triangle). Created in ArcMap with data from ArcGIS (Landcover Monitoring KAZA TFCA shapefile) and DIVAGIS (country administrative borders and water features).

The Kavango-East and Zambezi region experience a hot, semi-arid climate with annual average temperature of 20-22°C, and minimum and maximum temperatures of 2-4°C and 34-36°C respectively (Mendelsohn *et al.*, 2002). Annual rainfall occurs from November to March (Killingtveit and Hamududu, 2016) and is most intense during December to January during the development of a “moisture front” associated with

cumulus clouds of the ITCZ (Taljaard, 1986). The rainfall varies from 600mm to 540mm (Fick and Hijmans, 2017) from East to West with the Kavango-Zambezi region (Figure 4.) characterised as being on the boundary between rainfall regimes by Nicholson and Entekhabi (1986) with a significant decrease in rainfall towards the West coast of Namibia.

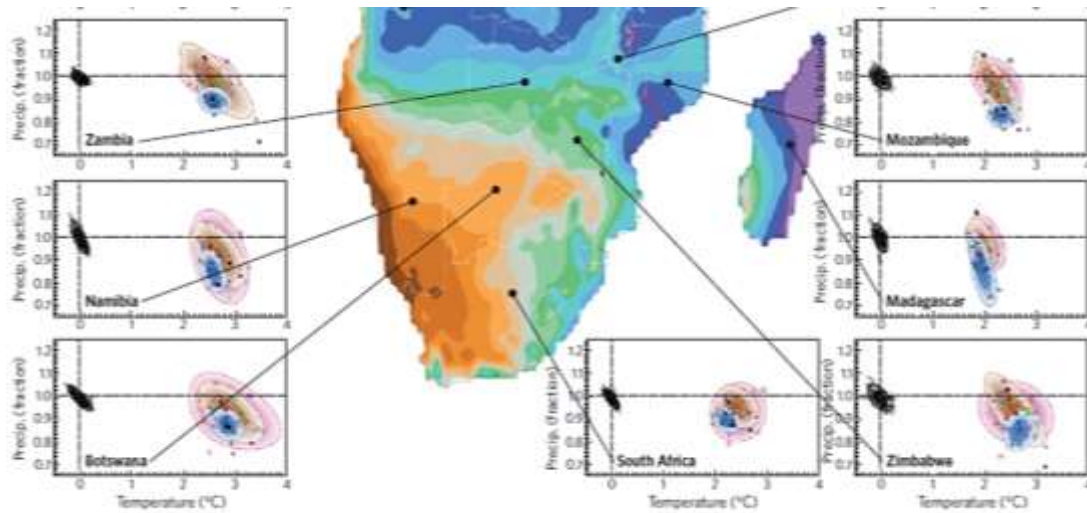


Figure 4. Map of Southern African rainfall for the period 1961-1990 with projected climate change plotted for each country (temperature on the x-axis and precipitation on the y-axis). Adapted from Conway *et al.* (2015).

The median rainfall value, described as “a better reflection” of normal rainfall for the Kavango-Zambezi region is ~550mm across a 30-year period (Mendelsohn *et al.*, 2002). While the average annual rainfall calculated from the WorldClim2 remote sensing model estimates ~800mm per annum with the coefficient of variation of rainfall <40% (Fick and Hijmans, 2017). The history of annual rainfall of the Kavango-East and Zambezi region is limited to 1945 (Figure 5.), with ~400mm variation in annual rainfall records observed at ~25 year cycles (Mendelsohn *et al.*, 2002).



Figure 5. Historic rainfall records from Katima Mulilo from 1940s to 2001 from Mendelsohn *et al.* (2002). The 5-year running average (red) show rainfall variability with above average rainfall in the early 1950s and early 1970s.

The vegetation of the Kavango-East and Zambezi region was described in the 1970s as a grassland landscape with patches of thorny shrubs (Giess, 1971). However, a more recent study gave a conflicting description defining the region as forested veld (Harring and Odendaal, 2012). Lushetile (2009) focused on the vegetation in and around the Sachinga Livestock Development Centre (a communal conservancy area), located 27km north west of the Zambezi basin, and identified two main vegetation classes: *Colophospermum mopane* Woodlands and *Baikiaea plurijuga* Woodlands which were exposed to frequent burning to improve livestock feed. According to the Atlas of Namibia (2002) (Figure 6.), the Kavango-East and Zambezi regions support a combination of Grassland and Woodland vegetation structure types with grass cover between 51-100% (Mendelsohn *et al.*, 2002). More recently Krawchuk and Moritz (2011) classified the region as an interplay of Tropical/subtropical grasslands, savannas and shrublands and Tropical/subtropical moist broadleaf forest, their work suggests the region is a fuel moisture-limited system – highly influenced by rainfall.

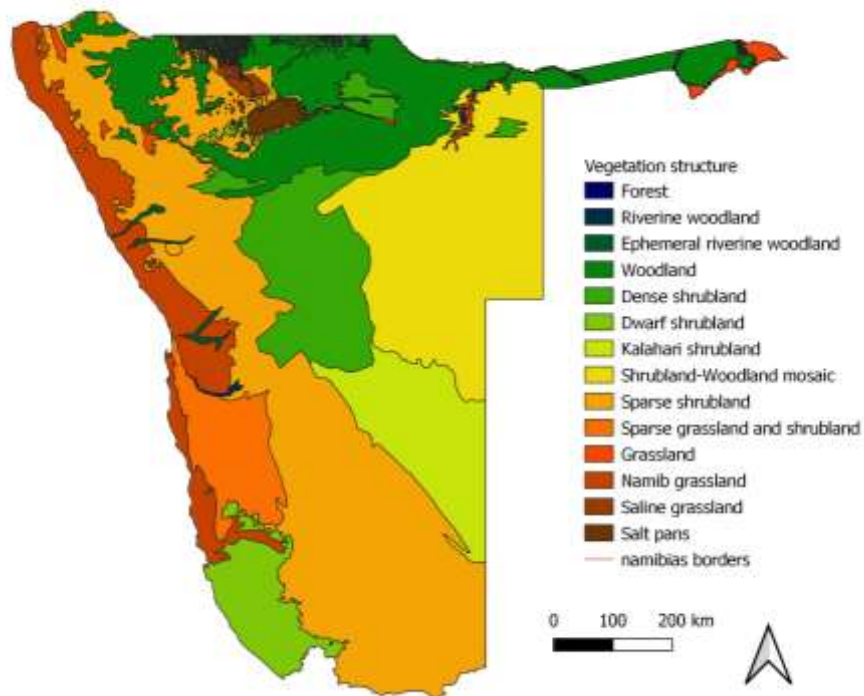


Figure 6. Map of the vegetation structure of Namibia (Map created in QGIS, data source: Mendelsohn *et al.*, 2002), which describes the high biomass regions in the North-Eastern region of Namibia.

Fires within the Kavango-East and Zambezi region are most common in April-November (Le Roux, 2011), which are prevented by management due to the threat to forest and wooded shrubland (Le Roux, 2017). Zambezi Teak (*Baikiaea plurijuga*) is an example of a fire sensitive species found in Eastern Namibia which fire suppression practices aim to protect (Le Roux, 2017). Current fire management in the region prescribes controlled patch burning annually, using early season fires to facilitate livestock feed and prevent intense fires (GFMC, 2001).

Chapter 2: Creating Chronologies

2.1. Introduction

Chronologies are the time intervals associated with finite events used to describe measurable archives of past biogeochemical states. They are a valuable resource for investigating historic environments, especially in Africa as an underrepresented region in palaeostudies (Gillson, 2015; Gillson and Marchant, 2014; Scholes *et al.*, 2015). Temporal constraint of environmental records can be complex and relies on effective sampling and interpretation to understand accumulation rates, post-depositional disturbances and the inherent taphonomic process of each environmental record. These range from sediment cores (Butzer *et al.*, 1972; Shanahan *et al.*, 2012), to tree cores (Gebrekirstos *et al.*, 2009; McCarroll and Loader, 2004), ice cores and many others. Within the range of environmental records different elements can be measured to quantify environmental conditions – including Oxygen-18 for water source or temperature (depending on the proxy investigated), Carbon-13 which indicates water stress in trees (Robertson *et al.*, 2006), pollen for plant community structure (Scott, 2016), charcoal for fire activity (Whitlock and Larsen, 2002) and fungal spores for species composition and herbivore abundance (van Geel *et al.*, 2011). Here I will be focusing on creating chronologies for a charcoal record generated from a sediment core and carbon-13 record from a Baobab tree core representing the Kavango-Zambezi region of North-East Namibia.

2.1.1. Radiocarbon Dating

In order to interpret past environmental records it is critical to accurately date these records, and this has been the subject of much research (Blaauw and Christen, 2011; Hagens, 2006; Telford *et al.*, 2004; Walker *et al.*, 2001). Radiocarbon dating is the preferred method for age determination of carbon rich materials such as sediments, bone and plant material younger than 50 000 years. The radiocarbon dating method uses the decay of carbon-14 to estimate when the carbon was sequestered based on its half-life (Broecker and Kulp, 1956). However, the quantity of radiocarbon within the atmosphere has varied in time and requires calibration to isolate calendar ages (Törnqvist *et al.*, 2015). The calibration of radiocarbon dates isolates periods in time when sequestration could have occurred. Often radiocarbon calibration can yield

multiple possible intercepts, each with an associated degree of error and probability of occurrence (Scott, 2007). Radiocarbon calibration is a well-established process with the newest internationally standardized calibration curves accepted in 2013 (Reimer *et al.*, 2013).

Accurate contextualization of events and variability within climate proxies form the basis for interpreting the environmental responses. The degree to which radiocarbon dating can be constrained is determined by the laboratory quoted error associated with each analyses and is unavoidable (Scott, 2007). The confidence intervals, or temporal constraint on a chronology is limited to the sample quality, quantity and placement of dates within proxy sequences (Telford *et al.*, 2004). To interpret proxy sequences multiple radiocarbon dates are used at intervals, each with a different range of error, which becomes statistically daunting and complex to quantify (Scott, 2007).

The selection of an appropriate chronology based on radiocarbon dates becomes problematic when dates do not clearly indicate the age-depth dynamics and there are multiple chronology possibilities (Bennett and Fuller, 2002; Richard J Telford *et al.*, 2004; R.J. Telford *et al.*, 2004). Most chronologies make use of linear interpolations based on few radiocarbon dates which are considered inaccurate in nature but of acceptable precision in the face of uncertainty (Bennett and Fuller, 2002). Bayesian statistical analyses are a statistical method introduced to generate age-depth models that reduces the subjectivity of radiocarbon date interpretations. These models reduce the use of poorly fitting chronologies which are unlikely approximations of the environment (Blaauw and Christen, 2011).

2.1.2. Radiocarbon Dating Sediments

Sediments accumulate by being transported by wind or water and collect where remobilization is prevented by sheltered local conditions or the presence of stagnant water. These depositional features can be dated using different components depending on the available sources of carbon such as shells (Heine, 1978; Williams *et al.*, 2010), fish bones (Shanahan *et al.*, 2012), humin (Pessenda *et al.*, 2001), pollen charcoal (Shanahan *et al.*, 2006), bulk organic matter (Peck *et al.*, 2004) or bulk sediments (Strobel *et al.*, 2019; Talbot and Johannessen, 1992). These different components can aid in the identification of proxy anomalies such as age reversals, hiatuses (Brauer *et*

al., 2001) or mixing where burrowing organisms or trampling can yield younger ages by disrupting the law of superposition (Rowe, 1961).

Sedimentary charcoal refers to plant material which has undergone incomplete combustion and is often characterized by a black or grey colour. It accumulates in sediments of fire-prone systems as either macroscopic charcoal associated with local fire activity, or microscopic charcoal which is used as a measure of regional fire (Higuera *et al.*, 2007; Whitlock and Larsen, 2002). However, sedimentary charcoal offers poor temporal constraint on chronologies because woody material can occur within the landscape for long periods of time before being incorporated into sediments (Schiffer, 1986) and undergoes different taphonomic processes in comparison to smaller sediment components (Scott, 2010). This inbuilt-age of charcoal has previously been estimated in different sediments using comparisons to fire records from tree rings (Gavin, 2001), Bayesian modelling analyses (Dee and Ramsey, 2014) and probability distributions of inherited age (Frueh and Lancaster, 2014). But, these studies are limited to tree dominated forests (Dee and Ramsey, 2014; Gavin, 2001) or perennial riverine systems (Frueh and Lancaster, 2014) and would overestimate the inbuilt charcoal age of semi-arid African environments where fire is frequent and maintains a continuous grass layer.

Radiocarbon dating determines the time of carbon sequestration, however this can be different from the target event (date of the fire that produced the charcoal) to which the dating strives (Dean, 1978) and highlights the importance of careful selection of dating material. In the case of dating sediments, bulk organic matter is favoured because it includes pollen (Scott, 2002) and humin (Pessenda *et al.*, 2001) which are considered more contemporary with sediment accumulation dates than charcoal which could have been sourced from a long-living tree. The identification of unsuitable or misrepresentative radiocarbon dates in sediments is restricted to well sampled proxies where there is sufficient dated material to identify outliers and deviations in the proxy accumulation (Bennett and Fuller, 2002; Heegaard *et al.*, 2005; Shanahan *et al.*, 2012; R.J. Telford *et al.*, 2004). Hence radiocarbon dating of sediments can require interpretations of the carbon source, usually by the percentage modern carbon (pMC), to identify non-contemporary (too old) or modern carbon (too young) contaminated samples (Santos *et al.*, 2016).

In complex systems, such as African semi-arid savannas, there are multiple feedbacks and processes which impact sediment accumulation processes that are not well understood (Marchant *et al.*, 2018) and poorly dated chronologies could easily be misinterpreted (Gillson, 2015). In addition, sub-Saharan African palaeoclimate studies are represented by a low-density network of proxies. Many are limited to wet systems (lakes, swamps and caves)(Burrough *et al.*, 2007; Butzer *et al.*, 1972; Heine, 1978; Scott, 2016; Scott *et al.*, 2003), with some extremely arid sequences (Scott, 1996; Stone and Thomas, 2008; Telfer and Thomas, 2007) which offer limited understanding with regards to semi-arid regions.

2.1.3. Radiocarbon Dating Tree Rings

Tree rings are used as indicators of past climate (Becker, 1992), growth rings are counted as the representation of years and the thickness measured as the climate indicator. But not all trees deposit rings regularly, with some depositing several rings in one year. The use of radiocarbon dating allowed for the inclusion of long-lived trees such as baobabs for climate records where the tree-rings are strongly correlated to rainfall (Robertson *et al.*, 2006). The combination of radiocarbon dated chronologies and use of stable carbon isotopes to analyse baobab rings have generated multiple rainfall histories for Southern Africa (Huffman and Woodborne, 2016; Woodborne *et al.*, 2016, 2015) in an absence of long-term rainfall data.

The concept of radiocarbon dating tree rings hinges on the ability of plants to photosynthesize: the regulated uptake of carbon from the atmosphere and subsequent sequestration into cellulose provides reliable sample material for radiocarbon dating due to the chronological sequence of tissue accumulation. The exception being tissue damage and regrowth where newly formed scar tissue introduces younger carbon (Patrut *et al.*, 2015). But the development of scar tissue is texturally different and can be easily observed within the wood of the sample. By using a reference section, or longitudinally sampling half the core, the woody tissue structure is maintained and allows for reference to '*in situ*' tree rings to identify scar tissue for exclusion.

2.2. Chapter Outline

Here I will be using Bayesian statistics to develop well-dated chronologies for radiocarbon dates generated from the Mukolo sediment core and Linyanti Baobab tree core. Bulk sediments and macroscopic contemporary charcoal organic (MCCO) components will be used to date the sediment core and new radiocarbon dates will be generated for the Baobab tree core from sampled material collected by Hamilton (2016). The chronologies created will provide temporally constrained timeline for fire history and historic rainfall of the Kavango-Zambezi region of Namibia.

2.3. Methods

2.3.1. *Field Sampling*

The Mukolo sediment core was collected from an oxbow lake off the Kwando river system (17.877598S 23.341643E) in October 2014 by L. Gillson and G. Humphreys. The sediment core of 85cm, was removed as a single continuous section using a hand-held Russian corer. The core was packaged and labelled before being transported to the Plant Conservation Unit (PCU) at the University of Cape Town.

The Linyanti Baobab tree core was collected by S. Woodborne in 2015 tissue using a 1.5m increment borer with a diameter of 12mm. The core was sampled continuously and analysed for stable carbon isotopes by Hamilton (2016).

2.3.2. *Lab Sampling*

The Mukolo sediment core was cut lengthwise to create two identical sections of the core, a sampling section and an un-sampled reference section. The soil texture limited the sampling resolution - sediment was non-cohesive, so as individual samples were removed from the core material collapse into the void created. In an effort to prevent sediment mixing between consecutive samples, five millimetres length from the sediment core was used to separate individual samples. Hence, the Mukolo sediment core samples were non-continuous and yielded a total of 84 one cubic centimetre samples. Two tablets of Lycopodium spores (batch number 3862) were added to each sample.

Sediment samples underwent standardized charcoal extraction procedures (Bennett and Willis 2001): 1) Hydrochloric Acid (7%) bath for 30 minutes (90°C) and rinsed to dissolve carbonates; 2) Sodium Hydroxide (10%) bath for 4 minutes (90°C) and rinsed repeatedly to remove humic acids; 3) sieved to separate the macroscopic and microscopic sediment components and rinsed repeatedly.

The macroscopic sediment components included macroscopic charcoal particles (>150µm), contemporary organic material - plant matter which was incorporated into the soil column at the time of sediment deposition; and coarse sedimentary grains.

The Microscopic sediment components include contemporary organic material, soil humin, charcoal particles (<150µm), pollen grains and the known quantity of Lycopodium spores (batch number 3862) that I added. The microscopic components were processed to remove silica and silicates - each sample was acidified with Hydrochloric Acid (7%) and then put in a 90°C Hydrofluoric Acid (>99.9%) bath for 60 minutes, colloidal silica and silicofluorides were removed with Hydrochloric Acid (7%) and rinsed. Cellulose was digested with Glaciated Acetic Acid; samples acetolyzed (acetic anhydride 90ml and concentrated sulfuric acid 10ml) for 2 minutes (90°C) and rehydrated with Glaciated Acetic Acid. Each sample was stained (with Safranin) and preserved (with Tert-Butyl Acid) before being mixed with Silicone Oil and prepared on glass slides for microscope counting.

2.3.3. Charcoal Counting

The macroscopic charcoal was manually counted from each sample under a Nikon SMZ1000 dissecting microscope at 10x magnification. The macroscopic charcoal particles were represented as the number of charcoal particles per 1cm³ of sediment sampled from the core.

The charcoal within the microscopic sediment component was quantified by Clark's Point-Count method (1982) under a HM-Lux compound microscope at 400x magnification. Microscopic charcoal was quantified by counting the number of charcoal pieces (Char) and Lycopodium spores which intersect the selected points on the reticule (nP). To ensure statistical significance, a minimum of 200 charcoal and/or

Lycopodium particles were observed for each sample (Bonny, 1972). This required multiple fields of view (FOV) to be observed for each microscope slide. The concentration of microscopic charcoal was calculated based on the number of Lycopodium spores observed (L_c) as a fraction of the total number of Lycopodium spores (L_a) within the volume of sediment (S_{vol}) sampled from the core (Bonny, 1972).

$$\text{Microscopic Charcoal Concentration} = \frac{(L_a/L_c) \times (FOV \times \frac{Char}{nP})}{S_{vol}}$$

2.3.4. Radiocarbon Dating the Mukolo Sediment

The Mukolo sediment core was radiocarbon dated using two components: macroscopic charcoal and contemporary organic matter (MCCO) and bulk sediments. Both components were pre-treated following the prescribed pre-treatment techniques of the Oxford Radiocarbon Accelerator Unit (ORAU) (Brock *et al.*, 2010).

The MCCO radiocarbon dates were generated from amalgamated macroscopic sediment material (>150 μ m) that was sampled, processed and counted from the Mukolo sediment core. These samples were selected at approximately 10-centimeter intervals, with a total of ten, collected from the length of the Mukolo core. Three consecutive samples (i.e. representing 3cm of core) were amalgamated into a single MCCO radiocarbon sample to acquire enough mass for Accelerator Mass Spectroscopy (AMS). The MCCO radiocarbon dating samples were acid washed in Hydrochloric Acid (1%) for 15 minutes (90°C), rinsed and dried overnight in preparation for radiocarbon dating, no further preparation was required due to prior exposure to Hydrochloric Acid and Sodium Hydroxide during the charcoal extraction process.

Eleven raw bulk sediment samples were selected at corresponding, or neighbouring depths if sediment was exhausted. I prepared the bulk sediment samples for radiocarbon dating using an Acid-Base-Acid pre-treatment: 1) Hydrochloric Acid (1%) bath for 30 minutes (90°C) and rinsed; 2) Sodium Hydroxide bath (1%) for 40 minutes and rinsed, 3) Hydrochloric Acid (1%) bath for 15 minutes (90°C) and rinsed repeatedly; 4) dried overnight in a 60 °C oven; and 5) homogenized with a pestle and mortar. The radiocarbon dating samples were prepared and measured at the iThemba LABS AMS facility.

Radiocarbon dates were calibrated within the BACON (version 2.3.9.1) package (Blaauw *et al.*, 2011) using the Southern Hemisphere calibration curve (Hogg *et al.*, 2013) and converted to percentage modern carbon using the CLAM (version 2.3.2) package (Blaauw, 2010) in R Studio. Radiocarbon dates yielded age date ranges within 1-sigma error and 2-sigma error. The radiocarbon age ranges of the bulk sediment and MCCO samples; and the Linyanti 1 radiocarbon age ranges; each with the associated high-confidence 1-sigma error ranges are presented below as Common Era (CE).

2.3.5. Radiocarbon Dating the Linyanti Tree Core

Four radiocarbon dates were used to constrain the Linyanti chronology by Hamilton (2016), one at each terminal end of the core and two more at equal intervals in-between. Further dating was necessary to reduce the large sample intervals between the initial radiocarbon dates, reduce error ranges, and increase the comparability with other proxies.

Eleven additional radiocarbon samples were selected at 10cm intervals through the length of the core. Radiocarbon samples were prepared by amalgamating consecutive aliquot samples (maximum of three) to acquire sufficient mass for AMS dating. The radiocarbon pre-treatment used was in accordance with the prescribed pre-treatment techniques of the Oxford Radiocarbon Accelerator Unit (ORAU) (Brock *et al.*, 2010) and in line with the dating methodology used for the previously generated radiocarbon dates from Hamilton (2016). The Linyanti baobab radiocarbon samples were combusted and graphitized on the iThemba LABS Accelerator Mass Spectroscopy preparation line before being measured on the AMS.

Addition of new radiocarbon dates led to reanalysis of the Linyanti reference section where I identified that the Linyanti Baobab core had passed the centre of the tree duplicating material on the other side and rendering the radiocarbon date at the deepest point of the core inappropriately young. The centre of the tree was then identified at sample 1330 with samples exceeding this point excluded from the study. Further dating was necessary to establish a new date for the centre of the tree as well as reduce the large sample intervals between initial radiocarbon dates, reduce error ranges, and increase comparability with other proxies.

2.3.6. Age-depth Modelling

The Bacon (Bayesian Accumulation) package (version 2.3.5 by Blaauw *et al.* 2019) was used to model age-depth relationships in RStudio (R Core Team 2018) using Bayesian statistics and Markov Chain Monte Carlo (MCMC) iterations to interpolate between radiocarbon dates. The BACON package requires the user to enter information about the proxy based on the sampling methodology and modelling outputs. The age-depth model parameters are the number of samples used to generate a segment of the age-depth model, average accumulation rate, sampling interval, number of samples within the core, radiocarbon calibration specifications. Age-depth model outputs are presented below with probabilistic curves for each calibrated radiocarbon date and modelled confidence intervals. A greyscale accumulation rate by depth ghost plot from Bacon was used to show the predicted sedimentation rates for the Mukolo core based on the age-depth model.

Age-depth models were adapted to the distribution of each dataset and tested for robustness using a measure of Markov Chain Monte Carlo (MCMC) convergence models. The Mukolo sediment age-depth model and the Linyanti baobab tree core were each tested for model convergence using the comparison of MCMC iterations across ten individual model runs (Blaauw *et al.* 2018) to generate the Gelman and Rubin Reduction (GRR) factors (Brooks and Gelman, 1998). The GRR factor is as an indicator of reproducibility of the age-model, the threshold is 1.05 with values closest to 1 considered best (Blaauw *et al.* 2018).

2.4. Results

2.4.1. Mukolo Sediment Core Age-Depth model

A total of 18 radiocarbon dates were produced from the Mukolo sediment core (Table 1.); the yield included 10 radiocarbon dates from the bulk sediments and 8 radiocarbon dates from the MCCO components. The radiocarbon samples from 5cm (MCCO), 15cm (MCCO), 30cm (MCCO) and 30cm (bulk) yielded too little carbon dioxide during sample combustion, thus provided no radiocarbon dates. The 0cm (MCCO), 1cm (bulk) and 16cm (bulk) samples yielded post-modern (1950) dates which

are shown by pMC values greater than 100. The MCCO and bulk sediments yielded contradictory radiocarbon dates for four (41, 51, 61 and 71cm) of the nine depths dated (Table 1). The radiocarbon dated sediment components show that samples from depths 0, 10, 20 and 84cm coincide, but the samples between 40 and 70cm deviate in the predicted ages with MCCO samples being older by more than 10 radiocarbon years.

The percentage of modern carbon within MCCO samples 1, 10 and 20 was greater than the Bulk sediment samples at the same depths, but by less than 5% deviation. Samples between 40 and 70cm had at least 8% less modern carbon than the Bulk sediments which coincides with the older radiocarbon ages. Dated material sampled at 80cm and 84cm depth had 1.6 % and 1.21% greater pMc respectively from the MCCO sample at 82cm, even though it was sampled between the bulk depths.

The calibrated radiocarbon dates from the MCCO samples estimate a surface age between 1956-1957AD or 2008-2011AD. The MCCO radiocarbon dates from depths greater than 60cm yield younger ages than the overlaying sediments; with the basal date of the Mukolo sediment core between 1229-1381AD (within 1-sigma error) at 83cm.

Table 1: Radiocarbon Dates from the Mukolo Sediment Core

Sample	Lab#	$\delta^{13}\text{C}$	pMC (pMC error)	Radiocarbon Date (+/-1sigma error)
Muko_0(mac)	IT-C-1376	-25.0	103.93 (0.8564)	*
Muko_10(mac)	IT-C-1378	-25.0	95.36 (0.93)	380 (78)
Muko_20(mac)	IT-C-1377	-25.0	91.77 (1.06)	690 (92)
Muko_40(mac)	IT-C-1372	-25.0	83.11 0.77	1490 (74)
Muko_50(mac)	IT-C-1371	-25.0	86.37 (0.98)	1180 (91)
Muko_60(mac)	IT-C-1375	-25.0	80.88 (1.12)	1710 (111)
Muko_72(mac)	IT-C-1374	-25.0	86.85 (0.86)	1130 (79)
Muko_1(bulk)	IT-C-1380	-24.7	109.68 (1.09)	*
Muko_10(bulk)	IT-C-1386	-23.6	94.97 (0.81)	410 (68)
Mukolo_16(bulk)	IT-C-1544	-23.2	119.90 (0.48)	*
Muko_20(bulk)	IT-C-1385	-22.9	91.57 (0.77)	710 (67)
Muko_40(bulk)	IT-C-1381	-23.2	99.38 (1.21)	50 (97)
Muko_50(bulk)	IT-C-1384	-23.3	93.12 (0.84)	570 (72)
Muko_61(bulk)	IT-C-1383	-21.9	94.07 (0.86)	490 (73)
Muko_70(bulk)	IT-C-1387	-22.8	94.70 (0.85)	440 (72)
Muko_80(bulk)	IT-C-1382	-22.6	92.82 (3.24)	600 (275)

*Post-bomb radiocarbon dates (after 1950) are reported in pMC with no Radiocarbon date according to Radiocarbon Reporting conventions.

The Bulk sediment samples estimate the surface age of the core between 1958-1959AD and 1997-2003AD (within 1-sigma error), with a reduced overall sediment accumulation rate in comparison to the MCCO radiocarbon dates (Figure 1.). The bulk sediment sample at 84cm depth estimates the basal date of the core between 1316-1355AD and 1328-1395AD (within 1-sigma error). The radiocarbon dates sampled from 16cm and 40cm depths deviate from the general trend of the bulk sediments, these two samples are dated much younger with the sample at 16cm yielding a post-bomb (1950) date.

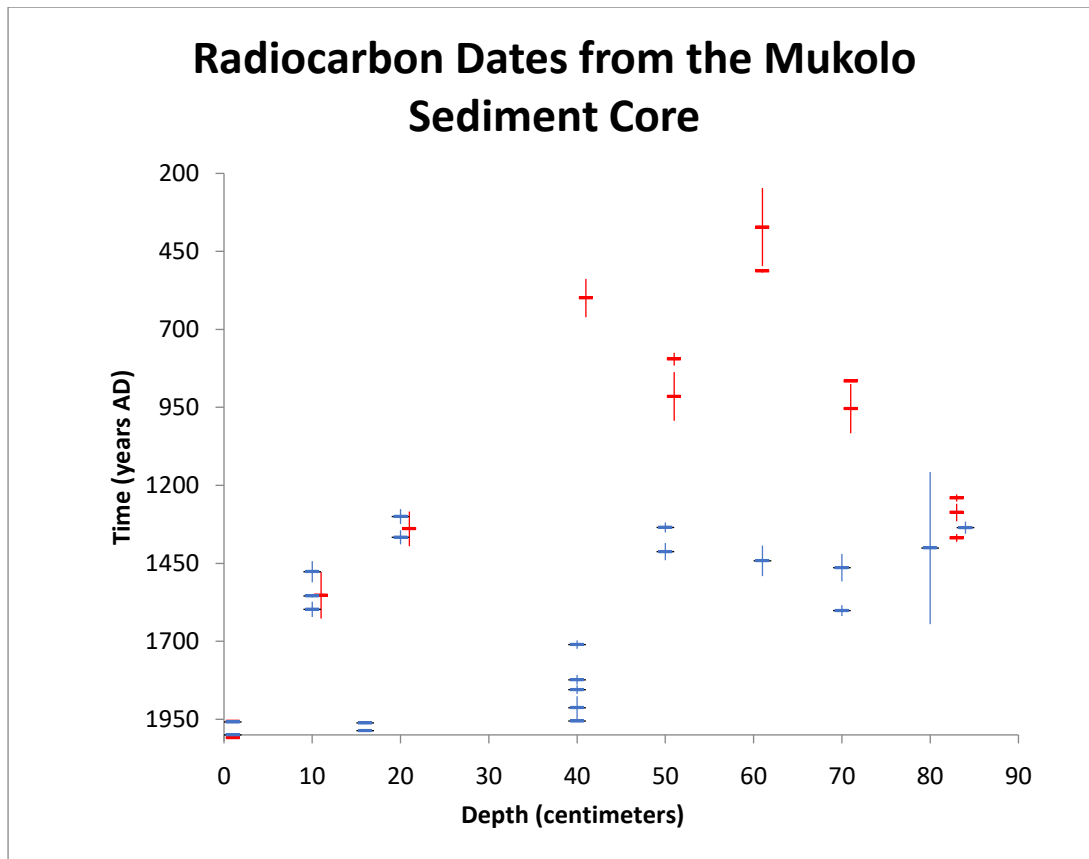


Figure 1. The radiocarbon dates generated from the macroscopic charcoal and contemporary organic material (MCCO) (red) and bulk sediment dates (blue) of the Mukolo sediment core. The calibrated age intercepts are represented by a horizontal bar, with vertical lines showing the range of error associated with each date (1-sigma error).

The Mukolo BACON age-depth model suggests a near-linear sediment accumulation rate based on 37620000 iterations of MCMC curves. The 95% confidence interval for the age-model is smallest at 0cm (204-148 years) and largest at 84cm depth (260 years). The 16cm and 20cm radiocarbon dates are disregarded by the model, neither of which intersect with the 95% confidence interval (Figure 2a.). The Mukolo age model represents the minimum ages of the sediment, transecting along the older error range for all the radiocarbon dates except 10cm and 50cm. The Mukolo age-depth model convergence, based on 10 individual model runs, yielded a GRR factor of 1.00073 which is safely below the threshold.

The sediment accumulation rates generated from the Mukolo age model show little fluctuation (Figure 2b), with slightly greater accumulation rates estimated around 16cm and 40cm, and a decreases accumulation rate at 60cm depth. The increased

sediment accumulation rates (16 and 40cm) are associated with less statistical certainty than the rest of the core at 95% confidence (Figure 2b). The final model indicates that the time resolution of each 1cm sample is approximately 7.5 [0, 16] years.

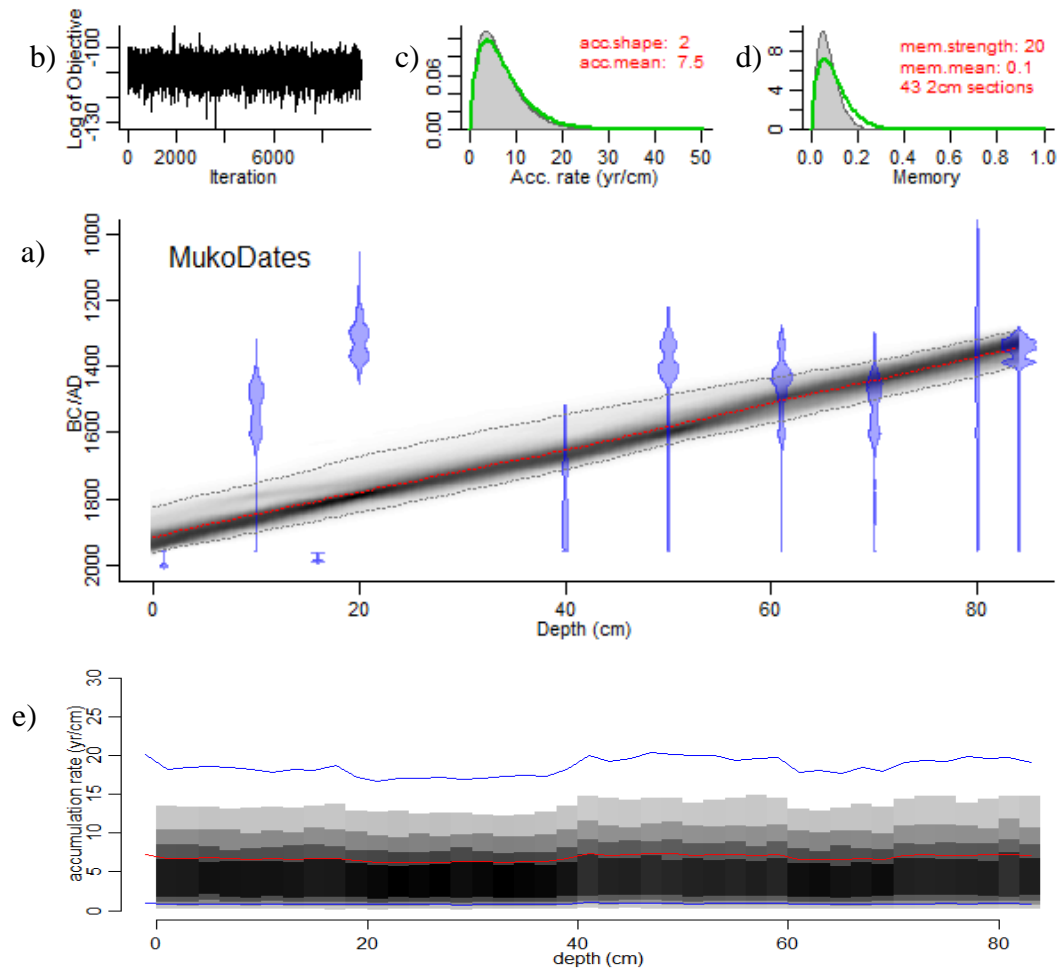


Figure 2. The Mukolo chronology (2a) is presented with age on the y-axis and depth of sampling on the x-axis. Bulk sediment calibrated radiocarbon dates are indicated as vertical bars with multiple intercepts and widths to indicate probability. BACON model MCMC iterations are displayed (2b) with the model fitted to the accumulation rate (2c) and influence on consecutive samples (2d). The predicted sediment accumulation rates are plotted (2e) with confidence intervals (blue) and the 7.5 years per cm average accumulation rate (red). Dark grey bars indicate higher levels of certainty.

2.4.2. Linyanti Rainfall Record Age-Depth model

The Linyanti Baobab tree core was radiocarbon dated using a total of twelve radiocarbon dates (Table 2), with two dates (sample number 648-649 and 750-760) which deviate from the overall trend. The youngest radiocarbon sample was taken from aliquot 49 where the radiocarbon date was negative indicating a post-modern (1950)

age. The radiocarbon samples taken between aliquot 200-505 show the widest range of radiocarbon error (Figure 3b), which span across a range of 285 years. The three radiocarbon samples between aliquots 800 and 1200 show well constrained date ranges, each with only two possible date ranges. The oldest part of the tree core (aliquot 1255) yields a single age range of 34.1 radiocarbon years at one sigma level of error.

Table 2: Radiocarbon Dates from the Linyanti Baobab Tree Core

Sample	Lab#	$\delta^{13}\text{C}$	pMC (pMC error)	Radiocarbon Date (+/-1sigma error)
49	IT-C-154	-24.3	107.87 (0.59)	*
220-229	IT-C-1063	-24.1	97.97 (0.52)	172.3 (42.4)
350-358	IT-C-1103	-34.8	98.45 (0.45)	127.3 (36.4)
496	IT-C-152	-24.8	99.01 (0.31)	98.94 (0.31)
505-506	IT-C-786	-24.6	97.61 (0.63)	197.5 (51.4)
648-649	IT-C-1830	-24.2	89.31 (0.48)	915 (42.9) *
743-749	IT-C-1108	-24.0	95.75 (0.42)	356.8 (35.2)
750-760	IT-C-859	-24.0	92.10 (0.46)	661.1 (40) *
850-858	IT-C-1104	-23.9	95.09 (0.46)	413.1 (38.8)
996-1003	IT-C-655	-24.4	94.94 (0.60)	421.8 (50.3)
1070-1075	IT-C-1106	-24.2	94.84 (0.39)	432.8 (50.3)
1250-1260	IT-C-855	-23.1	93.40 (0.40)	548.5 (34.1)

* Post-bomb radiocarbon dates (after 1950) are reported in pMC with no Radiocarbon date according to Radiocarbon Reporting conventions.

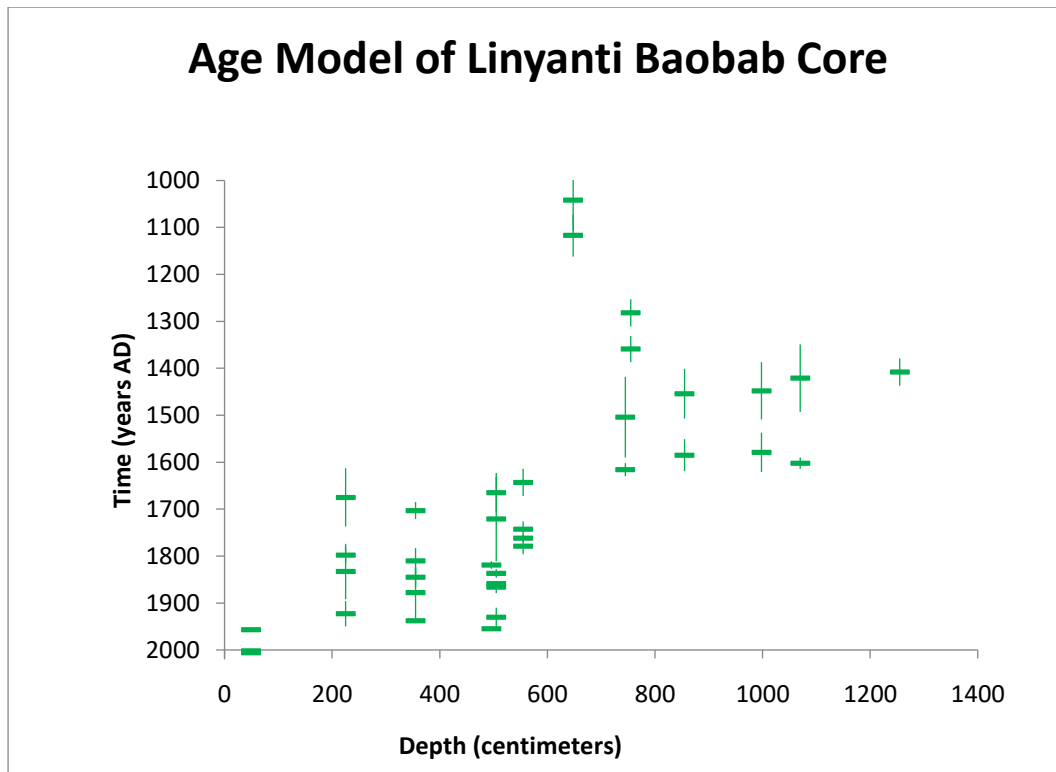


Figure 3. The radiocarbon dates generated for the Linyanti rainfall record are plotted by depth (green). The horizontal bars indicate the calibrated date, with vertical lines showing the error range associated with each date (1-sigma error).

The Linyanti age-depth model was generated using twelve radiocarbon dates sampled from different intervals of the tree core. The model predicts an almost linear accumulation of tree tissue for the length of the core (Figure 4a.), which intersects with nine of the twelve radiocarbon dates at the one-sigma error region of higher probability. There are two radiocarbon dates (sample 648-649 and 750-760) excluded by the model, and outside the 95% confidence interval (Figure 4a.). The 95% confidence interval for the age-model is smallest at aliquot 100 (83 years) and largest at aliquot 1200cm (100 years), with 91% of radiocarbon dates overlapping with the confidence interval.

The Linyanti age-depth model was tested for robustness by using a convergence model which combined ten individual age-depth model runs. A minimum of 143 000 000 MCMC iterations were used to generate a Gelman and Rubin Reduction factor of 1.01120, which is safely below the threshold. The resulting Linyanti age-depth model indicates a constant rate of proxy accumulation (Figure 4e). The average time resolution is 0.5 [0.5, 1.0] years per aliquot of wood sampled.

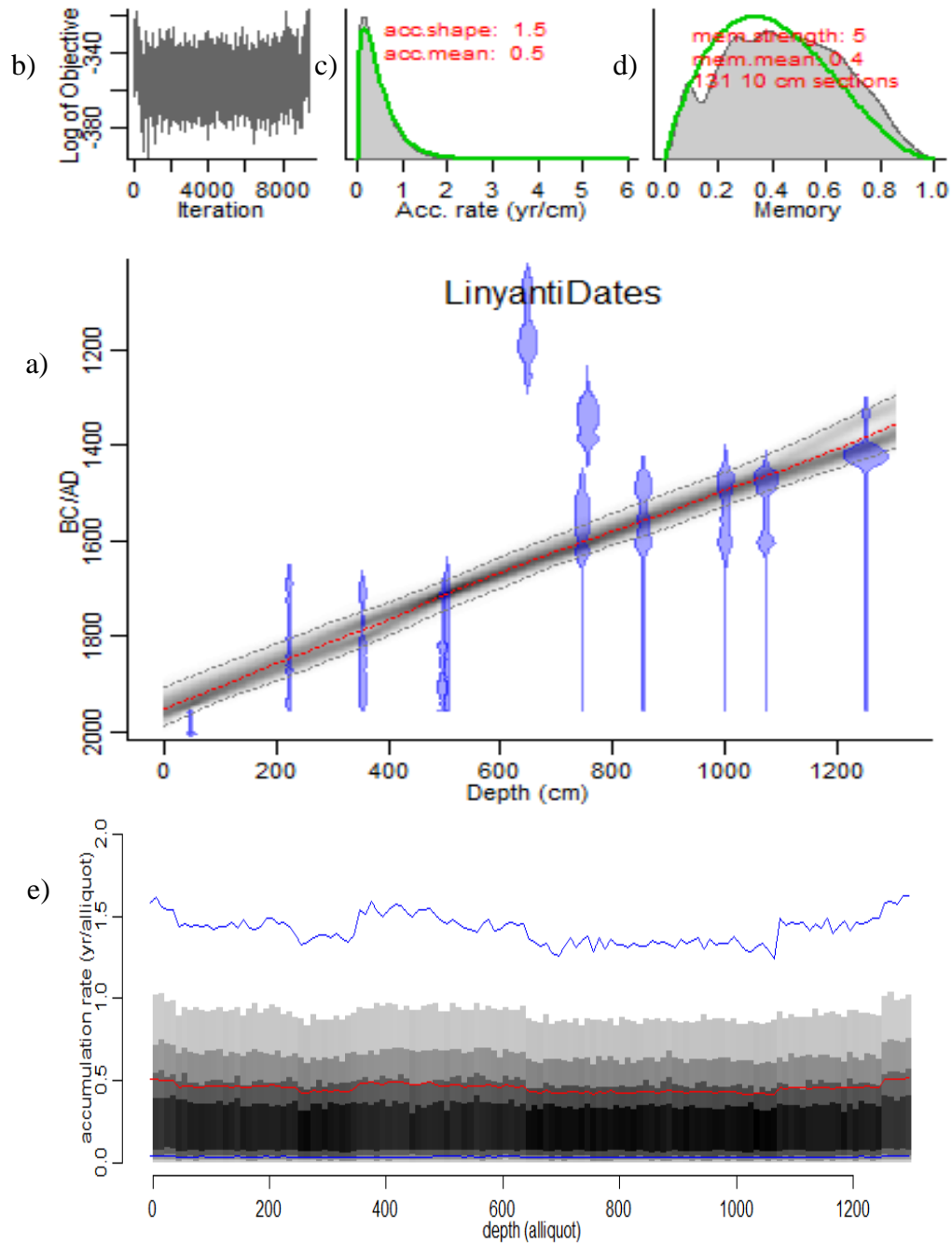


Figure 4. The BACON age-depth model for the Linyanti 1 baobab tree core is presented with date on the y-axis and depth of sampling on the x-axis. Calibrated radiocarbon dates are indicated as vertical bars (blue) with multiple intercepts and widths to indicate probability. Model MCMC iterations are displayed (4b) with the model fitted to the accumulation rate (4c) of sample material and the influence on consecutive samples (4d). The predicted Linyanti tissue accumulation rates are plotted (4e) with confidence intervals (blue) and the average accumulation rate of 0.5 years per aliquot (red). The dark grey colors are associated with higher levels of certainty.

2.5. Discussion

Using a relatively large number of radiocarbon dates from a sediment and tree core, I was able to produce statistically robust age-depth models to interpolate the sediment and tree cores. The charcoal samples are at a much coarser temporal resolution as opposed to the tree record (~7.5 years per cm in comparison with core samples which are sub-annual at ~0.5 years per mm). The interpretation of radiocarbon dates in the charcoal records showed some complexity with differences between bulk sediment and macroscopic organic material dated from the core which I will discuss below. The two environmental records overlap for a period of ~600 years, both going back to approximately 1300AD.

2.5.1. Chronology for the sedimentary sequence from Mukolo

The radiocarbon dates of both the bulk sediment and macroscopic contemporary charcoal and organic (MCCO) material suggest that the deepest part of the sediment core started accumulating at ~1300CE. The middle section of the sediment core presented a series of age discrepancies between the dated components with the MCCO samples being much older suggesting some disturbance which influenced the source of charcoal production within the landscape or accumulation within the sediment column. Potential sediment mixing by large mammals is expected within this site as the region is a renowned conservation area with large mammal populations.

The age discrepancy between the age of bulk sediments and MCCO samples highlights the importance of radiocarbon dating sample selection and the influence radiocarbon dates can have on proxy chronologies. The percentage of modern carbon within the MCCO samples confirms that the MCCO components are older than the bulk sediments for the middle section of the Mukolo core. The age difference between sampled material can be explained by the inbuilt age of woody material (Gavin, 2001) as the MCCO sample consistency was dominated by large charcoal particles and can be substantiated by the absence of contemporary material, such as pollen (Scott, 2002) and soil humin (Pessenda *et al.*, 2001) that were present in the bulk sediments. Hence the MCCO radiocarbon dates were excluded from age-depth modelling.

The MCCO and bulk sediments sampled from less than 20cm depth matched in age, thus the MCCO samples from the lowest depths were not influenced by the inbuilt-age but were possibly influenced by modern annual plant roots. These sub-surface dates

from the sediment core had convergent ages for both sampled components, showing that the sediment core terminated at ~1950.

2.5.2. *Changes in the Fire Regime over time based on the Microscopic and Macroscopic Charcoal Records*

Although the MCCO samples were ineffective for determining the sediment accumulation time, it does hold ecological value. The age difference between macroscopic organic material and bulk sediment dates suggest that much older wood was bunt and subsequently incorporated into the sediment column. The fact that the age difference between MCCO and bulk samples does not persist prior to 1400 or after 1800 suggests some change to the fire regime during this time which resulted in old trees being burnt.

This change in fire regime coincides with the Little Ice Age. A period well documented in the Northern hemisphere but sparsely identified in an African context. Environmental proxy records from southern Africa show reduced atmospheric temperatures between 1400 and 1800 (Sundqvist *et al.*, 2013; Tyson *et al.*, 2000) and a decline in rainfall from 1600 to 1800 (Woodborne *et al.*, 2016, 2015). This implies that variation in the amount of charcoal observed in the Mukolo sediment core could be a response to climate variability, but it is also possible that changing human activities, or changes in the ratio of tree to grass in the environment could have caused these differences.

2.5.3. *Linyanti Baobab Tree Core Chronology*

Radiocarbon dating of the Linyanti baobab tree core was used to revise the existing chronological sequence of the wood core. Rigorous radiocarbon dating facilitated a thorough understanding of the rate of growth for the individual Linyanti tree on par with studies by Patrut *et al.* (2019, 2013 and 2010). The chronology was used to interpolate the timeline for the 1230 $\delta^{13}\text{C}$ sub-samples collected by Hamilton (2016) where the chronology relied on a misleading radiocarbon date at the oldest section of the core.

The Linyanti age-depth model identified three radiocarbon dates as outliers from the model. Two radiocarbon dates overestimated the age of the middle section of the core by more than 100 years than the model predictions, lie far outside the model upper confidence intervals and deviates from the model at the region of greatest certainty. The remaining outlier underestimated the age of the sample with a minimum of 50 years deviation from a radiocarbon date sampled from neighbouring sample material and lies entirely outside the lower confidence interval. Removal of these outliers from the model made no impact to the age-depth model as the BACON package was able to exclude them from the age-depth model estimates. The presence of outlier radiocarbon dates can be attributed to contamination during sample combustion for which I was newly trained. These erroneous dates emphasize the importance of thorough dating of proxy records to prevent errors (Scott, 2007) in climate records.

2.5.4. Reliability of Mukolo and Linyanti Climate Records

The Mukolo core was dated with ten radiocarbon dates through a total length of 84cm and the Linyanti Baobab tree core was dated with eleven radiocarbon dates within a total length of 1250cm. The Mukolo age-depth model was able to exclude the clearly unrealistic dates because of the number of other samples available. If I had used three radiocarbon dates it would have been difficult to determine whether there was a large change in sediment accumulation rates over time for the Mukolo core. The same applies for the Linyanti tree core, although because there is less uncertainty about the way that this core accumulates - annual tree rings with limited potential for mixing and minimal risk of incorporation of older material into younger samples - it would probably have been sufficient to use fewer samples.

The age-depth models generated for each proxy are derived from multiple independent, discrete radiocarbon dates sampled through the length of each proxy. The number of radiocarbon dates used to model both cores exceeds the prescribed five dates per 1000years (Carleton *et al.*, 2018) and indicates that in semi-arid ecosystems such as the ones my proxies come from, fewer dates could easily be misinterpreted. The Bacon modelling package from Blaauw *et al.* (2018) reduced the subjectivity of model selection by generating multiple probabilistic MCMC runs to test potential accumulation models to allow for statistically defensible interpolation of proxy material

(Blaauw and Christen, 2011). Problems with age-depth model selection (Bennett and Fuller, 2002), interpreting radiocarbon dates with multiple calibration intercepts (Richard J Telford *et al.*, 2004), or outliers were avoided. The combination of thorough radiocarbon dating and objective interpolation of radiocarbon dates makes interpretations of the complex Mukolo sediment core and the Linyanti Baobab tree core possible for analysis and exploration of historic fire and rainfall.

2.6. Appendices

2.6.1. Appendix 1 – Summary of the Methods and Results of Hamilton (2016), the generation of the Linyanti 1 $\delta^{13}\text{C}$ record.

The Linyanti 1 Baobab tree core was collected by Dr Stephan Woodborne in 2015 with a 1.5m increment borer with a diameter of 12mm. The core was transported back to South Africa where it was air dried and sampled continuously. 1505 aliquots were collected, each was approximately 0.5-1mm taken from the top half of the core creating a longitudinal ‘witness’ section for reference. Each sample underwent two six-hour soxhlette treatments (an ethanol-toluene and an ethanol only) to remove soluble organic compounds; followed by a four-stage Alpha Cellulose Reduction process to remove resin as proposed by (Loader *et al.*, 1997) and weighed.

Stable Carbon Isotope analyses were performed at the Stable Isotope Laboratory of the University of Pretoria. Prepared samples were run intermittently with measured blanks from an in-house standard (*Shorea superba*) used to initiate each run and between every 12 samples (Woodborne *et al.*, 2015). A total of 104 batches were run to analyse the Linyanti 1 samples and blanks. Stable carbon isotope results were corrected for $\delta^{13}\text{C}$ based on correction values derived from (Farquhar *et al.*, 1989) to create the Linyanti 1 rainfall record.

The Linyanti 1 baobab core was radiocarbon dated at the iThemba LABS Accelerator Mass Spectroscopy (AMS) facility, Johannesburg. The core was radiocarbon dated with a total of four radiocarbon dates, one at each end and two evenly distributed in the length of the core. The radiocarbon dates were calibrated (Stuiver *et al.*, 2018) which provided an estimated maximum age of the core at 327years. However it is important to consider that the date from the deepest section of the core had in fact exceeded the centre of the tree (identified on re-examination in 2017 as part of MSc), thus provided a date describing a younger section of the tree core and not the centre (oldest part) of the tree.

The Linyanti 1 baobab tree core was presented as a high-resolution sub-annual rainfall record (Figure 1, top) and an annually averaged rainfall record (Figure 1, bottom).

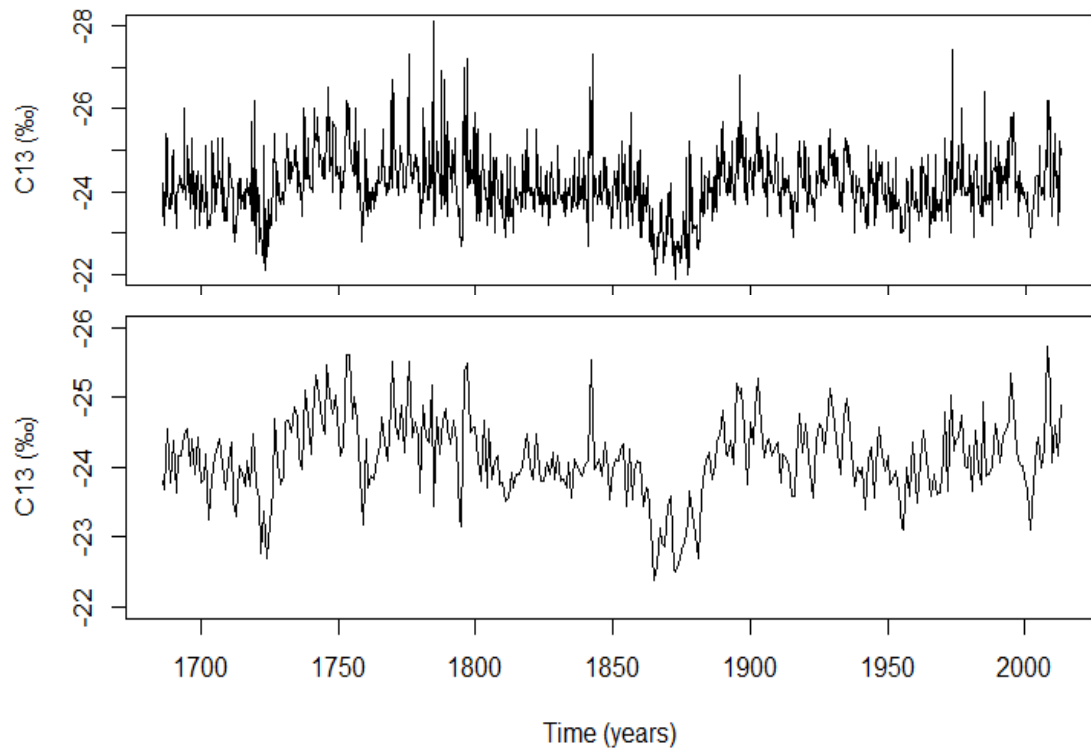


Figure 1. The sub-annual Linyanti rainfall record (top) and the annually averaged Linyanti rainfall record (bottom). The y-axis shows $\delta^{13}\text{C}$ values from stable carbon isotope analysis of a baobab core, more negative values indicate wetter conditions and less negative values indicate drier conditions. Note that the extreme drought occurring around 1860-1880CE is actually representative of the Little Ice Age of ~1700CE.

Chapter 3: Rainfall and Fire in the Kavango-Zambezi region

3.1. Introduction

Understanding environmental responses to past climate variability can improve our understanding of future environmental responses to climate change. In southern Africa climate change predictions forecast increased aridity and increased frequency of extreme events (Niang *et al.*, 2014). Environmental resilience refers to the ability of a landscape to provide the same functions after disturbance – for which savanna systems are renowned (Buisson *et al.*, 2019; Higgins *et al.*, 2007b; Walker and Noy-Meir, 1982).

Savannas depend on regular disturbances, such as fire, to maintain an open structure (Archibald and Hempson, 2016; Bond and Keeley, 2005; Govender *et al.*, 2006). The occurrence of fire in an ecosystem depends on rates of fuel accumulation, the dryness of this fuel, the occurrence of appropriate fire weather conditions and an ignition source (Bradstock, 2010). Rainfall strongly influences the state of the fuel within savannas and researchers find a unimodal relationship between rainfall and fire (Krawchuk and Moritz, 2011). At low rainfall, reduced biomass growth prevents fuel accumulation and limits the potential for fire to spread effectively within the landscape, and this is referred to as fuel-limited savannas. At higher rainfall, the biomass growth facilitates an abundance of fuel accumulation that does not cure sufficiently, and these are referred to as moisture-limited savannas because they are usually too wet to burn (Alvarado *et al.*, 2020; Archibald *et al.*, 2009; Lehmann *et al.*, 2011)(Figure 1). Between these extremes, biomass growth facilitates fuel accumulation which dries effectively during winter and provides a well cured fuel source with an increased probability of fire (Figure 1). Alvarado *et al.* (2020) find that in Africa at mean annual rainfall below 800mm ecosystems are generally fuel-limited and above 800mm they are more likely to be moisture-limited. The Kavango-Zambezi region therefore is expected currently to be a moisture limited system where rainfall is negatively correlated with fire (Krawchuk and Moritz, 2011), but it is possible that higher rainfall in the past might have altered this relationship over the last several centuries..

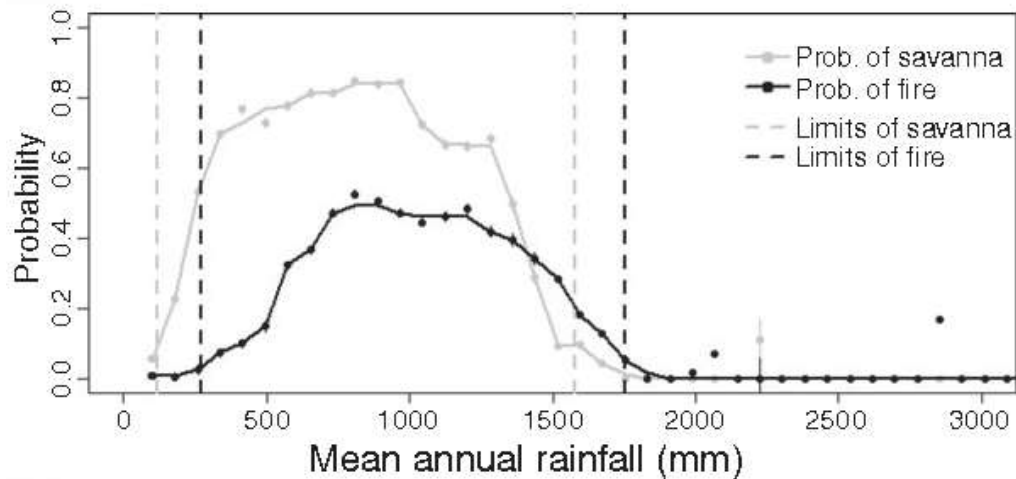


Figure 1. Graph showing the limits of fire within African savannas as found by (Lehmann *et al.*, 2011). The probability of fire is lower where rainfall is <1000mm and >1200mm which can be attributed to fuel-load limited (positive rainfall-fire correlation) and fuel-moisture limited (negative rainfall-fire correlation) savanna types respectively.

People have a strong influence on vegetation within African savannas, and are considered to diffuse the rainfall-fire relationship through reducing fuel with grazing, and burning at larger range of seasons thus preventing large, climate-driven wildfire events (Archibald *et al.*, 2010). Factors affecting burnt area were ranked in southern Africa with grazing livestock the highest human impact accounting for >35%, followed by human population size accounting for ~30% (Archibald *et al.*, 2009). Furthermore, human activities affect the landscape continuity and increase the number of ignitions within the landscape (Archibald, 2016) with effects on the timing, intensity and size of fires, also known as the fire regime (Bond and Keeley, 2005).

With climate change effects observable in daily weather (Sippel *et al.*, 2020), knowing past environmental responses to climate could help with knowing what to expect for the future and planning accordingly to reduce the impacts on agriculture, human health and society (Serdeczny *et al.*, 2016). Most global analyses assume that more frequent droughts will increase fire frequency and intensity (Meyn *et al.*, 2010). However, in semi-arid savannas it is possible that droughts will reduce the area burned and fire intensity by reducing the fuel load (Figure 1). Having a long-term perspective on this important, unresolved issues will be helpful for understanding responses of semi-arid savannas to climate change.

3.1.1. *Climate Proxies for Understanding the Past*

Recently there has been much focus on the development of historic climate records, most of which span long time scales from centuries to millennia (February, 2000; Scott, 2002; Whitlock and Larsen, 2002). Climate proxies are indirect measures of environmental factors which are used to understand past changes based on the accumulation of material in a regular or predictable way that is interpreted in terms of the contemporary environment. The crucial aspect for climate proxies is that they must be responsive and sensitive to capture incremental environmental changes such as the amount of ash deposited in sediments or physio-chemical changes in response to water availability in trees. By capturing small environmental changes over time climate proxies can inform about long-term trends and, depending on the sensitivity of the proxy, capture events on shorter-term scales. Changes observed in climate proxies can have immediate and prolonged effects on the environment (Colin Prentice, 1986) which vary within the landscape at different spatial scales (Bond *et al.*, 2005).

To overcome data scarcity in southern Africa multiple proxies are often used in conjunction to compare environmental signals (Scott 2002; Tyson *et al.* 2002; Hall 2010), fill hiatuses (Duffin 2008) or extend the temporal coverage further than that of a single record (Woodborne *et al.* 2015). But most long-term environmental records are incompatible with modern instrumental data due to relatively short instrumental records. The discontinuity between proxy and modern observational data describes a gap in temporal understanding where the short-term responses interface with long-term trends associated with climate. The historical data are key to understanding landscape responses to climate change and reducing uncertainty around topics such as bush-encroachment and drought responses in arid regions.

3.1.2. *Forcing at different time scales (event vs regime)*

When we interpret environmental records, there are two components driven by the same conditions, but operating on different timescales. The term “event” in the climate record refers to a deviation from the normal trend, the change can be interpreted as a disturbance in the form of amplitude, frequency or rate. Rainfall events can describe periods of above or below average precipitation, while fire events can indicate periods of increased fire activity or absence.

- The high frequency component of a climate record is driven by events, and is described by high variability over short-durations with a limited spatial expanse; often referred to as *weather* in this case. Historic weather data, such as rainfall records, are limited in southern Africa, the longest records reaching as far back as the colonial period (Nicholson *et al.*, 2018) and are often interrupted.
- The low frequency component, is the sum of high frequency events over a long period of time and is often described as the long-term trend or *climate*. Climate is dependent on large temporal- and spatial-scale drivers such as upper atmospheric circulation which facilitates planetary-level responses to solar radiation, volcanism and temperature. The impacts of which are detectable across the world and across a range of proxy materials (Brönnimann, 2016).

3.1.3. Forcing at different spatial scales (local vs regional)

The spatial aspect of environmental records varies according to the proxy used and the scale of the drivers associated with the accumulation of that proxy. Sedimentary charcoal records focus on two size-classes: macroscopic charcoal refers to larger particles with greater mass, often being transported short distances (Duffin *et al.*, 2008; Ekblom and Gillson, 2010; Oris *et al.*, 2014; Peters and Higuera, 2007; Scott, 2010); and microscopic charcoal particles which are smaller and can be carried greater distances from the source in convective air currents above fires or strong winds (Higuera *et al.*, 2007; Oris *et al.*, 2014; Scott, 2002; Tinner and Hu, 2003). Sedimentary charcoal source models have been developed to estimate particle dispersion, such as Oris *et al.* (2014), but these models are based on forest systems where fire intensity is greater (mean 4858 kW m⁻¹ and 6047 kW m⁻¹ observed by de Groot *et al.* (2013)) compared to savanna fires (mean 38 kWm⁻¹ to 2664 kW m⁻¹ observed by Govender *et al.* (2006)). This suggests that the microscopic charcoal dispersion limits from savannas could be less than the 32km observed by Oris *et al.* (2014) and has been attributed to a maximum distance of 15km by Duffin *et al.* (2008) under medium intensity fires in a South African savanna.

3.1.4. Age precision and Proxy Comparison

The taphonomic process involved with each proxy is different and requires individual sampling and dating (Gillson, 2015), but there will always be errors and temporal offsets derived from taphonomy and instrumental errors as noted by Scott (2002) and observed in Hamilton (2016). Therefore, even when there is a strong causal link between two environmental variables, proxies with poorly resolved chronologies can be misleading and result in mismatching of events yielding poor relationships and lack of correlation. This uncertainty becomes more problematic when working on sediments with high temporal resolution/short time periods. On geological timescales where radiocarbon dates span millennia age-depth modelling can provide adequate temporal constraint to detect large changes in the environment but at shorter timescales, where calibration plateaus span decades, interpretations around multiple intercepts from radiocarbon calibration make age-depth modelling a complex issue (Guilderson *et al.*, 2005) (Refer to Chapter 2 for more information).

Moreover, traditional analytical methods for sedimentary charcoal make use of smoothing windows (Duffin *et al.*, 2008) to separate peaks of local events from ‘noise’ attributed to the background climate signal. However this decomposition of the charcoal from background noise requires the application of a locally defined threshold (Higuera *et al.*, 2011; Peters and Higuera, 2007), which, in the case of tropical grasslands and savanna ecosystems is not always well understood or defined.

However, there are alternative analytical methods for comparing proxies that put less emphasis on the chronology, and do not require user-defined thresholds. Wavelet analyses converts the timeseries data to frequency-space and uses a range of wavelengths to identify trends on different timescales (Roesch and Schmidbauer, 2018). The timescale to which a wavelet length is compared is referred to as a period - i.e. larger wavelengths for longer timescales and shorter wavelengths for shorter timescales. At larger wavelengths, the terminal ends of the timeseries can be exceeded, this is referred to as the cone of influence and is associated with uncertainty (Roesch and Schmidbauer, 2018). Hence the cone of influence marks the extent of statistically defensible wavelet analysis within the timeseries. These wavelet analyses can identify trends within different timescales, or periodicity within a single timeseries (Hall *et al.*,

2009; Labat *et al.*, 2004) as well as comparisons between timeseries (Prokoph and El Bilali, 2008; Torrence and Compo, 1998).

3.2. Aims and Objectives of this Chapter

I will be using chronologies prepared in Chapter 2, and wavelet analytical techniques, to investigate the trends within each climate proxy as well as the relationship between rainfall and fire at local and regional scales. Based on current-day understanding of relationships between fire, vegetation, climate, and human activities it is expected that:

- a) An overall positive relationship between the rainfall proxy and the charcoal proxy – both at local and regional scales.
- b) That the influence of humans on the fire-rainfall relationship is identifiable through deviations from the above expected fire response to rainfall, and should be associated with known information of the type and amount of human activity in the region.
- c) That the effect of human activity is clearer in the macro-charcoal record than the micro-charcoal record, as the regional record should be integrated across a range of different human land uses, whereas the local record might more clearly reflect changes in local grazing/cultivation/wood harvesting and fire management.

3.3. Methods

3.3.1. *Scaling Mukolo and Linyanti Records*

The Mukolo and Linyanti environmental proxies were sampled and radiocarbon dated to generate age-depth models to interpolate between dated samples (Refer to Chapter 2). The different proxy material of the Linyanti and Mukolo core had different resolutions related to sampling limitations and taphonomy. To compare the proxy records in the frequency domain, they needed to have matching points in time, thus the higher resolution Linyanti record needed to be sampled at intervals equal to that of the Mukolo sampling resolution. Hence the Linyanti record was sub-sampled by averaging

the $\delta^{13}\text{C}$ values for the year that matched the Mukolo sample depths to create the Linyanti “stepped” timeseries.

The Linyanti stepped timeseries resolution equates to 8.0 years per sample. The Linyanti stepped timeseries was compared against the Mukolo fire records (microscopic and macroscopic charcoal) over time using a linear regression.

3.3.2. *Morlet Wavelet Analysis*

Timeseries were transformed to the frequency domain using the WaveletComp package (Roesch and Schmidbauer, 2018) in RStudio (R Core Team, 2019). A Wavelet Coherency model (Appendix 1 and 2) was used to evaluate the trends within each environmental record, with each model simulated 1000 times at 95% level of significance.

To compare between two timeseries a Cross-Wavelet Analysis Model was generated for each pair of records: macroscopic & microscopic charcoal, Linyanti rainfall & macroscopic charcoal and Linyanti rainfall & microscopic charcoal. Timeseries were compared within the model and identified by coinciding frequencies in time, or when the timeseries showed changes at the same time. The phase, or lag of timeseries is indicated by arrows within the Cross-Wavelet Analysis Models. Arrows pointing to the right represent in-phase responses of the timeseries, or a positive correlation; while arrows pointing left represent anti-phase responses with a negative correlation. Arrows pointing upwards or downwards indicate a lagged response between the timeseries.

The Wavelet Coherency and Cross-Wavelet Analysis Models require comparison of the timeseries data against a surrogate timeseries, a white noise surrogate was selected (method $z = \text{"white.noise"}$) to simulate a null-hypothesis that the Mukolo and Linyanti timeseries are random. The WaveletComp analysis performs user-defined levels of detrending for which I selected none (loess.span = 0). Time resolution was allocated within the wavelet analysis by the average time interval between each sample ($dt = 7.694117647$) and the period resolution was set to represent number of years on the y-axis ($dj = 0.1299694$). Boxcar smoothing was used for both time and period ($window.type.t = 3$, $window.type.s = 3$), the smoothing window was defined as the

default of five years in both time and frequency directions ($\text{window.size.t} = 5 \cdot 1/\text{dt}$, $\text{window.size.s} = 5 \cdot 1/\text{dj}$).

3.4. Results

3.4.1. Mukolo Fire Record

The Mukolo charcoal record spans 708 years from 1288 to 1996. The record includes a regional (microscopic charcoal) and local (macroscopic charcoal) fire history, both of which are highly variable, but show similar overall trends. It is not clear from charcoal concentrations (Figure 2) whether the two different charcoal records are correlated over any of the proxy record.

The local fire history is associated with the macroscopic charcoal component (Figure 2) and is highly variable (ranges between 11 and 1298 charcoal particles per cm^3). The average is 376 particles per sample which yields an average macroscopic charcoal accumulation of 49 particles per year. The local fire record is characterised by reoccurring spikes throughout the record and several notable low periods, the most extreme occurring around 1924. The linear regression shows a highly significant correlation which accounts for ~12% ($R^2 = 0.1285$, $p = 0.0007$) of the variation and indicates that time is a poor predictor of macroscopic charcoal accumulation.

The regional-scale fire activity, represented by microscopic charcoal component (Figure 2) is even more variable than the macroscopic charcoal with a charcoal concentration range of $0.066 \text{ cm}^2/\text{cm}^3$ to $30.338 \text{ cm}^2/\text{cm}^3$. The average concentration per sample is $2.935 \text{ cm}^2/\text{cm}^3$, which equates to an average annual microscopic charcoal accumulation of $0.382 \text{ cm}^2/\text{year}$. There are a series of major peaks prior to 1400, at ~1700 and ~1900 which show rapid increases in charcoal accumulation and sudden, rapid declines. These peaks show a sudden increase in charcoal concentration within a single sample, which then goes back to background levels (Figure 2). The linear regression shows that time accounts for almost none of the variation observed in the microscopic charcoal record ($R^2 = 0.009$, $p = 0.9212$).

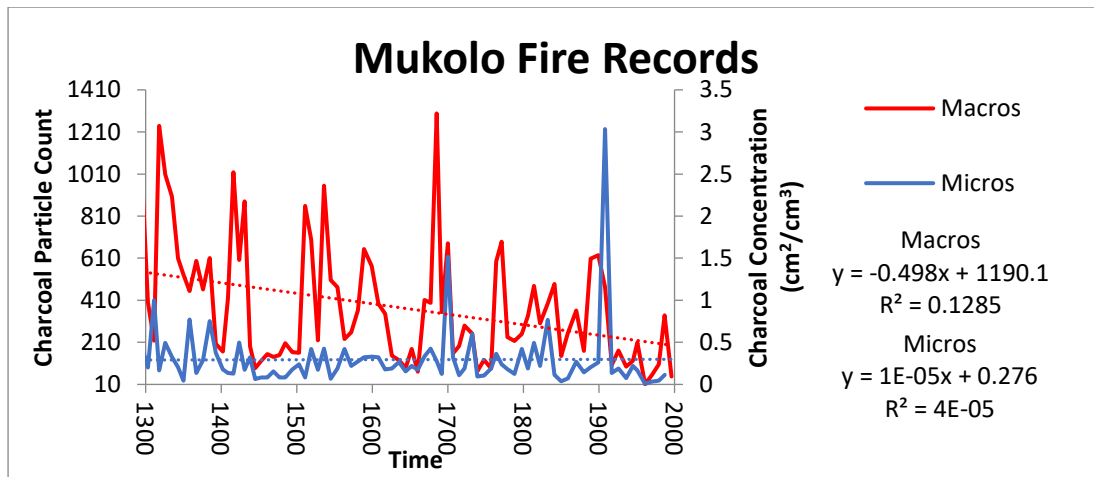


Figure 2. The Mukolo fire record, indication of fire activity is shown as concentration of charcoal within sediment samples through time. The macroscopic charcoal (red) is associated with local fire activity and the Microscopic charcoal (blue) is indicative of larger-scale regional fire activity. Trendlines (dashed lines) for each fire record show the linear regression of charcoal concentration over time.

3.4.2. Linyanti Rainfall Record

The Linyanti age-depth model was used to assign ages to the sample depths from Linyanti stable isotopic values from Hamilton (2016), the result is the Linyanti Rainfall record (Figure 3) which includes a total of 1230 samples from a timespan of around 1307CE to 1947CE.

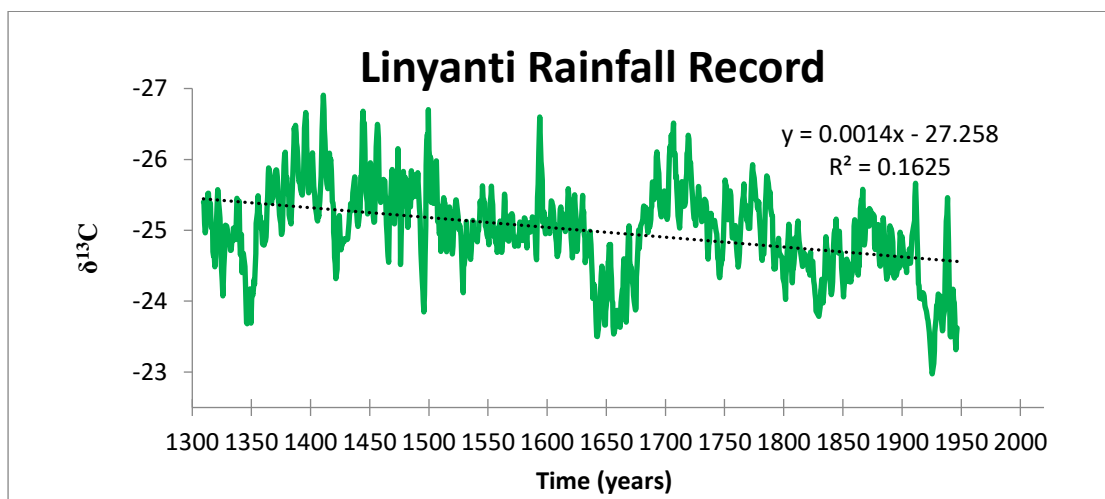


Figure 3. The high frequency Linyanti rainfall record (green) generated from stable carbon isotopic analysis from Hamilton (2016) is plotted using the BACON age-depth model generated from thirteen radiocarbon dates. More negative $\delta^{13}C$ values (towards the top of the y axis) are associated with wet conditions and less negative $\delta^{13}C$ values indicate water-stressed conditions.

The Linyanti rainfall record shows highly variable rainfall over the past ~640 years, with extreme events which persist for decades. For example there is an extended period of below average rainfall in the mid 1600's and again from 1900CE onwards. From this record it appears that the current rainfall in the Caprivi region is lower than it has been over much of the last ~600 years.

3.4.3. *Wavelet Analyses of Environmental Records*

Wavelet analysis of the Mukolo Fire record and Linyanti Rainfall record spanned ~640 years from around 1307CE to 1947CE, where the two records overlapped. The wavelet analyses show that all the environmental records undergo variability in time with periodicity observed across all the periods within each record.

The macroscopic charcoal power spectrum initially shows predictable trend of strong event pulses at 16 to 32-year periods, but this trend stops after 1750CE when there is an absence of frequency correspondence (Figure 4a). There are three isolated periods where strong trends occur: at 16-32 years with three out of four strong ~50 year-long events being statistically significant ($p=0.05$); at ~50years with two strong events of approximately 100 years duration; and at 64 to 100-years with periodicity which persists throughout the record.

The microscopic charcoal (Figure 4b) shows two strong event pulses prior to 1400 which occur in almost complete succession between the 15- and 32-year periods. There is a weak fire trend from around 1400CE to 1550CE, followed by two statistically significant events around 1700CE and 1900CE which persist into higher periods. The first event at around 1700CE occurs across the 10 to 32-year periods and lasts approximately 50 years, with the second event persisting further across the periods into the 100-year period and lasting approximately 100 years.

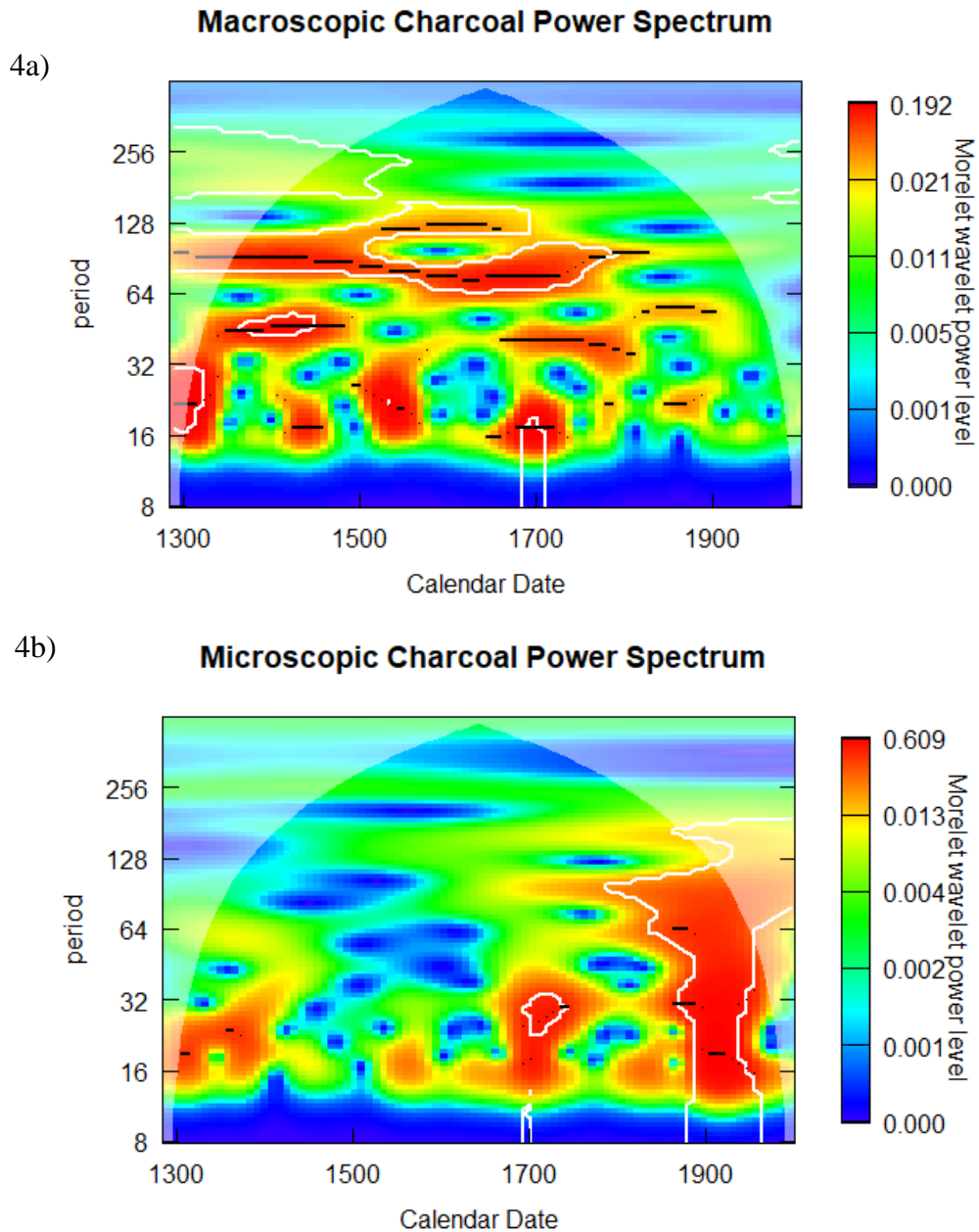


Figure 4. Wavelet Power spectra for Macroscopic Charcoal (a) and Microscopic Charcoal (b) showing the response of each proxy at different temporal scales. The macroscopic and microscopic charcoal, although from the same sediment samples, have very different spectra, and together the two spectra indicate a switch from local to regional drivers of fire at 1700CE (Figure 4a and 4b). Regions with a strong trend are shown in red with white lines encircling regions associated with statistical significance ($\alpha=0.05$).

The Linyanti rainfall wavelet analysis shows at least four events of corresponding timeseries frequency at low (16-32 year) periods (Figure 5) Events of strong wavelet correspondence are restricted to periods greater than 64-years, but are

always statistically significant. Events in higher periods (> 64 years) identified after 1900CE are not considered significant due to exclusion by the cone of influence.

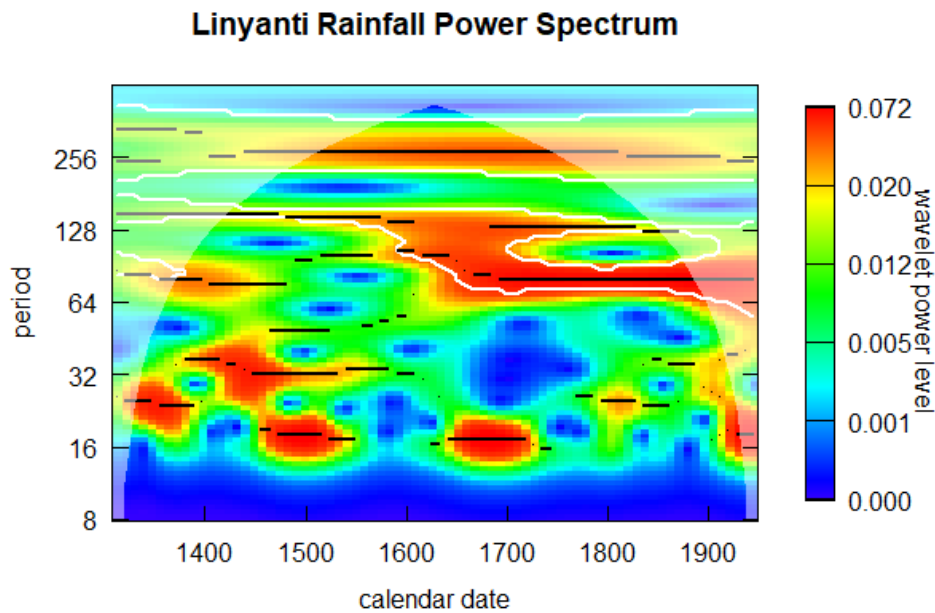


Figure 5. Wavelet Power spectrum for the Linyanti rainfall record, it shows a high degree of long-term periodicity. Regions with a strong trend are shown in red with white lines encircling regions associated with statistical significance ($\alpha = 0.05$).

The cross-wavelet analysis of the macroscopic and microscopic charcoal (Figure 6) compares the sedimentary charcoal components collected from the same sample and separated during preparation. The two large sedimentary charcoal spikes at ~ 1700 and ~ 1900 visible in the Sedimentary charcoal record in Figure 3 are also clear in the correspondence analysis. The event at ~ 1700 was replicated in both individual power spectra (Figure 4a and 4b), the phase arrows of this event show that macroscopic charcoal is leading (with microscopic charcoal lagging). The event at ~ 1900 was at a longer period (64 years) and, although it is not apparent in the individual macroscopic charcoal spectrum (Figure 4a) the phase arrows show that the two charcoal records are in phase. The event of strong corresponding frequency pre-1300 suggests an anti-phase relationship between the charcoal components, but is disregarded due to the cone of influence. The lack of frequency corresponding events between 1350CE and 1700CE corresponds with the lack of significant events in the microscopic charcoal power

spectra, however the mild event at 1550CE matches with a strong event in the macroscopic charcoal and a weak event within the microscopic charcoal record.

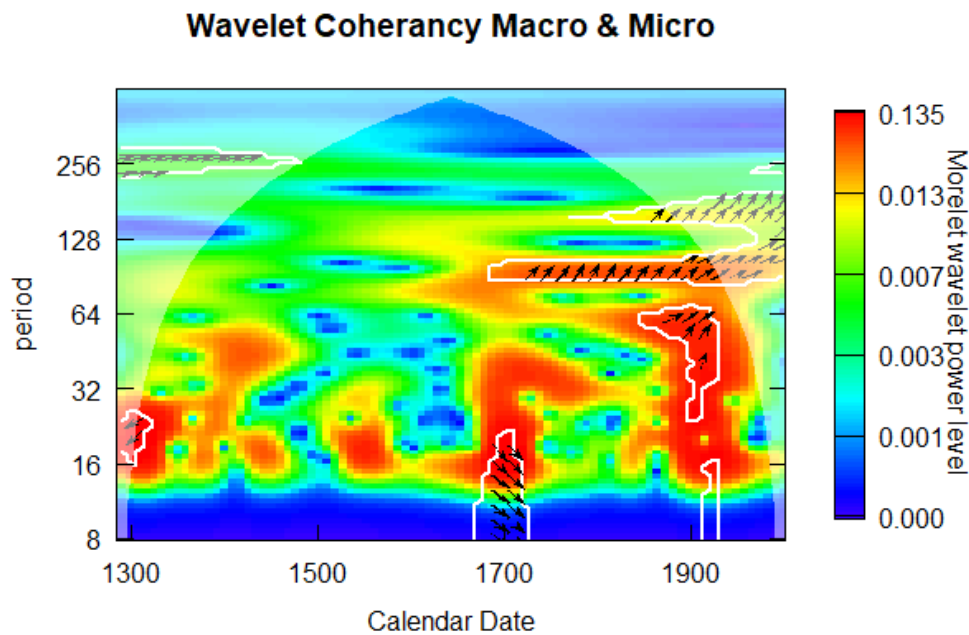


Figure 6. Cross Wavelet Transform of the macroscopic and microscopic charcoal from the Mukolo sediment core. Regions highlighted in red show strong correlation between the two timeseries, the white lines indicate statistical significance ($\alpha = 95\%$). The South-East to North-East direction change of the arrows within the significant events indicate a shift from macroscopic charcoal leading to lagging. This plot shows that although there are points in time when the two timeseries show corresponding signals, they are overall different records.

The cross-wavelet analysis model comparing the macroscopic charcoal and Linyanti rainfall (Figure 7) shows limited correlation at shorter periods. However, there is a strong indication that after the multi-decadal drought in the 1600s the increasing rainfall correlated with increasing macro-charcoal abundance, both at longer periods (64-128), and also in terms of time-step to time-step variability (16 years). There is also a correlated event in ~1420 with a 45-year periodicity, also associated with the end of a drought in the rainfall record. The strongest point of correlation between the macroscopic charcoal and Linyanti rainfall is at >64-year periods throughout the record.

Wavelet Coherency Macros & Lin

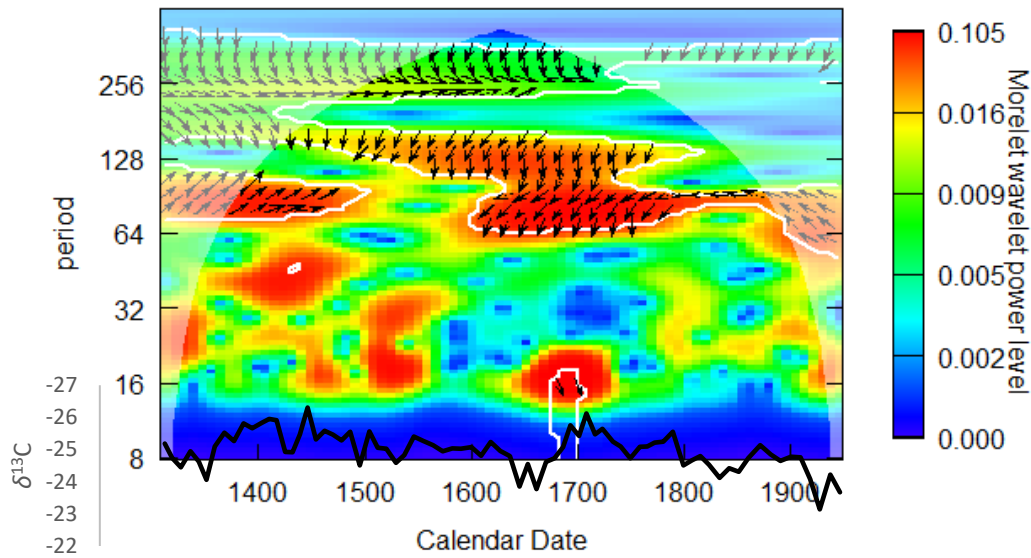


Figure 7. Cross Wavelet Analysis of Linyanti rainfall and macroscopic charcoal. Regions highlighted in red show strong frequency correlation between the two timeseries, while regions marked in blue show no correlation. White lines indicate statistical significance ($\alpha = 95\%$). The black line graph overlay shows the Linyanti rainfall record (more negative $\delta^{13}C$ values indicate drier conditions and less negative values indicate wetter conditions).

The cross-wavelet comparison model for Microscopic charcoal and Linyanti rainfall (Figure 8) shows a very different relationship with all the statistically significant frequency coherency located in the more recent part of the record. There is a lack of frequency coherency prior to 1700CE, except for two low period, strongly correlated events at 1400CE-1450CE and 1580CE-1600CE. After ~1700 there is a highly correlated event which spans 16 to 32-year periods. The largest event is that of around 1930CE which persists from the low periods up to 128-year period and is statistically significant ($\alpha = 95\%$) almost throughout. In contrast, the non-coherent events occurring at ~1500 and between 1650CE and 1700CE persists across all the lower periods and terminates at approximately 90-year period.

Wavelet Coherency of Micros & Lin

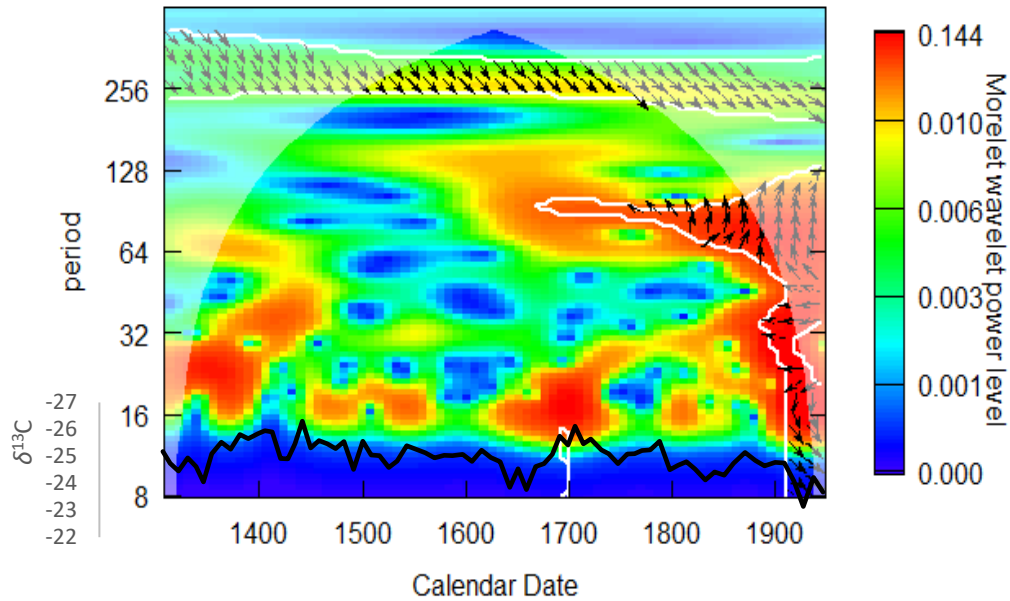


Figure 8. Cross Wavelet comparison of Linyanti rainfall and Microscopic charcoal. Regions highlighted in red show strong correlation between the two timeseries, while the white lines indicate statistical significance ($\alpha = 95\%$). The arrows pointing left indicate that the timeseries are in anti-phase with a negative relationship. The black line graph overlay shows the Linyanti rainfall record (more negative $\delta^{13}\text{C}$ values indicate drier conditions and less negative values indicate wetter conditions).

3.5. Discussion

The time-series presented here provide unique insight into patterns of rainfall and fire over ~600 years in an important region of southern Africa. Independently, and combined, they can be used to quantify past variability and help interpret environmental change in the region which can be tested against other environmental proxies.

3.5.1. The Linyanti Rainfall Record

The Linyanti record shows high variability at all temporal scales – interannual, decadal and centennial. This variability is expected in a semi-arid savanna and aligns with patterns found in other tree ring cores (Woodborne *et al.*, 2016, 2015), coral proxies (Zinke *et al.*, 2014) (Figure 9) as well as instrumental records (Nicholson *et al.*, 2018). Overall there was a decreasing rainfall trend which was replicated in the fire

record over the time period, but this was largely driven by a large drop in $\delta^{13}\text{C}$ values in the last 50 years of the record. If these 50 years are excluded then there is no trend in rainfall, but large oscillations around the mean. The reduced rainfall at the beginning of the century is not surprising, as other climate proxies also show a low-rainfall period over this time.

The Linyanti rainfall record shows a strong link to trends in the Agulhas current, global sea surface temperatures and coral proxy records off the West coast of Madagascar (Zinke *et al.*, 2014) (Figure 9). From ~1750 to ~1920 the climate proxies show strong cohesion, however there is a major sustained deviation at 1670-1740CE where the Kavango-Zambezi region receives increased rainfall in comparison with what the SSTs and Coral proxies predict. This deviation occurs over the period where maximum cooling was observed in the Makapansgat stalagmite record in South Africa (Tyson *et al.*, 2000) and could be explained by prolonged south-east Atlantic warm events within the tropics that delivers moisture inland (Rouault *et al.*, 2003). A stronger South-Indian monsoon during the Little Ice Age (Hong *et al.*, 2005), attributed to warmer equatorial sea surface temperatures, could have facilitated increased rainfall in the region.

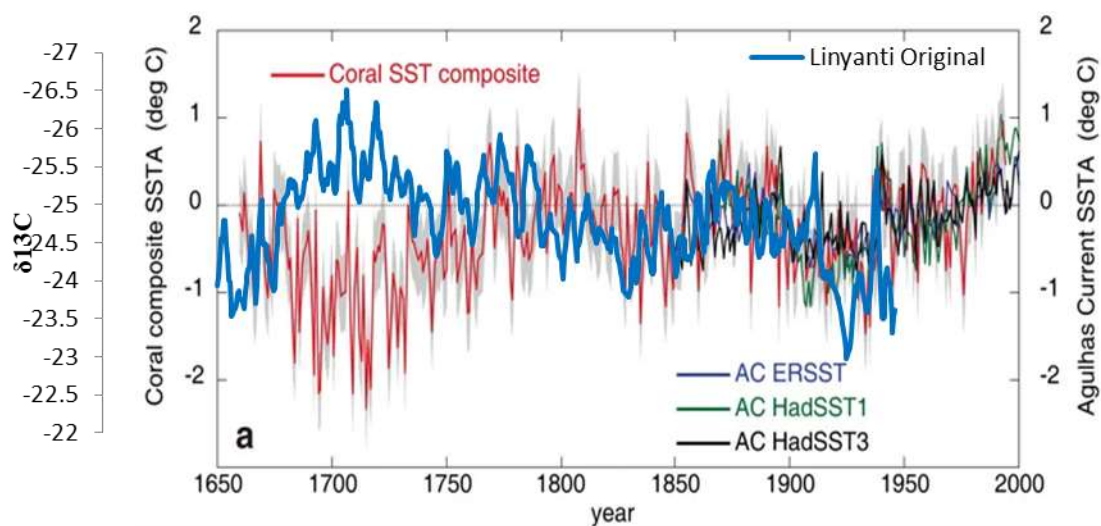


Figure 9. Composite record of sea-surface temperatures from the East coast of Africa adapted from Zinke *et al.* (2014) overlaid with the Linyanti rainfall record. This graph demonstrates the teleconnection between the historic rainfall described by the Linyanti rainfall record and large-scale oceanic currents. More negative $\delta^{13}\text{C}$ values are associated with higher rainfall.

Comparisons of the Linyanti rainfall record with instrumental rainfall records are limited by the absence of continuous data within the region, but comparison against regionally aggregated instrumental records from southern Africa (Nicholson and Entekhabi, 1986) show similarities with the Linyanti rainfall from 1900-1950CE. However, the location of the Kavango-Zambezi region along the border between North and South Kalahari regions (Figure 10) indicates the variability and undefined nature of the rainfall within the region.

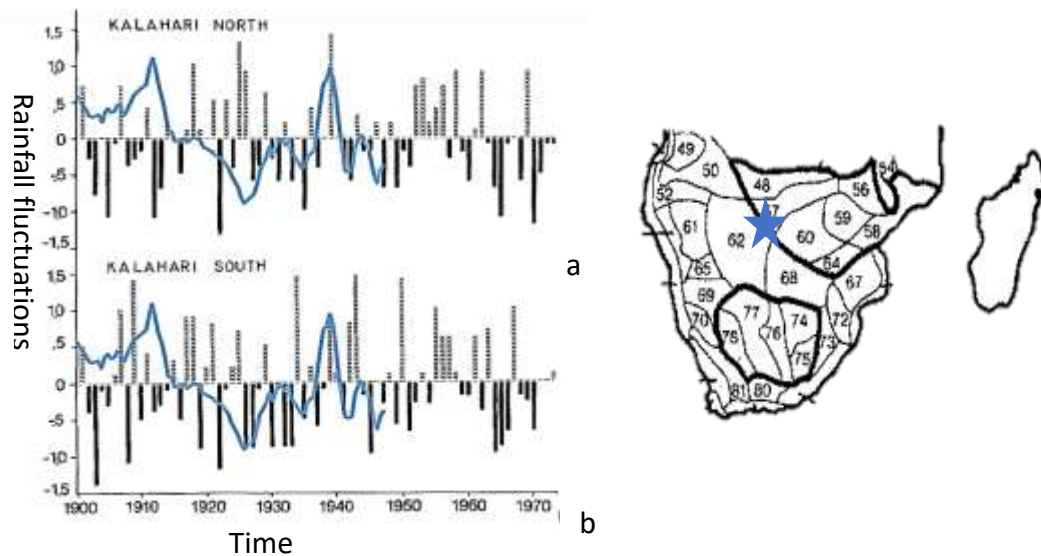


Figure 10. Regionally aggregated instrumental records for the North (10a) and South Kalahari (10b) overlaid with the High-resolution Linyanti rainfall record (blue) from 1900-1950CE (adapted from Nicholson and Entekhabi, 1986).

The wavelet analysis of the Linyanti rainfall record shows regular 16-32-year cycles that persist for ~100 years at a time, meaning that historic rainfall underwent predictable trends of high and low rainfall in the past. The oscillating nature of the Linyanti rainfall record highlights the long-term rainfall variability within the Kavango-Zambezi region driven at a decadal scale. Decadal and bi-decadal rainfall correlations have been observed in instrumental rainfall records from 1903-1981 in South Africa which have been linked to upper-atmospheric dynamics (Reason and Rouault, 2002) and tropical cyclone activity along the Eastern coast of the sub-continent (Malherbe *et al.*, 2014).

The long-term rainfall signals at >64-year frequency that starts at 1600 suggests a large-scale rainfall driver operating on at least 200-year cycles. However this long-term rainfall driver cannot be limited to 200 years because of the potential effect of the

cone of influence within the high frequency bands of the Linyanti rainfall record. These centennial rainfall responses are also not unexpected, as Tyson (1991) and (Holmgren *et al.*, 1999) also identified similar long-term periodicities from proxies in South Africa.

3.5.2. *The Mukolo Fire record*

The macroscopic and microscopic charcoal, although sampled from the same core, show variation between the two fire records which can be hypothesised to reflect different charcoal source areas (Higuera *et al.*, 2007) with drivers operating differently at local and regional scales.

The local fire record showed regular intervals of high charcoal concentration (>650 particles per cm^3) which reduced (<650 particles cm^3) after 1700. The accumulation rate of macroscopic charcoal (49 particles per year) was much higher than those observed within various savanna vegetation types of the Kruger National Park (Gillson and Ekblom, 2009). This suggests that the fluvial landscape where the Mukolo core was collected possibly offered better preservation for large charcoal particles. Wavelet analysis of the local fire record showed that trends in fire regime were consistent until ~ 1700 . Local fire was driven at regular intervals on 16-32 year cycles with a consistent 64-100 year driver from 1300-1700CE. After ~ 1700 the local fire trends disappear, or are likely degraded by a disturbance within the landscape.

The regional fire record showed variability with consistent charcoal concentrations prior to ~ 1700 . Thereafter, charcoal concentrations increased by several orders of magnitude at isolated events at ~ 1700 and ~ 1900 . The average microscopic charcoal influx is considered low ($0.382 \text{ cm}^2/\text{year}$)(Gillson and Ekblom, 2009). However, during the periods of high charcoal accumulation in sediments around 1700CE and 1900CE ($1.972 \text{ cm}^2/\text{year}$ and $3.943 \text{ cm}^2/\text{year}$ respectively) the influx rates are considered moderate and high respectively, in comparison to savanna vegetation types observed in the Kruger National Park by Gillson and Ekblom (2009). The increase in fire activity post-1700 was replicated in the wavelet analysis where trends were limited to short-term (16-32 year) cycles until 1700CE when fire became strongly correlated at longer periods (64 year and 100 year).

By comparing these two components from the Mukolo sediment core we can confirm that the charcoal accumulations from the two different size classes are different and proves that trampling did not take place which would have crushed macroscopic charcoal particles and yielded absolute coherency in the charcoal comparison. The events which coincide across both local and regional fire proxies should be noted as persistent features in history and observed as significant trends in overall (local and regional) fire. Comparison of the Mukolo fire records to other fire records is problematic because of a lack of long-term fire information, for example MODIS burnt area products only go back to 1999. In addition to this, most pollen studies provide little insight in to fire dynamics and the lack of pollen records from the region prevent any comparisons.

3.5.3. *The Fire-Rainfall Relationship*

Only the local fire (macroscopic charcoal) record showed pulses of strong correlation with the rainfall record prior to ~1700 which, at low periods, coincided with decreases in rainfall showing an unexpected negative relationship. The rainfall-fire coherency at higher periods (64 to 128 -years) are attributed to long-term environmental responses to rainfall within the local area. The long-term cycles observed in the rainfall and local fire record prior to 1700CE would have direct effects on the vegetation structure potentially resulting in local shifts between tree and grass dominance. Similar long-term oscillations (~100 years) of tree-grass dominance were observed in pollen analyses of an Ethiopian savanna by Gil-Romera *et al.* (2010).

The rainfall-fire relationship from 1700-1750CE becomes positively correlated for both fire records (Figure 11) and matches with Krawchuk and Moritz' (2011) observations, showing that the Kavango-Zambezi region has been a fuel-moisture limited system for >300 years. Local fire shows the strongest periodicity within the record during a consistent increase in rainfall. The relationship between rainfall and local fire during this period of time occurs when atmospheric temperatures reach their minimum during the Little Ice Age (Tyson *et al.*, 2000).

After ~1700CE the regional fire and rainfall relationship has an opposite relationship to that of the local fire with increased periodicity thereafter. The absence of locally driven fire post-1750, even with observed decreases in rainfall where fire

previously occurred, suggests that fire in the local area was no longer driven by rainfall. Alternative local-scale drivers for fire are herbivory and human activity (Archibald and Hempson, 2016), so either there was an influx of humans into the local area or increased herbivore numbers had an impact on vegetation (Archibald *et al.*, 2005; Savadogo *et al.*, 2007). Both are possible based on records of a rich cattle farming history within the Kavango-Zambezi region (Boden, 2009). The change in regional and local fire regimes around 1700CE could be associated with the influence of colonial settlers in the area from 1650-1800s (Boden, 2009), and the subsequent fire exclusion management strategy (Botha, 2005) could be a major contributor to the reduction in local fires within the area.

After 1900CE the persistence of the strong coherency signal across all frequencies suggests a driver at both long and short timescales. The increased fire-rainfall coherency coincides with a rapid decline in rainfall, increases in African human population size (Frankema and Jerven, 2014) and the onset of rapid global atmospheric temperature increases (Leclercq and Oerlemans, 2012).

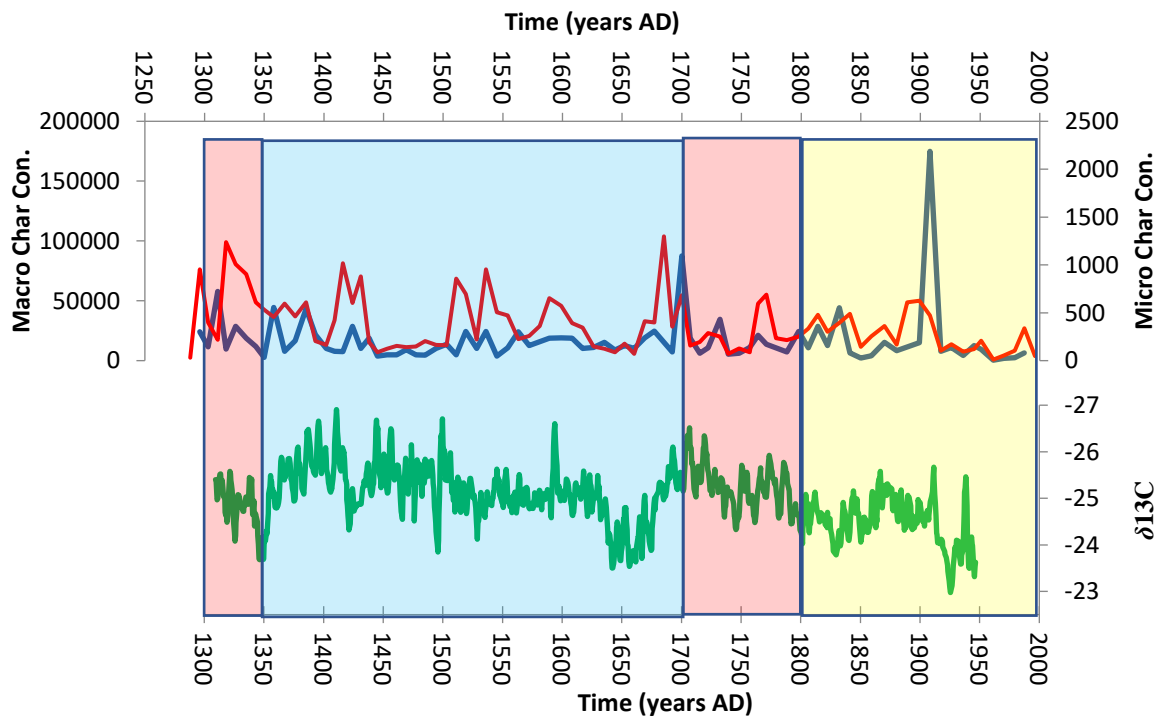


Figure 11. The Mukolo Fire (above, Local fire record shown in red and Regional fire record in blue) and Linyanti Rainfall (below, green) climate proxies are separated into sections and discussed based on the time periods where trends in the fire-rainfall relationship occur. Red shading indicates periods when the fire-rainfall relationship is fuel-load limited (positively correlated), blue indicates periods when the fire-

rainfall relationship is fuel-moisture limited (negatively correlated) and yellow indicates when the fire-rainfall relationship has been degraded and rainfall no longer predicts fire.

3.5.4. Conclusions

The findings of this chapter indicate that the fire-rainfall relationship has varied over time within the local and regional scales of the Mukolo fire record. This contradicts the original hypothesis that the fire-rainfall relationship would be positive across fire-scales and has implications for our understanding of savanna responses to climate variability. These findings highlight the potential for savannas to vary, not just in vegetation structure in response to climate variability, but also in the drivers of fire at different scales.

The influence of human activity on the fire-rainfall relationship was expected to be identifiable through deviations from the anticipated positive trend, however deviations observed in the relationship during significant climatic events, such as the Little Ice Age, could have prolonged effects on the vegetation structure with direct implications for the fire regime regardless of current climate. To clarify this, pollen analyses would be required to define historic community structure.

Finally, the absence of local fire and coinciding increases in regional fire after 1750CE suggests that a possible response to human activity. The implications of absent local fire suggest that humans had a great impact on the immediate area by preventing fuel accumulation, possibly through livestock grazing or agriculture. While the increase in regional fire suggests a growing population but could also be a symptom of reduced rainfall and general drying of the landscape.

3.5.5. Integration with current research

The wavelet analysis of rainfall and fire at different scales highlights the importance of the concept of scale within ecology. The data and analyses produced here, while limited by uncertainty associated with radiocarbon dating and sediment accumulation processes, still provide valuable perspective on the spatial and temporal patterns of fire and rainfall in an important and dynamic region of the sub-continent. The degree to which vegetation structure and composition has been influenced by the

environmental changes document here is a pending question. I hypothesize that pollen records would show cyclical patterns of woody thickening and opening, related to the patterns of drought and fire described here. It is also possible that the vegetation record will give more insights into the patterns of fire, as the effect of climate on fire regimes depends strongly on the type of fuel (i.e. vegetation) (Pausas and Ribeiro, 2013).

The limitation on this study was the sample resolution of the Mukolo sediments. Improved sediment sampling techniques could offer further insight into short-term response of the rainfall and fire relationship to climatic change. To improve the study, I would recommend the inclusion of pollen analysis to investigate vegetation community structure to climate changes and tree recruitment rates.

3.6. Appendices

3.6.1. Appendix 1

```
Wavelet Coherency Model<- analyze.wavelet(my.data, "x",  
method = "white.noise",  
loess.span = ,  
dt =7.694117647,  
dj = 0.1299694,  
lowerPeriod = 8,  
upperPeriod = 512,  
n.sim = 1000)
```

3.6.2. Appendix 2

```
Cross Wavelet Model<- analyze.coherency( comparison,  
c( "x", "y"),  
    loess.span = ,  
    dt = 7.694117647, dj = 0.06498471,  
    window.type.t = 3, window.type.s = 3,  
    window.size.t = 5,  
window.size.s = 1/4,  
    lowerPeriod = 8, upperPeriod = 512,  
    method = "white.noise",  
    n.sim = 1000)
```

Chapter 4: Interpretations of historic climate fire numbering

4.1. Dissertation Overview

Savanna variability and dynamics are introduced in Chapter 1 with an emphasis on the abiotic drivers of savanna structure - climate and fire. The chronologies developed in Chapter 2 create a timeline for important environmental drivers for savanna structure within the Kavango-Zambezi region. The wavelet analyses in Chapter 3 explored the relationship between rainfall and fire through history and indicated a shift in the fire-rainfall relationship around ~1700. An absence of local fire and increase in regional fire activity thereafter coincided with an overall decline in rainfall, thus, directly affecting savanna structure, with implied changes to the vegetation.

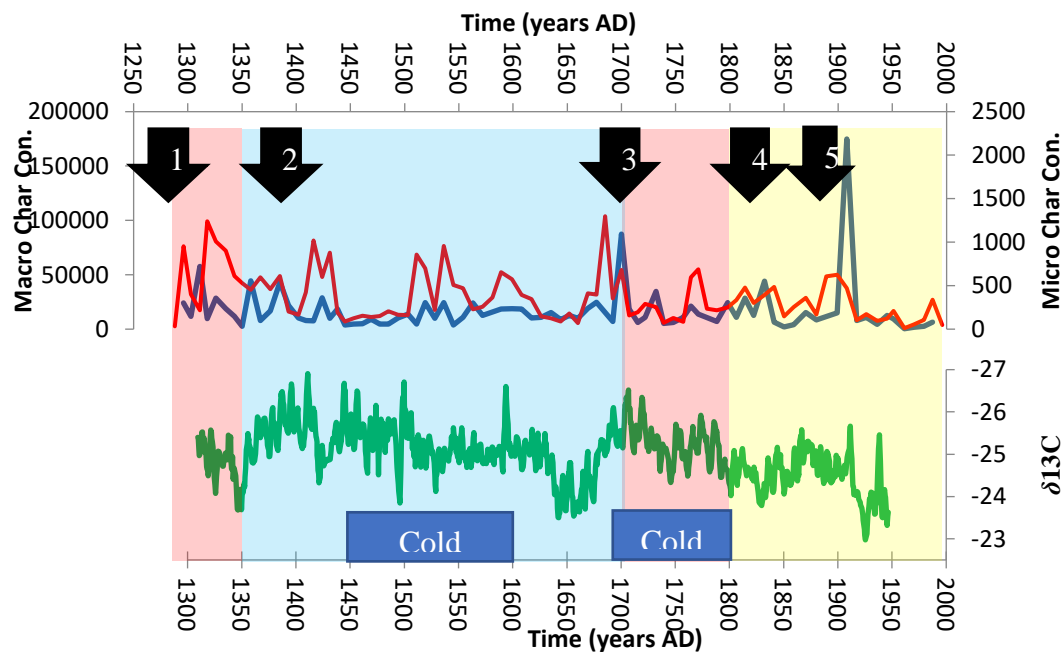


Figure 1. The Mukolo Fire (above, local fire record shown in red and regional fire record in blue) and Linyanti Rainfall (below, green) climate proxies are separated into time periods where the fire-rainfall relationship is discussed. Red shading indicates periods when the fire-rainfall relationship is fuel-load limited (positively correlated), blue indicates where the fire-rainfall relationship is fuel-moisture limited (negatively correlated) and yellow indicates when the fire-rainfall relationship has been degraded and rainfall no longer predicts fire. The black arrows indicate important events in human history (1 - Decline of Mapungubwe, 2 - Peak of Great Zimbabwe, 3 - Lozi Expansion, 4 -Difaqane, 5 - German colonial governance).

The changes observed within the environmental records overlap with human habitation of the region, and cannot be separated from human activities. Thus, the environmental records can include human manipulations of fire activity that precede climatic responses as well as human responses to climate. The Linyanti rainfall and Mukolo fire records are presented below (Figure 2) and discussed with the aid of relevant historic literature to contextualize the environmental records.

4.1.1. Pre-1400

Both charcoal records indicate strong trends prior to 1400CE, suggesting that local fire regimes are correlated with regional patterns of fire at this time (i.e. fire probably associated with large-scale environmental drivers). This is supported by the fact that rainfall and fire strongly coincide in this part of the record, both decreasing until at least 1350CE (Figure 1), thus describing a fuel-load limited system. This is also the region of the Mukolo sediment core where macroscopic and bulk material have overlapping radiocarbon dates suggesting that the source is contemporary vegetation, most likely grasses. Over this time atmospheric temperatures were relatively cooler (Scott *et al.*, 2003) and coincided with drought conditions that lead to the abandonment of Mapungubwe (Huffman, 2008). The drought conditions observed in the Linyanti record in combination with low atmospheric temperatures imply low fire intensities as well as reduced biomass burned, that could have limited the ability of fire to burn trees and prevent woody thickening (Trollope and Potgieter, 1985). In contrast, the low temperatures and reduced rainfall would have reduced tree growth – but occasional years of above-average rainfall might still have resulted in recruitment events. The overall interpretation is of a grassy dominated landscape, with periods of high and low fire associated with periods of high and low rainfall, respectively.

Increased rainfall is observed from 1350-1420CE, while fire activity continued to decline – a possible explanation is that the system switched to a fuel moisture-limited savanna (i.e. high enough rainfall that there was an abundance of fuel, and very wet years meant less favourable conditions for fire to burn). An alternative explanation is that humans had settled in the area and reduced fire buffering the climate response of vegetation. This seems unlikely because historic records for the inland regions of southern Africa for this time are limited to Mapungubwe, Great Zimbabwe and the

Ingombe Ilede which are >600km East and South-East from the Kavango Zambezi region and are associated with generally higher rainfall. Archaeological studies show that human societies at Mapungubwe were abandoned and there was a subsequent expansion of activity in Great Zimbabwe (Huffman, 2008; O'Connor and Kiker, 2004). The agricultural economy of Great Zimbabwe would have flourished under the high rainfall conditions at this time, facilitating the increase in population size and development of agriculture which is observed in the archaeological record (Chirikure and Pikirayi, 2008). At the Ingombe Ilede burial site in Southern Zambia, society flourished from 1300-1500CE (Davidson, 1974). The advancement of these African societies does not however confirm the presence or influence of people in the Kavango-Zambezi region, but does confirm that the wet climate observed in the Linyanti record was probably a regional phenomenon.

4.1.2. *Old Wood Burning: 1400-1600*

Between 1400CE and 1600CE the microscopic charcoal shows the lowest fire activity, while the macroscopic charcoal shows relatively high concentrations. The absence of coinciding fire signals suggests fire activity was spatially limited due to the short deposition distances associated with larger charcoal particles. Potentially, fires were unable to spread across the landscape while rainfall was higher than the modern average (see Chapter 3, Figure 6), suggesting a moisture-limited system. The strong rainfall-fire signal shortly after ~1500 (see Chapter 3, Figure 6) in both fire records marks the only strong regional-scale fire signal within this period of time – it coincides with a spike in atmospheric temperatures observed at the Makapansgat cold air caves (Holmgren *et al.*, 1999). Moreover, there is a great discrepancy (>500 years) in radiocarbon dates between the macroscopic charcoal and bulk sediment material from this section of the Mukolo charcoal record: the macroscopic charcoal is clearly composed of the wood from long-lived trees (see Chapter 2). This could be associated either with increased human activity (breaking up the landscape and preventing large fires – Archibald *et al* 2016), or increased grazer abundance. The implications for fuel loads and grazing lawns would have facilitated patchy burning and approximated the small-scale fires observed in the macroscopic charcoal record. However Smith (1992) (as cited by Sheuyange *et al.* (2005)) limits the uses of fire by pastoralists to ~1800CE,

suggesting there is no influence of human-driven fires on grazing strategies during this time. The alternative is that the Kavango-Zambezi region switched to a closed canopy, less flammable ecosystem that only burns under more extreme conditions (Hoffman *et al* 2012), where the ignitions were at times of year when fires can be more intense (dry season fires) to facilitate old wood burning.

Without pollen data to substantiate this, it is not possible to confirm if humans or a switch to closed canopy system was the cause of the change in fire regimes. However, it should be noted that the increased rainfall observed in the record prior to 1500CE suggests that vegetation was not load-limited, and that fuels would have naturally accumulated within the landscape. The small peaks observed in the fire record coincide with 16-32 year pulses in periodicity which are onset by decreases in rainfall and small increase in atmospheric temperature (Tyson *et al.*, 2000). The generally low air temperatures from 1400-1600CE (Tyson *et al.*, 2000) (Chapter 3, Figure 1) would have reduced the potential for fuel to dry, hence facilitating a fuel-moisture limited system with implications for patchy, intense burns (Govender *et al.*, 2006). Hence creating open spaces between dense vegetation, allowing the development of grassy patches with increased resource availability and landscape heterogeneity as observed by (Sheuyange *et al.*, 2005).

4.1.3. *Fire Transition Zone: 1600-1800*

Between 1600CE and 1650CE there is a rapid decline in rainfall observed in the Linyanti record followed by the onset of a severe, prolonged drought during which both fire records decline. During this period there is a strong periodicity of Linyanti rainfall with fire from ~1670 to 1720CE – where increases in rainfall are associated with spikes in both charcoal records that continue until ~1750CE suggesting a fuel-load limited savanna responding to increases in biomass. During this period it appears that the fire-climate system was following patterns described by Van Wilgen *et al.* (2004) and Archibald *et al.* (2010) for semi-arid savannas. Immediately following the drought conditions, the macroscopic charcoal concentrations increased strongly with rainfall, but suddenly ceased around ~1750; while the relationship became stronger at a regional-scale over longer timescales (>64years).

Other proxies from the southern hemisphere, including coral sea-surface temperatures from Madagascar (Zinke *et al.*, 2014) and air temperatures from stalagmites (Huffman, 2008; Sundqvist *et al.*, 2013), show persisting cold conditions from 1690 to 1800CE (Figure 1). The Linyanti rainfall record shows increased rainfall during this period, peaking at ~1700CE. This event is from a well-dated section of the Linyanti Baobab tree core and is further replicated in multiple independently dated baobab tree-core records across southern Africa (Woodborne *et al.*, 2015). The phenomenon can potentially be explained by eastward moisture influxes from temperature anomalies in the Eastern Atlantic, such as those observed by Rouault *et al.* (2003).

The lack of drought conditions post-1650 observed in the Linyanti record is further substantiated by the historic expansion of the Lozi people in the Kavango-Zambezi regions (Figure 1). The Lozi, a tribe with well-known fishing and cattle economies (Ocaya, 1993), were documented to have displaced the Hambukushu people from Katimo Mulilo (100km East of the sediment coring site) in the early 1700s (Pretorius, 1975; Unzicker, 1996). Further Lozi expansion during the mid-1700s led to a second displacement of the Hambukushu people and their settlement in Andara (Tlou, 1972; Unzicker, 1996), 200km West of the sediment coring site. The timing of historic Lozi expansion coincides with the peak and high sustained rainfall in the Linyanti rainfall record suggesting that the Kavango-Zambezi region provided an abundance of fishing potential which favoured the Lozi economies.

4.1.4. Degraded Fire-Rainfall Relationship: 1800 to 1880

From ~1800CE the fire-rainfall relationship is completely absent in the macroscopic charcoal record, while weak periodicity occurs in the microscopic record until ~1900. The microscopic record responds weakly to rainfall over this period but is clearly negative: we observe a series of small peaks in both charcoal records between 1800CE and 1900CE which coincides with decreases in rainfall. But the overall negative relationship implied between fire and rainfall indicates a fuel-moisture limited savanna system which coincides with the modern observations of Krawchuk and Moritz (2011) and persists to the end of the record.

The absence of strong fire periodicities in response to rainfall fluctuations which previously predicted fire under both fuel-limited and moisture-limited conditions, suggests that the charcoal deposition is no longer as strongly linked to rainfall as it was in earlier parts of the record. Overall, the lack of macroscopic charcoal from 1800-1880CE shows that within the smaller spatial extent of shorter deposition distance, the fire-rainfall relationship became degraded by some disturbance. Alternatively, this break-down of the fire-rainfall relationship could be caused by people - these conditions overlap with the Difaqane (Figure 2) when masses of South African Bantu-speaking people fled Northwards from South Africa (Botha, 2005). From 1820 to 1880 the influx of South African Bantu people, arrival of the Kololo, and the return of the Lozi was described as a time of great unrest, slavery and conflict for resources within the Kavango-Zambezi regions (Boden, 2009; Botha, 2005; Rohde and Hoffman, 2012). The increased human population within the region is likely to have resulted in greater land transformation (land clearing) and reduction in fuel loads due to grazing. Moreover, human fire ignitions, which can occur at any time of year (Archibald *et al.*, 2010), would also likely have weakened the impact of rainfall on fire activity and biomass burned.

4.1.5. *Regional Burning: 1880-1950*

Rainfall declines rapidly from ~1880 onward. Microscopic charcoal concentrations are also very low and declining. Potentially, this reduction in fire is linked with the decline in rainfall, but I attribute it to a continuation of the disrupted rainfall and fire relationship observed in the 1800's. It is possible that the intensification of human activities in the region could have long-term impacts on vegetation structure causing the sustained strong correlation of rainfall and fire at longer periods. Andela *et al.* (2019) demonstrate a global decline in the area burned in recent years associated with increased human cultivation and land use. Therefore, a more parsimonious explanation is that post-1800 the fire-rainfall relationship no longer acts strongly at local levels, and only at very large, regional scales where rainfall drives the fire regime. This is consistent with information from Australia (Bird *et al.*, 2016), as well as other parts of Africa (Alvarado *et al.*, 2020; Archibald *et al.*, 2010).

The Linyanti rainfall record matches with sea surface temperatures from the Eastern coast of southern Africa (Zinke *et al.*, 2014) between 1880 and 1950CE, while only matching along the extreme minimum of other tree-core records (Woodborne *et al.*, 2015). The fact that the Linyanti tree is somewhat further West suggests the influence of the East-West rainfall gradient causing the difference between the Linyanti record and other Baobab records, at least since ~1900CE.

The lowest point in the rainfall record is in 1926, which agrees with historic accounts of drought in the early 1930s (Botha, 2005) and is thought to have precipitated the bush-encroachment problem to the south and west of the Kavango-Zambezi regions of Namibia. The fact that this well-documented drought, coupled with heavy grazing regimes resulted in bush encroachment suggests that this might also have occurred during past droughts in the record. By the 1950s bush encroachment reached higher densities with negative impacts on livestock densities and by 1966 was declared an environmental disaster (De Klerk, 2004). The only region that remained un-encroached was the communal part of the Kavango-Zambezi region – which had been subjected to frequent burning and fuel harvesting. The fact that the Kavango-Zambezi region, dominated by communal cattle grazing, was un-encroached lead to the development of current management plans which include regular prescribed burning and stocking rates that approximate the fire regime and grazing in savannas which maintain open grassland.

4.2. Conclusions

The Linyanti rainfall and Mukolo fire proxies have been quantified, well-dated and explored to interpret the fire-rainfall relationship within the Kavango-Zambezi region. These proxies prove that there have been major shifts in historic rainfall and fire activity in the past that have influenced the relationship between fire and rainfall. The use of microscopic and macroscopic charcoal revealed that the fire-rainfall relationship can differ both temporally and spatially in response to rainfall. That macroscopic charcoal correlated better with climate in the first half of the record, when human impacts were more spatially localised, corroborates my assumption that macroscopic charcoal is representative of a local fire signal. Whilst the microscopic charcoal signal strength increased towards the end of the record when human

populations increased and habitation became more widespread supports the theory that microscopic charcoal is attributed to a larger spatial extent.

However, the impact of humans on the fire-rainfall relationship cannot be isolated from the climate proxies in the Kavango-Zambezi region owing to the lack of local context on semi-nomadic settlement patterns, migrations and unknown population sizes in the past. From ~1800CE onward there is a noticeable change in the local-scale fire-rainfall relationship suggesting a locally driven influence affecting the fire activity.

4.3. Reflections on the study aims and objectives

The aim of this project was to create proxy records for fire and rainfall for the South-Central African region and investigate the relationship between rainfall and fire over time to assess the impact of human activities on the fire regime. This was to be achieved through exploration of the Mukolo sediment core and Linyanti Baobab tree core with the aid of radiocarbon dating techniques and comparisons between the environmental records to describe the relationship between fire and rainfall throughout history. Identification of human impacts on the fire-rainfall relationship were expected to be apparent in the record as a break-down of this relationship, where rainfall poorly predicts fire activity.

4.4. Recommendations for Land-users and Policy-makers

By combining information from climate proxies, ecology and historic records of human activities I was able to identify environmental conditions which are relevant to assessing current ecosystem resilience under a changing climate. Predictions of increased atmospheric temperatures, changes in mean annual precipitation, and the frequency of extreme events as a result of climate change have implications for future fire regimes in Southern Africa (Tadross *et al.*, 2011). These conditions have anticipated impacts on ecosystems with associated environmental responses such as woody encroachment observed in Namibian rangelands. The impacts of which affect the economy, food security, human health and society (Serdeczny *et al.*, 2016). All of these environmental conditions (except elevated CO²) have been present at some point during the last several centuries in the records I studied. This implies that the projected

changes in climate – while they will certainly impact human livelihoods and alter ecosystem functioning – are without precedent. The organisms living in the region currently should be adapted to a degree of rainfall and fire variability and – given sufficient space to move and adapt to allow the ecosystem as a whole to remain intact. This conclusion would be more substantial if we had pollen data to confirm that the changes we observe were not dramatic enough to alter ecosystem states and ecosystem functioning.

From the evidence I present here it appears that the Kavango-Zambezi region is in a transition zone for rainfall – fire relationships. Changes in the amount of mean annual rainfall can alter the response of fire from positive to negative – i.e. it will be difficult to predict how fire regimes in the region will respond to changing climates unless we have good details about the projected rainfall. From 1800 onwards it appears that locally human activities have more impact on fire than larger climate signals. This is encouraging as it means that it should be possible to focus efforts on human management of fire in order to mitigate potential global-change related increases in woody cover (bush encroachment) which is a documented problem in the region.

4.5. Potential Sources of Error

Mukolo sediment sampling - although every effort was made to ensure no sediment mixing occurred during the sub-sampling of the Mukolo core, a sample was spilled during lab processing. The chemical preparation of the sediment samples themselves includes a sieving procedure which has potential to break charcoal pieces and exaggerate microscopic charcoal concentrations (Whitlock and Larsen, 2002).

Wavelet analysis - comparisons are made between annually averaged rainfall and the Mukolo charcoal concentrations. In hindsight, these correlations could be more meaningful if compared against summed rainfall because each charcoal sample represents multiple years of fire activity. However, this would require further understanding of the duration of which each sediment sample is representative (i.e. sediment traps), which is not currently available within southern Africa.

4.6. How this study could be improved

The end of the Linyanti rainfall record, at 1945, and Mukolo fire records, at 1996, show that South-Central Africa has experienced increased aridity since 1880 with strongly correlated increase in large-scale fire activity that has not been observed before. Although the comparison of the fire-rainfall relationship between the climate proxy records ends prior to 1950, reference has been made to numerous modern instrumental records (Nicolas Fauchereau *et al.*, 2003; Nicholson *et al.*, 2018; Nicholson and Entekhabi, 1986; Rouault *et al.*, 2003), observational reports (Govender *et al.*, 2006; Joubert, 2014; Krawchuk and Moritz, 2011; Sheuyange *et al.*, 2005) and satellite imagery (Archibald *et al.*, 2010; K. P. Vadrevu *et al.*, 2013) which relate the past trends to modern interpretations of the landscape.

The lack of historic information (historic photos, long-term instrumental records or other proxies) from the North-Eastern part of Namibia prevented any comparison against local sources. This study was further limited by the coarse temporal sampling of the Mukolo sediment core which restricted the rainfall records comparison in the wavelet analysis. Thus, short-term periodicity (<16years) could not be accounted for when comparing the rainfall and fire records. Furthermore, the interpretations of the historic ecology of the Kavango-Zambezi region could be improved by pollen analysis of the Mukolo sediment samples. It is likely that the relationship between fire and rainfall is mediated by vegetation – i.e. that fire in open grasslands responds positively to increases in rainfall, and fire in closed shrublands responds negatively. Thus, shifts from open to woody systems that can be attributed to the ‘alternative stable states’ hypothesis are likely to have occurred during the time period of my study and more information on vegetation patterns (i.e. pollen data) would help me to identify the causes of the changes I observe more clearly.

Finally, radiocarbon dating introduces a range of error to each chronology. These errors have been reduced through Bayesian statistical analyses to determine the most probable timeline for each environmental record, however in the case of the Mukolo sediment core it is likely that the radiocarbon dates are not accurate. By radiocarbon dating both the Macroscopic Charcoal and Contemporary Organic (MCCO) material and bulk sediments, we were able to see the range in potential ages estimated for each depth. Although, estimations of in-built age have been modelled previously (Dee and Ramsey, 2014; Gavin, 2001), those estimations are not specific to savanna systems and could prove to be highly inaccurate. Thus, the chronology

provided for the Mukolo sediment core was considered the minimum age of the environmental proxy.

References

- Adolf, C., Doyon, F., Klimmek, F., Tinner, W., 2018a. Validating a continental European charcoal calibration dataset. *The Holocene* 28, 1642–1652. <https://doi.org/10.1177/0959683618782607>
- Adolf, C., Wunderle, S., Colombaroli, D., Weber, H., Gobet, E., Heiri, O., van Leeuwen, J.F.N., Bigler, C., Connor, S.E., Gałka, M., La Mantia, T., Makhortykh, S., Svitavská-Svobodová, H., Vannièrè, B., Tinner, W., 2018b. The sedimentary and remote-sensing reflection of biomass burning in Europe. *Global Ecol Biogeogr* 27, 199–212. <https://doi.org/10.1111/geb.12682>
- Alexander, M.E., 1982. Calculating and interpreting forest fire intensities. *Canadian Journal of Botany* 60, 349–357.
- Alvarado, S.T., Andela, N., Silva, T.S.F., Archibald, S., 2020. Thresholds of fire response to moisture and fuel load differ between tropical savannas and grasslands across continents. *Global Ecol Biogeogr* 29, 331–344. <https://doi.org/10.1111/geb.13034>
- Andela, N., Morton, D.C., Giglio, L., Paugam, R., Chen, Y., Hantson, S., Van Der Werf, G.R., Randerson, J.T., 2019. The Global Fire Atlas of individual fire size, duration, speed and direction. *Earth System Science Data* 11, 529–552.
- Archibald, S., 2016. Managing the human component of fire regimes: lessons from Africa. *Philosophical Transactions of the Royal Society B: Biological Sciences* 371, 20150346.
- Archibald, S., 2010. Fire Regimes in Southern Africa - Determinants, Drivers and Feedbacks 176.
- Archibald, S., Bond, W., Stock, W., Fairbanks, D., 2005. Shaping the landscape: Fire-grazer interactions in an African savanna. *Ecological Applications* 15, 96–109. <https://doi.org/10.1890/03-5210>
- Archibald, S., Bond, W.J., Hoffmann, W., Lehmann, C., Staver, C., Stevens, N., 2019. Distribution and Determinants of Savannas, in: *Savanna Woody Plants and Large Herbivores*. John Wiley & Sons, Ltd, pp. 1–24. <https://doi.org/10.1002/9781119081111.ch1>
- Archibald, S., Hempson, G.P., 2016. Competing consumers: contrasting the patterns and impacts of fire and mammalian herbivory in Africa. *Phil. Trans. R. Soc. B* 371, 20150309. <https://doi.org/10.1098/rstb.2015.0309>

- Archibald, S., Roy, D.P., van Wilgen, B.W., Scholes, R.J., 2009. What limits fire? An examination of drivers of burnt area in Southern Africa. *Global Change Biology* 15, 613–630. <https://doi.org/10.1111/j.1365-2486.2008.01754.x>
- Archibald, S., Scholes, R.J., Roy, D.P., Roberts, G., Boschetti, L., 2010. Southern African fire regimes as revealed by remote sensing. *International Journal of Wildland Fire* 19, 861. <https://doi.org/10.1071/WF10008>
- Archibald, S., Staver, A.C., Levin, S.A., 2012. Evolution of human-driven fire regimes in Africa. *Proceedings of the National Academy of Sciences* 109, 847–852. <https://doi.org/10.1073/pnas.1118648109>
- Beach, D., 1998. Cognitive Archaeology and Imaginary History at Great Zimbabwe. *Current Anthropology* 39, 47–72. <https://doi.org/10.1086/204698>
- Becker, B., 1992. The History of Dendrochronology and Radiocarbon Calibration, in: Taylor, R.E., Long, A., Kra, R.S. (Eds.), *Radiocarbon After Four Decades*. Springer New York, New York, NY, pp. 34–49.
- Beerling, D.J., Osborne, C.P., 2006. The origin of the savanna biome. *Global Change Biology* 12, 2023–2031. <https://doi.org/10.1111/j.1365-2486.2006.01239.x>
- Bennett, K.D., Fuller, J.L., 2002. Determining the age of the mid-Holocene *Tsuga cana densis* (hemlock) decline, eastern North America. *The Holocene* 12, 421–429. <https://doi.org/10.1191/0959683602hl556rp>
- Bird, R.B., Bird, D.W., Coddling, B.F., 2016. People, El Nino southern oscillation and fire in Australia: fire regimes and climate controls in hummock grasslands. *Philosophical Transactions of the Royal Society B: Biological Sciences* 371, 20150343.
- Blaauw, M., 2010. Clam - “classic” age-depth modelling.
- Blaauw, M., Christen, J.A., 2011. Flexible Paleoclimate Age-Depth Models Using an Autoregressive Gamma Process 19.
- Blaauw, M., Christen, J.A., Aquino, M.A., Esquivel Vazquez, J., Gonzalez, O.M., Belding, T., Theiler, J., Gough, B., Karney, C., 2011. Age-Depth Modelling using Bayesian Statistics.
- Boden, G., 2009. The Khwe and West Caprivi before Namibian independence: Matters of land, labour, power and alliance. *Journal of Namibian Studies : History Politics Culture* 5, 27–71.

- Bond, W., Keeley, J., 2005. Fire as a global ‘herbivore’: the ecology and evolution of flammable ecosystems. *Trends in Ecology & Evolution* 20, 387–394.
<https://doi.org/10.1016/j.tree.2005.04.025>
- Bond, W.J., 2008. What limits trees in C4 grasslands and savannas? *Annual review of ecology, evolution, and systematics* 39, 641–659.
- Bond, W.J., Woodward, F.I., Midgley, G.F., 2005. The global distribution of ecosystems in a world without fire. *New phytologist* 165, 525–538.
- Bonny, A.P., 1972. A method for determining absolute pollen frequencies in lake sediments. *New Phytologist* 71, 393–405.
- Botha, C., 2005. People and the Environment in Colonial Namibia. *South African Historical Journal* 52, 170–190. <https://doi.org/10.1080/02582470509464869>
- Bradstock, R.A., 2010. A biogeographic model of fire regimes in Australia: current and future implications. *Global Ecology and Biogeography* 19, 145–158.
<https://doi.org/10.1111/j.1466-8238.2009.00512.x>
- Brauer, A., Litt, T., Negendank, J., Zolitschka, B., 2001. Lateglacial varve chronology and biostratigraphy of lakes Holzmaar and Meerfelder Maar, Germany. *Boreas* 30, 83–88. <https://doi.org/10.1111/j.1502-3885.2001.tb00991.x>
- Brock, F., Higham, T., Ditchfield, P., Ramsey, C.B., 2010. Current pretreatment methods for AMS radiocarbon dating at the Oxford Radiocarbon Accelerator Unit (ORAU). *Radiocarbon* 52, 103–112.
- Broecker, W.S., Kulp, J.L., 1956. The Radiocarbon Method of Age Determination. *Am. antiq.* 22, 1–11. <https://doi.org/10.2307/276163>
- Brönnimann, S., 2016. Tabora and the “year without a summer” of 1816: a perspective on earth and human systems science. *Geographica Bernensia*, Geographisches Institut der Universität Bern, Bern.
- Brooks, S., Gelman, A., 1998. General Methods for Monitoring Convergence of Iterative Simulations. *J. Comput. Graphi. Stat.* 7, 434–455.
<https://doi.org/10.1080/10618600.1998.10474787>
- Buisson, E., Le Stradic, S., Silveira, F.A.O., Durigan, G., Overbeck, G.E., Fidelis, A., Fernandes, G.W., Bond, W.J., Hermann, J.-M., Mahy, G., Alvarado, S.T., Zaloumis, N.P., Veldman, J.W., 2019. Resilience and restoration of tropical and subtropical grasslands, savannas, and grassy woodlands: Tropical grassland resilience and restoration. *Biol Rev* 94, 590–609.
<https://doi.org/10.1111/brv.12470>

- Buitenwerf, R., Bond, W.J., Stevens, N., Trollope, W.S.W., 2012. Increased tree densities in South African savannas: >50 years of data suggests CO₂ as a driver. *Global Change Biology* 18, 675–684. <https://doi.org/10.1111/j.1365-2486.2011.02561.x>
- Burrough, S.L., Thomas, D.S., Shaw, P.A., Bailey, R.M., 2007. Multiphase quaternary highstands at lake Ngami, Kalahari, northern Botswana. *Palaeogeography, Palaeoclimatology, Palaeoecology* 253, 280–299.
- Butzer, K.W., Isaac, G.L., Richardson, J.L., Washbourn-Kamau, C., 1972. Radiocarbon Dating of East African Lake Levels. *Science* 175, 1069–1076. <https://doi.org/10.1126/science.175.4026.1069>
- Carleton, W.C., Campbell, D., Collard, M., 2018. Radiocarbon dating uncertainty and the reliability of the PEWMA method of time-series analysis for research on long-term human-environment interaction. *PloS one* 13.
- Chemello, C., Davis, S., 2014. Dry/Desert Conditions: Preservation and Conservation, in: Smith, C. (Ed.), *Encyclopedia of Global Archaeology*. Springer New York, New York, NY, pp. 2194–2199. https://doi.org/10.1007/978-1-4419-0465-2_493
- Chirikure, S., Pikirayi, I., 2008. Inside and outside the dry stone walls: revisiting the material culture of Great Zimbabwe. *Antiquity* 82, 976–993. <https://doi.org/10.1017/S0003598X00097726>
- Clark, J.S., 1988. Particle motion and the theory of charcoal analysis: source area, transport, deposition, and sampling. *Quaternary Research* 30, 67–80.
- Colin Prentice, I., 1986. Vegetation responses to past climatic variation. *Vegetatio* 67, 131–141. <https://doi.org/10.1007/BF00037363>
- Collins, S.L., Sinsabaugh, R.L., Crenshaw, C., Green, L., Porrás-Alfaro, A., Stursova, M., Zeglin, L.H., 2008. Pulse dynamics and microbial processes in aridland ecosystems. *Journal of Ecology* 96, 413–420.
- Conway, D., Van Garderen, E.A., Deryng, D., Dorling, S., Krueger, T., Landman, W., Lankford, B., Lebek, K., Osborn, T., Ringler, C., 2015. Climate and southern Africa’s water–energy–food nexus. *Nature Climate Change* 5, 837–846.
- Crawford, A.J., Belcher, C.M., 2014. Charcoal Morphometry for Paleoecological Analysis: The Effects of Fuel Type and Transportation on Morphological Parameters. *Applications in Plant Sciences* 2, 1400004. <https://doi.org/10.3732/apps.1400004>

- Cromsigt, J.P.G.M., Archibald, S., Owen-Smith, N. (Eds.), 2017. *Conserving Africa's Mega-Diversity in the Anthropocene: The Hluhluwe-iMfolozi Park Story, Ecology, Biodiversity and Conservation*. Cambridge University Press, Cambridge. <https://doi.org/10.1017/9781139382793>
- Cumming, D.H., 2008. Large scale conservation planning and priorities for the Kavango-Zambezi Transfrontier Conservation Area. Unpublished report commissioned by Conservation International.
- Daniau, A.-L., d'Errico, F., Goñi, M.F.S., 2010. Testing the hypothesis of fire use for ecosystem management by Neanderthal and Upper Palaeolithic modern human populations. *Plos one* 5.
- Davidson, B., 1974. *Africa in History*. paladin Books.
- de Groot, W.J., Cantin, A.S., Flannigan, M.D., Soja, A.J., Gowman, L.M., Newbery, A., 2013. A comparison of Canadian and Russian boreal forest fire regimes. *Forest Ecology and Management* 294, 23–34. <https://doi.org/10.1016/j.foreco.2012.07.033>
- De Klerk, J.N., 2004. Bush encroachment in Namibia: report on phase 1 of the Bush Encroachment Research, Monitoring, and Management Project. Ministry of Environment and Tourism, Directorate of Environmental Affairs, Windhoek, Namibia.
- Dean, J.S., 1978. Independent Dating in Archaeological Analysis. *Advances in Archaeological Method and Theory* 1, 223–255.
- Dee, M.W., Ramsey, C.B., 2014. High-Precision Bayesian Modeling of Samples Susceptible to Inbuilt Age. *Radiocarbon* 56, 83–94. <https://doi.org/10.2458/56.16685>
- Duffin, K.I., 2008. The representation of rainfall and fire intensity in fossil pollen and charcoal records from a South African savanna. *Review of Palaeobotany and Palynology* 151, 59–71. <https://doi.org/10.1016/j.revpalbo.2008.02.004>
- Duffin, K.I., Gillson, L., Willis, K.J., 2008. Testing the sensitivity of charcoal as an indicator of fire events in savanna environments: quantitative predictions of fire proximity, area and intensity. *The Holocene* 18, 279–291. <https://doi.org/10.1177/0959683607086766>
- Ekblom, A., Gillson, L., 2010. Fire history and fire ecology of Northern Kruger (KNP) and Limpopo National Park (PNL), southern Africa. *The Holocene* 20, 1063–1077. <https://doi.org/10.1177/0959683610369499>

- Farquhar, G., O'Leary, M., Berry, J., 1982. On the Relationship Between Carbon Isotope Discrimination and the Intercellular Carbon Dioxide Concentration in Leaves. *Functional Plant Biol.* 9, 121–137.
- Farquhar, G.D., Hubick, K.T., Condon, A.G., Richards, R.A., 1989. Carbon Isotope Fractionation and Plant Water-Use Efficiency, in: Rundel, P.W., Ehleringer, J.R., Nagy, K.A. (Eds.), *Stable Isotopes in Ecological Research*. Springer New York, New York, NY, pp. 21–40.
- Farquhar, G.D., Sharkey, T.D., 1982. Stomatal Conductance and Photosynthesis. *Annu. Rev. Plant. Physiol.* 33, 317–345.
<https://doi.org/10.1146/annurev.pp.33.060182.001533>
- Fauchereau, N., Trzaska, S., Richard, Y., Roucou, P., Camberlin, P., 2003. Sea-surface temperature co-variability in the Southern Atlantic and Indian Oceans and its connections with the atmospheric circulation in the Southern Hemisphere. *International Journal of Climatology* 23, 663–677.
<https://doi.org/10.1002/joc.905>
- Fauchereau, Nicolas, Trzaska, S., Rouault, M., Richard, Y., 2003. Rainfall variability and changes in southern Africa during the 20th century in the global warming context. *Natural Hazards* 29, 139–154.
- Favier, C., Chave, J., Fabing, A., Schwartz, D., Dubois, M.A., 2004. Modelling forest–savanna mosaic dynamics in man-influenced environments: effects of fire, climate and soil heterogeneity. *Ecological Modelling* 171, 85–102.
<https://doi.org/10.1016/j.ecolmodel.2003.07.003>
- February, E., 2000. Archaeological charcoal and dendrochronology to reconstruct past environments of southern Africa. *South African Journal of Science* 96, 111–115.
- February, E.C., Higgins, S.I., Bond, W.J., Swemmer, L., 2013. Influence of competition and rainfall manipulation on the growth responses of savanna trees and grasses. *Ecology* 94, 1155–1164.
- Fenner, M., 1980. Some Measurements on the Water Relations of Baobab Trees. *Biotropica* 12, 205. <https://doi.org/10.2307/2387972>
- Fichtler, E., Trouet, V., Beekman, H., Coppin, P., Worbes, M., 2004. Climatic signals in tree rings of *Burkea africana* and *Pterocarpus angolensis* from semiarid forests in Namibia. *Trees* 18, 442–451.
<https://doi.org/10.1007/s00468-004-0324-0>

- Fick, S.E., Hijmans, R.J., 2017. WorldClim 2: new 1km spatial resolution climate surfaces for global land areas. *International Journal of Climatology* 37, 4302–4315.
- Fleming, F., 1856. *Southern Africa: a geography and natural history of the country colonies and inhabitants from the Cape of Good Hope to Angola*. Arthur Hall.
- Frankema, E., Jerven, M., 2014. Writing history backwards or sideways: towards a consensus on African population, 1850–2010. *The Economic History Review* 67, 907–931.
- Frueh, W., Lancaster, S., 2014. Correction of deposit ages for inherited ages of charcoal: Implications for sediment dynamics inferred from random sampling of deposits on headwater valley floors. *Quaternary Science Reviews* 88, 110–124. <https://doi.org/10.1016/j.quascirev.2013.10.029>
- Gavin, D.G., 2001. Estimation of Inbuilt Age in Radiocarbon Ages of Soil Charcoal for Fire History Studies. *Radiocarbon* 43, 27–44. <https://doi.org/10.1017/S003382220003160X>
- Gebrekirstos, A., Worbes, M., Teketay, D., Fetene, M., Mitlöhner, R., 2009. Stable carbon isotope ratios in tree rings of co-occurring species from semi-arid tropics in Africa: Patterns and climatic signals. *Global and Planetary Change* 66, 253–260. <https://doi.org/10.1016/j.gloplacha.2009.01.002>
- GFMC, 2001. National guidelines on Forest Fire Management in Namibia – GFMC. URL https://gfmc.online/iffn/country/na/na_8f.html (accessed 3.7.20).
- Giess, W., 1971. A preliminary vegetation map of South West Africa. *Dinteria* 1971, 05–14.
- Gillson, 2015. *Biodiversity Conservation and Environmental Change: Using palaeoecology to manage dynamic landscapes in the Anthropocene*. OUP Oxford.
- Gillson, L., Ekblom, A., 2009. Untangling anthropogenic and climatic influence on riverine forest in the Kruger National Park, South Africa. *Vegetation History and Archaeobotany* 18, 171–185. <https://doi.org/10.1007/s00334-008-0202-6>
- Gillson, L., Marchant, R., 2014. From myopia to clarity: sharpening the focus of ecosystem management through the lens of palaeoecology. *Trends in Ecology & Evolution* 29, 317–325. <https://doi.org/10.1016/j.tree.2014.03.010>
- Gil-Romera, G., Lamb, H.F., Turton, D., Sevilla-Callejo, M., Umer, M., 2010. Long-term resilience, bush encroachment patterns and local knowledge in a

- Northeast African savanna. *Global Environmental Change* 20, 612–626.
<https://doi.org/10.1016/j.gloenvcha.2010.04.008>
- Giorgi, F., Mearns, L.O., 1991. Approaches to the simulation of regional climate change: a review. *Reviews of Geophysics* 29, 191–216.
- Goldammer, J., 2001. Namibia Round Table on Fire Windhoek 1999. *International Forest Fire News* 25, 57–72.
- Govender, N., Trollope, W.S.W., Van Wilgen, B.W., 2006. The effect of fire season, fire frequency, rainfall and management on fire intensity in savanna vegetation in South Africa: Fire intensity in savanna. *Journal of Applied Ecology* 43, 748–758. <https://doi.org/10.1111/j.1365-2664.2006.01184.x>
- Grady, J.M., Hoffmann, W.A., 2012. Caught in a fire trap: recurring fire creates stable size equilibria in woody resprouters. *Ecology* 93, 2052–2060.
- Guilderson, T.P., Reimer, P.J., Brown, T.A., 2005. The Boon and Bane of Radiocarbon Dating. *Science* 307, 362.
<https://doi.org/10.1126/science.1104164>
- Guy, R.D., Fogel, M.L., Berry, J.A., 1993. Photosynthetic Fractionation of the Stable Isotopes of Oxygen and Carbon. *Plant Physiol.* 101, 37.
<https://doi.org/10.1104/pp.101.1.37>
- Hagens, G., 2006. Testing the Limits: Radiocarbon Dating and the End of the Late Bronze Age. *Radiocarbon* 48, 83–100.
<https://doi.org/10.1017/S0033822200035414>
- Hall, G., Woodborne, S., Pienaar, M., 2009. Rainfall control of the $\delta^{13}\text{C}$ ratios of *Mimusops caffra* from KwaZulu-Natal, South Africa. *The Holocene* 19, 251–260. <https://doi.org/10.1177/0959683608100569>
- Hamilton, T., 2016. Fire, Water and Carbon Isotopes. University of Witwatersrand, Johannesburg, South Africa.
- Harring, S.L., Odendaal, W., 2012. “God stopped making land!”: land rights, conflict and law in Namibia’s Caprivi region. Legal Assistance Center, Windhoek, Namibia.
- Harrison, M., 1984. A generalized classification of South African summer rain-bearing synoptic systems. *Journal of Climatology* 4, 547–560.
- Heegaard, E., Birks, H.J.B., Telford, R.J., 2005. Relationships between calibrated ages and depth in stratigraphical sequences: an estimation procedure by

- mixed-effect regression. *The Holocene* 15, 612–618.
<https://doi.org/10.1191/0959683605hl836rr>
- Heine, K., 1978. Radiocarbon chronology of late quaternary lakes in the Kalahari, southern Africa. *CATENA* 5, 145–149. [https://doi.org/10.1016/0341-8162\(78\)90005-X](https://doi.org/10.1016/0341-8162(78)90005-X)
- Hempson, G.P., Archibald, S., Bond, W.J., Ellis, R.P., Grant, C.C., Kruger, F.J., Kruger, L.M., Moxley, C., Owen-Smith, N., Peel, M.J.S., Smit, I.P.J., Vickers, K.J., 2015. Ecology of grazing lawns in Africa: African grazing lawns. *Biol Rev* 90, 979–994. <https://doi.org/10.1111/brv.12145>
- Hennenberg, K.J., Goetze, D., Kouamé, L., Orthmann, B., Porembski, S., 2005. Border and ecotone detection by vegetation composition along forest-savanna transects in Ivory Coast. *Journal of Vegetation Science* 16, 301–310.
- Herrera, C.M., Medrano, M., Bazaga, P., 2015. Continuous within-plant variation as a source of intraspecific functional diversity: Patterns, magnitude, and genetic correlates of leaf variability in *Helleborus foetidus* (Ranunculaceae). *American Journal of Botany* 102, 225–232.
<https://doi.org/10.3732/ajb.1400437>
- Higgins, S.I., Bond, W.J., February, E.C., Bronn, A., Euston-Brown, D.I., Enslin, B., Govender, N., Rademan, L., O'Regan, S., Potgieter, A.L., 2007a. Effects of four decades of fire manipulation on woody vegetation structure in savanna. *Ecology* 88, 1119–1125.
- Higgins, S.I., Bond, W.J., February, E.C., Bronn, A., Euston-Brown, D.I.W., Enslin, B., Govender, N., Rademan, L., O'Regan, S., Potgieter, A.L.F., Scheiter, S., Sowry, R., Trollope, L., Trollope, W.S.W., 2007b. Effects of four decades of fire manipulation on woody vegetation structure in savanna. *Ecology* 88, 1119–1125. <https://doi.org/10.1890/06-1664>
- Higgins, S.I., Bond, W.J., Trollope, W.S., 2000. Fire, resprouting and variability: a recipe for grass–tree coexistence in savanna. *Journal of Ecology* 88, 213–229.
- Higuera, P., Peters, M., Brubaker, L., Gavin, D., 2007. Understanding the origin and analysis of sediment-charcoal records with a simulation model. *Quaternary Science Reviews* 26, 1790–1809.
<https://doi.org/10.1016/j.quascirev.2007.03.010>
- Higuera, P.E., Gavin, D.G., Bartlein, P.J., Hallett, D.J., 2011. Peak detection in sediment–charcoal records: impacts of alternative data analysis methods on

- fire-history interpretations. *International Journal of Wildland Fire* 19, 996–1014.
- Hoffmann, W.A., Flake, S.W., Abreu, R.C., Pilon, N.A., Rossatto, D.R., Durigan, G., 2019. Rare frost events reinforce tropical savanna–forest boundaries. *Journal of Ecology* 107, 468–477.
- Holdo, R.M., 2006. Elephant herbivory, frost damage and topkill in Kalahari sand woodland savanna trees. *Journal of Vegetation Science* 17, 509–518.
- Holmgren, K., Karlén, W., Lauritzen, S., Lee-Thorp, J., Partridge, T., Piketh, S., Repinski, P., Stevenson, C., Svanered, O., Tyson, P., 1999. A 3000-year high-resolution stalagmitebased record of palaeoclimate for northeastern South Africa. *The Holocene* 9, 295–309.
- Hong, Y.T., Hong, B., Lin, Q.H., Shibata, Y., Hirota, M., Zhu, Y.X., Leng, X.T., Wang, Y., Wang, H., Yi, L., 2005. Inverse phase oscillations between the East Asian and Indian Ocean summer monsoons during the last 12000 years and paleo-El Niño. *Earth and Planetary Science Letters* 231, 337–346.
<https://doi.org/10.1016/j.epsl.2004.12.025>
- Hu, Y., Li, D., Liu, J., 2007. Abrupt seasonal variation of the ITCZ and the Hadley circulation. *Geophysical Research Letters* 34.
<https://doi.org/10.1029/2007GL030950>
- Huffman, T.N., 2008. Climate change during the Iron Age in the Shashe-Limpopo Basin, southern Africa. *Journal of Archaeological Science* 35, 2032–2047.
<https://doi.org/10.1016/j.jas.2008.01.005>
- Huffman, T.N., 2000. Mapungubwe and the Origins of the Zimbabwe Culture. *Goodwin Series* 8, 14–29. <https://doi.org/10.2307/3858043>
- Huffman, T.N., Vogel, J.C., 1991. The Chronology of Great Zimbabwe. *The South African Archaeological Bulletin* 46, 61–70. <https://doi.org/10.2307/3889086>
- Huffman, T.N., Woodborne, S., 2016. Archaeology, baobabs and drought: Cultural proxies and environmental data from the Mapungubwe landscape, southern Africa. *The Holocene* 26, 464–470.
- Joubert, D.F., 2014. The dynamics of bush thickening by *Acacia mellifera* in the Highland Savanna of Namibia. University of the Free State.
- Joubert, D.F., Rothauge, A., Smit, G.N., 2008. A conceptual model of vegetation dynamics in the semiarid Highland savanna of Namibia, with particular

- reference to bush thickening by *Acacia mellifera*. *Journal of Arid Environments* 72, 2201–2210. <https://doi.org/10.1016/j.jaridenv.2008.07.004>
- Jury, M.R., Parker, B., Waliser, D., 1994. Evolution and variability of the ITCZ in the SW Indian Ocean: 1988–90. *Theoretical and Applied Climatology* 48, 187–194. <https://doi.org/10.1007/BF00867048>
- K. P. Vadrevu, I. Csiszar, E. Ellicott, L. Giglio, K. V. S. Badarinath, E. Vermote, C. Justice, 2013. Hotspot Analysis of Vegetation Fires and Intensity in the Indian Region. *IEEE Journal of Selected Topics in Applied Earth Observations and Remote Sensing* 6, 224–238. <https://doi.org/10.1109/JSTARS.2012.2210699>
- Kane, R.P., 2009. Periodicities, ENSO effects and trends of some South African rainfall series: an update. *South African Journal of Science* 105, 199–207.
- Kaplan, M., 2012. Million-year-old ash hints at origins of cooking. *Nature*. <https://doi.org/10.1038/nature.2012.10372>
- Killingtveit, Å., Hamududu, B., 2016. Hydropower Production in Future Climate Scenarios; the Case for the Zambezi River. *Energies* 9. <https://doi.org/10.3390/en9070502>
- Kinahan, J., 2011a. *A History of Namibia: From the Beginning to 1990*. Columbia University Press.
- Kinahan, J., 2011b. *A History of Namibia: From the Beginning to 1990*. Columbia University Press.
- Krawchuk, M.A., Moritz, M.A., 2011. Constraints on global fire activity vary across a resource gradient. *Ecology* 92, 121–132.
- Labat, D., Ronchail, J., Calde, J., Guyot, J.L., De Oliveira, E., Guimarães, W., 2004. Wavelet analysis of Amazon hydrological regime variability. *Geophysical Research Letters* 31. <https://doi.org/10.1029/2003GL018741>
- Le Roux, J., 2017. Namibia: Fire Situation (IFFN No. 25) – GFMC. URL https://gfmc.online/iffn/country/na/na_4.html (accessed 3.7.20).
- Le Roux, J., 2011. The effect of land use practices on the spatial and temporal characteristics of savanna fires in Namibia.
- Leclercq, P.W., Oerlemans, J., 2012. Global and hemispheric temperature reconstruction from glacier length fluctuations. *Climate Dynamics* 38, 1065–1079. <https://doi.org/10.1007/s00382-011-1145-7>

- Leduc, G., Vidal, L., Tachikawa, K., Bard, E., 2009. ITCZ rather than ENSO signature for abrupt climate changes across the tropical Pacific? *Quaternary Research* 72, 123–131. <https://doi.org/10.1016/j.yqres.2009.03.006>
- Lehmann, C.E.R., Archibald, S.A., Hoffmann, W.A., Bond, W.J., 2011. Deciphering the distribution of the savanna biome. *New Phytologist* 191, 197–209. <https://doi.org/10.1111/j.1469-8137.2011.03689.x>
- Loader, N.J., Robertson, I., Barker, A.C., Switsur, V.R., Waterhouse, J.S., 1997. An improved technique for the batch processing of small wholewood samples to α -cellulose. *Chemical Geology* 136, 313–317.
- Lushetile, K., 2009. Vegetation Description of Sachinga Livestock Development Centre and Surroundings, Caprivi, Namibia. B. Sc. Honours Mini Dissertation. University of Pretoria, South Africa.
- Malherbe, J., Landman, W.A., Engelbrecht, F.A., 2014. The bi-decadal rainfall cycle, Southern Annular Mode and tropical cyclones over the Limpopo River Basin, southern Africa. *Climate Dynamics* 42, 3121–3138. <https://doi.org/10.1007/s00382-013-2027-y>
- Mann, M.E., Rutherford, S., 2002. Climate reconstruction using ‘Pseudoproxies.’ *Geophysical Research Letters* 29, 139–1. <https://doi.org/10.1029/2001GL014554>
- Marchant, R., Richer, S., Boles, O., Capitani, C., Courtney-Mustaphi, C.J., Lane, P., Prendergast, M.E., Stump, D., De Cort, G., Kaplan, J.O., 2018. Drivers and trajectories of land cover change in East Africa: Human and environmental interactions from 6000 years ago to present. *Earth-Science Reviews* 178, 322–378.
- Marlon, J.R., Bartlein, P.J., Daniau, A.-L., Harrison, S.P., Maezumi, S.Y., Power, M.J., Tinner, W., Vanni re, B., 2013. Global biomass burning: a synthesis and review of Holocene paleofire records and their controls. *Quaternary Science Reviews* 65, 5–25. <https://doi.org/10.1016/j.quascirev.2012.11.029>
- McCarroll, D., Gagen, M.H., Loader, N.J., Robertson, I., Anchukaitis, K.J., Los, S., Young, G.H.F., Jalkanen, R., Kirchhefer, A., Waterhouse, J.S., 2009. Correction of tree ring stable carbon isotope chronologies for changes in the carbon dioxide content of the atmosphere. *Geochimica et Cosmochimica Acta* 73, 1539–1547. <https://doi.org/10.1016/j.gca.2008.11.041>

- McCarroll, D., Loader, N.J., 2004. Stable isotopes in tree rings. *Quaternary Science Reviews* 23, 771–801. <https://doi.org/10.1016/j.quascirev.2003.06.017>
- Mendelsohn, J., Jarvis, A., Roberts, C., Robertson, T., 2002. Atlas of Namibia.
- Meyn, A., Taylor, S.W., Flannigan, M.D., Thonicke, K., Cramer, W., 2010. Relationship between fire, climate oscillations, and drought in British Columbia, Canada, 1920–2000. *Global Change Biology* 16, 977–989. <https://doi.org/10.1111/j.1365-2486.2009.02061.x>
- Moleele, N.M., Ringrose, S., Matheson, W., Vanderpost, C., 2002. More woody plants? the status of bush encroachment in Botswana’s grazing areas. *Journal of Environmental Management* 64, 3–11. <https://doi.org/10.1006/jema.2001.0486>
- Niang, I., O.C. Ruppel, M.A. Abdrabo, A. Essel, C. Lennard, J. Padgham, P. Urquhart, 2014. Africa, in: *Climate Change 2014: Impacts, Adaptation, and Vulnerability. Part B: Regional Aspects. Contribution of Working Group II to the Fifth Assessment Report of the Intergovernmental Panel on Climate Change*. Cambridge University Press, Cambridge, United Kingdom and New York, NY, USA, pp. 1199–1265.
- Nicholson, S.E., 2018. The ITCZ and the Seasonal Cycle over Equatorial Africa. *Bull. Amer. Meteor. Soc.* 99, 337–348. <https://doi.org/10.1175/BAMS-D-16-0287.1>
- Nicholson, S.E., Entekhabi, D., 1986. The quasi-periodic behavior of rainfall variability in Africa and its relationship to the southern oscillation. *Arch. Met. Geoph. Biocl. A.* 34, 311–348. <https://doi.org/10.1007/BF02257765>
- Nicholson, S.E., Funk, C., Fink, A.H., 2018. Rainfall over the African continent from the 19th through the 21st century. *Global and Planetary Change* 165, 114–127. <https://doi.org/10.1016/j.gloplacha.2017.12.014>
- Nicholson, S.E., Kim, J., 1997. The Relationship of the El Nino-Southern Oscillation to African Rainfall. *International Journal of Climatology* 17, 117–135. [https://doi.org/10.1002/\(SICI\)1097-0088\(199702\)17:2<117::AID-JOC84>3.0.CO;2-O](https://doi.org/10.1002/(SICI)1097-0088(199702)17:2<117::AID-JOC84>3.0.CO;2-O)
- Ocaya, V., 1993. Corporate Kingship: The Lozi of Zambia and the Ultimately Meaningful and Real. *Ultimate Reality and Meaning* 16, 173–184. <https://doi.org/10.3138/uram.16.3-4.173>

- O'connor, T.G., Kiker, G.A., 2004. Collapse of the Mapungubwe Society: Vulnerability of Pastoralism to Increasing Aridity. *Climatic Change* 66, 49–66. <https://doi.org/10.1023/B:CLIM.0000043192.19088.9d>
- Oris, F., Ali, A.A., Asselin, H., Paradis, L., Bergeron, Y., Finsinger, W., 2014. Charcoal dispersion and deposition in boreal lakes from 3 years of monitoring: Differences between local and regional fires: Monitoring charcoal deposition in lakes. *Geophys. Res. Lett.* 41, 6743–6752. <https://doi.org/10.1002/2014GL060984>
- Patrut, A., Mayne, D.H., von Reden, K.F., Lowy, D.A., Venter, S., McNichol, A.P., Roberts, M.L., Margineanu, D., 2010. Age and growth rate dynamics of an old African baobab determined by radiocarbon dating. *Radiocarbon* 52, 727–734.
- Patrut, A., Von Reden, K.F., Lowy, D.A., Alberts, A.H., Pohlman, J.W., Wittmann, R., Gerlach, D., Xu, L., Mitchell, C.S., 2007. Radiocarbon dating of a very large African baobab. *Tree Physiology* 27, 1569–1574.
- Patrut, A., von Reden, K.F., Mayne, D.H., Lowy, D.A., Patrut, R.T., 2013. AMS radiocarbon investigation of the African baobab: Searching for the oldest tree. *Nuclear Instruments and Methods in Physics Research Section B: Beam Interactions with Materials and Atoms* 294, 622–626. <https://doi.org/10.1016/j.nimb.2012.04.025>
- Patrut, A., Woodborne, S., Patrut, R.T., Hall, G., Rakosy, L., Winterbach, C., von Reden, K.F., 2019. Age, Growth and Death of a National Icon: The Historic Chapman Baobab of Botswana. *Forests* 10, 983. <https://doi.org/10.3390/f10110983>
- Patrut, A., Woodborne, S., von Reden, K.F., Hall, G., Hofmeyr, M., Lowy, D.A., Patrut, R.T., 2015. African baobabs with false inner cavities: the radiocarbon investigation of the Lebombo Eco Trail baobab. *PLoS One* 10, e0117193–e0117193. <https://doi.org/10.1371/journal.pone.0117193>
- Pausas, J., Ribeiro, E., 2013. The global fire–productivity relationship. *Global Ecology and Biogeography* 22. <https://doi.org/10.1111/geb.12043>
- Pausas, J.G., Keeley, J.E., 2009. A Burning Story: The Role of Fire in the History of Life. *BioScience* 59, 593–601. <https://doi.org/10.1525/bio.2009.59.7.10>
- Pearson, R.G., Dawson, T.P., 2003. Predicting the impacts of climate change on the distribution of species: are bioclimate envelope models useful? *Global*

- Ecology and Biogeography 12, 361–371. <https://doi.org/10.1046/j.1466-822X.2003.00042.x>
- Peck, J.A., Green, R.R., Shanahan, T., King, J.W., Overpeck, J.T., Scholz, C.A., 2004. A magnetic mineral record of Late Quaternary tropical climate variability from Lake Bosumtwi, Ghana. *Palaeogeography, Palaeoclimatology, Palaeoecology* 215, 37–57. <https://doi.org/10.1016/j.palaeo.2004.08.003>
- Pessenda, L.C.R., Gouveia, S.E.M., Aravena, R., 2001. Radiocarbon Dating of Total Soil Organic Matter and Humin Fraction and Its Comparison with ¹⁴C Ages of Fossil Charcoal. *Radiocarbon* 43, 595–601. <https://doi.org/10.1017/S0033822200041242>
- Peters, M.E., Higuera, P.E., 2007. Quantifying the source area of macroscopic charcoal with a particle dispersal model. *Quaternary Research* 67, 304–310. <https://doi.org/10.1016/j.yqres.2006.10.004>
- Pretorius, J.L., 1975. The Fwe of the Eastern Caprivi Zipfel: a study of their historical and geographical background, tribal structure and legal system, with special reference to Fwe family law and succession.
- Priyadarshini, K.V.R., Prins, H.H.T., de Bie, S., Heitkönig, I.M.A., Woodborne, S., Gort, G., Kirkman, K., Ludwig, F., Dawson, T.E., de Kroon, H., 2016. Seasonality of hydraulic redistribution by trees to grasses and changes in their water-source use that change tree-grass interactions: HYDRAULIC REDISTRIBUTION BY TREES TO GRASSES AND CHANGES IN THEIR WATER SOURCES. *Ecohydrology* 9, 218–228. <https://doi.org/10.1002/eco.1624>
- Prokoph, A., El Bilali, H., 2008. Cross-Wavelet Analysis: a Tool for Detection of Relationships between Paleoclimate Proxy Records. *Mathematical Geosciences* 40, 575–586. <https://doi.org/10.1007/s11004-008-9170-8>
- Pyne, S.J., 1997. *World fire: the culture of fire on earth*. University of Washington press.
- R Core Team, 2019. *R: A Language and Environment for Statistical Computing*. R Foundation for Statistical Computing.
- Reason, C.J.C., Rouault, M., 2002. ENSO-like decadal variability and South African rainfall. *Geophysical Research Letters* 29, 16–1. <https://doi.org/10.1029/2002GL014663>

- Reimer, P.J., Bard, E., Bayliss, A., Beck, J.W., Blackwell, P.G., Ramsey, C.B., Buck, C.E., Cheng, H., Edwards, R.L., Friedrich, M., Grootes, P.M., Guilderson, T.P., Haflidason, H., Hajdas, I., Hatté, C., Heaton, T.J., Hoffmann, D.L., Hogg, A.G., Hughen, K.A., Kaiser, K.F., Kromer, B., Manning, S.W., Niu, M., Reimer, R.W., Richards, D.A., Scott, E.M., Southon, J.R., Staff, R.A., Turney, C.S.M., van der Plicht, J., 2013. IntCal13 and Marine13 Radiocarbon Age Calibration Curves 0–50,000 Years cal BP. *Radiocarbon* 55, 1869–1887. https://doi.org/10.2458/azu_js_rc.55.16947
- Robertson, I., Loader, N.J., Froyd, C.A., Zambatis, N., Whyte, I., Woodborne, S., 2006. The potential of the baobab (*Adansonia digitata* L.) as a proxy climate archive. *Applied Geochemistry* 21, 1674–1680. <https://doi.org/10.1016/j.apgeochem.2006.07.005>
- Robertson, J., 2001. South African Early Iron Age in Zambia. pp. 260–271. https://doi.org/10.1007/978-1-4615-1193-9_20
- Roesch, A., Schmidbauer, H., 2018. WaveletComp: Computational Wavelet Analysis.
- Rohde, R.F., Hoffman, M.T., 2012. The historical ecology of Namibian rangelands: Vegetation change since 1876 in response to local and global drivers. *Science of The Total Environment* 416, 276–288. <https://doi.org/10.1016/j.scitotenv.2011.10.067>
- Roques, K.G., O’connor, T.G., Watkinson, A.R., 2001. Dynamics of shrub encroachment in an African savanna: relative influences of fire, herbivory, rainfall and density dependence. *Journal of Applied Ecology* 38, 268–280.
- Rouault, M., Florenchie, P., Fauchereau, N., Reason, C.J.C., 2003. South East tropical Atlantic warm events and southern African rainfall. *Geophysical Research Letters* 30. <https://doi.org/10.1029/2002GL014840>
- Rowe, J.H., 1961. Stratigraphy and Seriation. *American Antiquity* 26, 324–330. <https://doi.org/10.2307/277399>
- Saha, M.V., Scanlon, T.M., D’Odorico, P., 2015. Examining the linkage between shrub encroachment and recent greening in water-limited southern Africa. *Ecosphere* 6, art156. <https://doi.org/10.1890/ES15-00098.1>
- Sankaran, M., Hanan, N., Scholes, R., Ratnam, J., Augustine, D., Cade, B., Gignoux, J., Higgins, S., Roux, X., Ludwig, F., Ardö, J., Banyikwa, F., Bronn, A., Bucini, G., Caylor, K., Coughenour, M., Diouf, A., Ekaya, W., Feral, C.,

- Zambatis, N., 2005. Determinants of woody cover in African savannas: a continental scale analysis.
- Santos, G.M., Alexandre, A., Prior, C.A., 2016. From radiocarbon analysis to interpretation: A comment on “Phytolith Radiocarbon Dating in Archaeological and Paleoecological Research: A Case Study of Phytoliths from Modern Neotropical Plants and a Review of the Previous Dating Evidence”, *Journal of Archaeological Science* (2015), doi: 10.1016/j.jas.2015.06.002.” by Dolores R. Piperno. *Journal of Archaeological Science* 71, 51–58. <https://doi.org/10.1016/j.jas.2016.04.015>
- Savadogo, P., Zida, D., Sawadogo, L., Tiveau, D., Tigabu, M., Odén, P.C., 2007. Fuel and fire characteristics in savanna–woodland of West Africa in relation to grazing and dominant grass type. *Int. J. Wildland Fire* 16, 531–539. <https://doi.org/10.1071/WF07011>
- Schiffer, M.B., 1986. Radiocarbon dating and the “old wood” problem: The case of the Hohokam chronology. *Journal of Archaeological Science* 13, 13–30. [https://doi.org/10.1016/0305-4403\(86\)90024-5](https://doi.org/10.1016/0305-4403(86)90024-5)
- Schlachter, K.J., Horn, S.P., 2010. Sample preparation methods and replicability in macroscopic charcoal analysis. *Journal of Paleolimnology* 44, 701–708.
- Schneider, T., Bischoff, T., Haug, G.H., 2014. Migrations and dynamics of the intertropical convergence zone. *Nature* 513, 45–53. <https://doi.org/10.1038/nature13636>
- Scholes, B., Scholes, M., Lucas, M., 2015. *Climate Change: Briefings from Southern Africa*. Wits University Press.
- Schwinning, S., Sala, O.E., 2004. Hierarchy of responses to resource pulses in arid and semi-arid ecosystems. *Oecologia* 141, 211–220. <https://doi.org/10.1007/s00442-004-1520-8>
- Scott, A.C., 2010. Charcoal recognition, taphonomy and uses in palaeoenvironmental analysis. *Palaeogeography, Palaeoclimatology, Palaeoecology* 291, 11–39. <https://doi.org/10.1016/j.palaeo.2009.12.012>
- Scott, E.M., 2007. Radiocarbon dating: sources of error. *Encyclopedia of Quaternary Science* 2918–2923. <https://doi.org/10.1016/B0-44-452747-8/00042-9>
- Scott, L., 2016. Fluctuations of vegetation and climate over the last 75 000 years in the Savanna Biome, South Africa: Tswaing Crater and Wonderkrater pollen

- sequences reviewed. *Quaternary Science Reviews* 145, 117–133.
<https://doi.org/10.1016/j.quascirev.2016.05.035>
- Scott, L., 2002. Microscopic charcoal in sediments: Quaternary fire history of the grassland and savanna regions in South Africa. *Journal of Quaternary Science* 17, 77–86. <https://doi.org/10.1002/jqs.641>
- Scott, L., 1996. Palynology of hyrax middens: 2000 years of palaeoenvironmental history in Namibia. *Quaternary International* 33, 73–79.
[https://doi.org/10.1016/1040-6182\(95\)00093-3](https://doi.org/10.1016/1040-6182(95)00093-3)
- Scott, L., Holmgren, K., Talma, A.S., Woodborne, S., Vogel, J.C., 2003. Age interpretation of the Wonderkrater spring sediments and vegetation change in the Savanna Biome, Limpopo province, South Africa. *South African Journal of Science* 99, 484–488.
- Seddon, D., 1968. The Origins and Development of Agriculture in East and Southern Africa. *Current Anthropology* 9, 489–509. <https://doi.org/10.1086/200947>
- Serdeczny, O., Adams, S., Baarsch, F., Coumou, D., Robinson, A., Hare, B., Schaeffer, M., Perrette, M., Reinhardt, J., 2016. Climate change impacts in Sub-Saharan Africa: from physical changes to their social repercussions. *Regional Environmental Change* 1–16. <https://doi.org/10.1007/s10113-015-0910-2>
- Shanahan, T.M., Beck, J.W., Overpeck, J.T., McKay, N.P., Pigati, J.S., Peck, J.A., Scholz, C.A., Heil, C.W., King, J., 2012. Late Quaternary sedimentological and climate changes at Lake Bosumtwi Ghana: New constraints from laminae analysis and radiocarbon age modeling. *Palaeogeography, Palaeoclimatology, Palaeoecology* 361–362, 49–60. <https://doi.org/10.1016/j.palaeo.2012.08.001>
- Shanahan, T.M., Overpeck, J.T., Wheeler, C.W., Beck, J.W., Pigati, J.S., Talbot, M.R., Scholz, C.A., Peck, J., King, J.W., 2006. Paleoclimatic variations in West Africa from a record of late Pleistocene and Holocene lake level stands of Lake Bosumtwi, Ghana. *Palaeogeography, Palaeoclimatology, Palaeoecology* 242, 287–302. <https://doi.org/10.1016/j.palaeo.2006.06.007>
- Sheuyange, A., Oba, G., Weladji, R.B., 2005. Effects of anthropogenic fire history on savanna vegetation in northeastern Namibia. *Journal of Environmental Management* 75, 189–198. <https://doi.org/10.1016/j.jenvman.2004.11.004>
- Shorrocks, B., Bates, W., 2015. *The biology of African savannahs*. Oxford University Press, USA.

- Singleton, A.T., Reason, C.J.C., 2007. Variability in the characteristics of cut-off low pressure systems over subtropical southern Africa. *International Journal of Climatology* 27, 295–310. <https://doi.org/10.1002/joc.1399>
- Sippel, S., Meinshausen, N., Fischer, E.M., Székely, E., Knutti, R., 2020. Climate change now detectable from any single day of weather at global scale. *Nat. Clim. Chang.* 10, 35–41. <https://doi.org/10.1038/s41558-019-0666-7>
- Smith, A.B., 1992. *Pastoralism in Africa: origins and development ecology*. Hurst & Company.
- Staver, A.C., Archibald, S., Levin, S., 2011. Tree cover in sub-Saharan Africa: Rainfall and fire constrain forest and savanna as alternative stable states. *Ecology* 92, 1063–1072. <https://doi.org/10.1890/10-1684.1>
- Stevens, N., Lehmann, C.E., Murphy, B.P., Durigan, G., 2017. Savanna woody encroachment is widespread across three continents. *Global change biology* 23, 235–244.
- Stone, A., Thomas, D., 2008. Linear dune accumulation chronologies from the southwest Kalahari, Namibia: challenges of reconstructing late Quaternary palaeoenvironments from aeolian landforms. *Quaternary Science Reviews* 27, 1667–1681.
- Strobel, P., Kasper, T., Frenzel, P., Schitteck, K., Quick, L.J., Meadows, M.E., Mäusbacher, R., Haberzettl, T., 2019. Late Quaternary palaeoenvironmental change in the year-round rainfall zone of South Africa derived from peat sediments from Vankervelsvlei. *Quaternary Science Reviews* 218, 200–214. <https://doi.org/10.1016/j.quascirev.2019.06.014>
- Stuiver, M., Reimer, P., Reimer, R., 2018. CALIB 7.1. 2017. URL: <http://calib.org> (accessed: 30.11. 2017).
- Sundqvist, H.S., Holmgren, K., Fohlmeister, J., Zhang, Q., Matthews, M.B., Spötl, C., Körnich, H., 2013. Evidence of a large cooling between 1690 and 1740 AD in southern Africa. *Scientific Reports* 3, 1–6. <https://doi.org/10.1038/srep01767>
- Tadross, M., Davis, C., Engelbrecht, F., Joubert, A., Archer, E.R., 2011. Regional scenarios of future climate change over southern Africa. CSIR.
- Talbot, M.R., Johannessen, T., 1992. A high resolution palaeoclimatic record for the last 27,500 years in tropical West Africa from the carbon and nitrogen isotopic composition of lacustrine organic matter. *Earth and Planetary Science Letters* 110, 23–37. [https://doi.org/10.1016/0012-821X\(92\)90036-U](https://doi.org/10.1016/0012-821X(92)90036-U)

- Taljaard, J., 1986. Change of rainfall distribution and circulation patterns over southern Africa in summer. *Journal of climatology* 6, 579–592.
- Telfer, M., Thomas, D., 2007. Late Quaternary linear dune accumulation and chronostratigraphy of the southwestern Kalahari: implications for aeolian palaeoclimatic reconstructions and predictions of future dynamics. *Quaternary Science Reviews* 26, 2617–2630.
- Telford, Richard J, Heegaard, E., Birks, H.J., 2004. The intercept is a poor estimate of a calibrated radiocarbon age. *The Holocene* 14, 296–298.
- Telford, R.J., Heegaard, E., Birks, H.J.B., 2004. All age–depth models are wrong: but how badly? *Quaternary Science Reviews* 23, 1–5.
<https://doi.org/10.1016/j.quascirev.2003.11.003>
- Tinner, W., Hofstetter, S., Zeuglin, F., Conedera, M., Wohlgemuth, T., Zimmermann, L., Zweifel, R., 2006. Long-distance transport of macroscopic charcoal by an intensive crown fire in the Swiss Alps - implications for fire history reconstruction, *The Holocene* 16, 287–292.
<https://doi.org/10.1191/0959683606hl925rr>
- Tinner, W., Hu, F.S., 2003. Size parameters, size-class distribution and area-number relationship of microscopic charcoal: relevance for fire reconstruction. *The Holocene* 13, 499–505. <https://doi.org/10.1191/0959683603hl615rp>
- Tlou, T., 1972. The Taming of the Okavango Swamps—the Utilization of a Riverine Environment \pm 1750– \pm 1800. *Botswana Notes and Records* 147–159.
- Todd, M.C., Washington, R., Palmer, P.I., 2004. Water vapour transport associated with tropical–temperate trough systems over southern Africa and the southwest Indian Ocean. *International Journal of Climatology* 24, 555–568.
<https://doi.org/10.1002/joc.1023>
- Törnqvist, T., Rosenheim, B., Hu, P., Fernandez, A., 2015. Radiocarbon dating and calibration. pp. 349–360. <https://doi.org/10.1002/9781118452547.ch23>
- Torrence, C., Compo, G.P., 1998. A Practical Guide to Wavelet Analysis. *Bull. Amer. Meteor. Soc.* 79, 61–78. [https://doi.org/10.1175/1520-0477\(1998\)079<0061:APGTWA>2.0.CO;2](https://doi.org/10.1175/1520-0477(1998)079<0061:APGTWA>2.0.CO;2)
- Trollope, W.S.W., Potgieter, A.L.F., 1985. Fire behaviour in the Kruger National Park. *Journal of the Grassland Society of Southern Africa* 2, 17–22.
<https://doi.org/10.1080/02566702.1985.9648000>

- Tyson, P., Karlén, W., Holmgren, K., Heiss, G., 2000. The Little Ice Age and medieval warming in South Africa. *South African Journal of Science* 96, 121–126.
- Tyson, P.D., 1991. Climatic change in southern Africa: past and present conditions and possible future scenarios. *Climatic Change* 18, 241–258.
- Unzicker, A.B., 1996. Hambukushu Marriage Traditions: Past and Present. *Botswana Notes and Records* 28, 97–106.
- Usman, M.T., Reason, C.J.C., 2004. Dry spell frequencies and their variability over southern Africa. *Climate Research* 26, 199–211.
- Van de Vijver, C.A.D.M., Poot, P., Prins, H.H.T., 1999. Causes of increased nutrient concentrations in post-fire regrowth in an East African savanna. *Plant and Soil* 214, 173–185. <https://doi.org/10.1023/A:1004753406424>
- van Geel, B., Gelorini, V., Lyaruu, A., Aptroot, A., Rucina, S., Marchant, R., Damsté, J.S.S., Verschuren, D., 2011. Diversity and ecology of tropical African fungal spores from a 25,000-year palaeoenvironmental record in southeastern Kenya. *Review of Palaeobotany and Palynology* 164, 174–190.
- Van Langevelde, F., Van De Vijver, C.A., Kumar, L., Van De Koppel, J., De Ridder, N., Van Andel, J., Skidmore, A.K., Hearne, J.W., Stroosnijder, L., Bond, W.J., 2003. Effects of fire and herbivory on the stability of savanna ecosystems. *Ecology* 84, 337–350.
- Van Wilgen, B.W., Govender, N., Biggs, H.C., Ntsala, D., Funda, X.N., 2004. Response of savanna fire regimes to changing fire-management policies in a large African national park. *Conservation Biology* 18, 1533–1540.
- Verlinden, A., Laamanen, R., 2006. Long Term Fire Scar Monitoring with Remote Sensing in Northern Namibia: Relations Between Fire Frequency, Rainfall, Land Cover, Fire Management and Trees. *Environmental Monitoring and Assessment* 112, 231–253. <https://doi.org/10.1007/s10661-006-1705-1>
- Walker, B.H., Noy-Meir, I., 1982. Aspects of the Stability and Resilience of Savanna Ecosystems, in: Huntley, B.J., Walker, Brian H. (Eds.), *Ecology of Tropical Savannas*. Springer Berlin Heidelberg, Berlin, Heidelberg, pp. 556–590.
- Walker, M.J.C., Bryant, C., Coope, G.R., Harkness, D.D., Lowe, J.J., Scott, E.M., 2001. Towards a Radiocarbon Chronology of the Late-Glacial: Sample Selection Strategies. *Radiocarbon* 43, 1007–1019. <https://doi.org/10.1017/S0033822200041679>

- Ward, D., 2005. Do we understand the causes of bush encroachment in African savannas? *African Journal of Range & Forage Science* 22, 101–105.
<https://doi.org/10.2989/10220110509485867>
- Wei, Y., Wu, X., Cai, C., Wang, Jie, Xia, J., Wang, Junguang, Guo, Z., Yuan, Z., 2019. Impact of erosion-induced land degradation on rainfall infiltration in different types of soils under field simulation. *Land Degrad Dev* 30, 1751–1764. <https://doi.org/10.1002/ldr.3382>
- Whitlock, C., Larsen, C., 2002. Charcoal as a Fire Proxy, in: Smol, J.P., Birks, H.J.B., Last, W.M., Bradley, R.S., Alverson, K. (Eds.), *Tracking Environmental Change Using Lake Sediments*. Springer Netherlands, Dordrecht, pp. 75–97.
https://doi.org/10.1007/0-306-47668-1_5
- Whittaker, R.H., 1962. Classification of natural communities. *The Botanical Review* 28, 1–239.
- Williams, C.A., Hanan, N., Scholes, R.J., Kutsch, W., 2009. Complexity in water and carbon dioxide fluxes following rain pulses in an African savanna. *Oecologia* 161, 469–480.
- Williams, M.A.J., Williams, F.M., Duller, G.A.T., Munro, R.N., El Tom, O.A.M., Barrows, T.T., Macklin, M., Woodward, J., Talbot, M.R., Haberlah, D., 2010. Late Quaternary floods and droughts in the Nile valley, Sudan: new evidence from optically stimulated luminescence and AMS radiocarbon dating. *Quaternary Science Reviews* 29, 1116–1137.
<https://doi.org/10.1016/j.quascirev.2010.02.018>
- Woodborne, S., Gandiwa, P., Hall, G., Patrut, A., Finch, J., 2016. A Regional Stable Carbon Isotope Dendro-Climatology from the South African Summer Rainfall Area. *PLOS ONE* 11, e0159361.
<https://doi.org/10.1371/journal.pone.0159361>
- Woodborne, S., Hall, G., Robertson, I., Patrut, A., Rouault, M., Loader, N.J., Hofmeyr, M., 2015. A 1000-Year Carbon Isotope Rainfall Proxy Record from South African Baobab Trees (*Adansonia digitata* L.). *PLoS ONE* 10, e0124202. <https://doi.org/10.1371/journal.pone.0124202>
- Zhang, W., Brandt, M., Penuelas, J., Guichard, F., Tong, X., Tian, F., Fensholt, R., 2019. Ecosystem structural changes controlled by altered rainfall climatology in tropical savannas. *Nat Commun* 10, 671. <https://doi.org/10.1038/s41467-019-08602-6>

Zinke, J., Loveday, B.R., Reason, C.J.C., Dullo, W.-C., Kroon, D., 2014. Madagascar corals track sea surface temperature variability in the Agulhas Current core region over the past 334 years. *Scientific Reports* 4, 1–8.
<https://doi.org/10.1038/srep04393>